



University of Tennessee Health Science Center
UTHSC Digital Commons

Theses and Dissertations (ETD)

College of Graduate Health Sciences

11-2022

Cerebellar Coordination of Neuronal and Behavioral Rhythms

Brittany Correia Chapman
University of Tennessee Health Science Center

Follow this and additional works at: <https://dc.uthsc.edu/dissertations>



Part of the [Medical Neurobiology Commons](#), [Nervous System Diseases Commons](#), and the [Neurosciences Commons](#)

Recommended Citation

Chapman, Brittany Correia (<https://orcid.org/0000-0001-7480-5977>), "Cerebellar Coordination of Neuronal and Behavioral Rhythms" (2022). *Theses and Dissertations (ETD)*. Paper 618. <http://dx.doi.org/10.21007/etd.cghs.2022.0605>.

This Dissertation is brought to you for free and open access by the College of Graduate Health Sciences at UTHSC Digital Commons. It has been accepted for inclusion in Theses and Dissertations (ETD) by an authorized administrator of UTHSC Digital Commons. For more information, please contact jwelch30@uthsc.edu.

Cerebellar Coordination of Neuronal and Behavioral Rhythms

Abstract

Long known for its role in motor control, it is increasingly clear that the cerebellum is also involved in numerous cognitive and affective behaviors. Though the neuronal mechanism for the role of the cerebellum in cognition is still unclear, there is a consensus that it involves cerebellar interactions with the cerebral cortex. Recent studies suggest that the cerebellum monitors, and possibly coordinates, the precise phase alignment or coherence of neuronal oscillations in cerebral cortical areas. Here, we asked how loss of cerebellar function affects respiratory rhythms and the interactions of local field potential (LFP) oscillations between the lobulus simplex (LS) in the cerebellum, medial prefrontal cortex (mPFC), and dorsal CA1 (dCA1) using multisite in vivo extracellular recordings in freely moving mice. We compared a mouse model of cerebellar ataxia and their littermate controls. The ataxic mice were designed to have a genetically induced loss of Purkinje cell neurotransmission, resulting in an expected repertoire of cerebellar motor deficits. Here we asked whether these mice also have neurophysiological defects that are indicative of cognitive circuit dysfunction. We quantified respiratory interval regularity and rhythmicity, power spectra of LFP oscillations in each structure, the magnitudes of coherence of oscillations and Granger causality between each pair of structures using a nonparametric spectral method, and the phase amplitude coupling (PAC) of LFP oscillations within and between each structure. Resting-state coherence of gamma oscillations between LS and mPFC was significantly increased in ataxic mice relative to their controls. Ataxic animals also showed significantly larger Granger causality from the mPFC to cerebellar LS in gamma frequencies compared to littermate controls. Significant PAC within LS was observed at very high gamma frequencies. Our findings reveal that Purkinje cell neurotransmission is required for normal functional interactions between the cerebellum and cerebral cortex and between cerebral cortical areas involved in cognitive functions, suggesting an involvement of the cerebellum in the modulation or coordination of functional communication between brain areas.

Document Type

Dissertation

Degree Name

Doctor of Philosophy (PhD)

Program

Biomedical Sciences

Research Advisor

Detlef H. Heck, PhD

Keywords

Cerebellum; Coherence, Oscillations, Phase Amplitude Coupling, Respiration

Subject Categories

Medical Neurobiology | Medical Sciences | Medicine and Health Sciences | Nervous System Diseases | Neurosciences

UNIVERSITY OF TENNESSEE HEALTH SCIENCE CENTER

DOCTORAL DISSERTATION

**Cerebellar Coordination of Neuronal
and Behavioral Rhythms**

Author:
Brittany Correia Chapman

Advisor:
Detlef Heck, Ph.D.

*A Dissertation Presented for The Graduate Studies Council of
The University of Tennessee Health Science Center
in Partial Fulfillment of Requirements for the Doctor of Philosophy degree from
The University of Tennessee*

in

*Biomedical Sciences: Neuroscience
College of Graduate Health Sciences*

November 2022

Portions of Chapter 2 © 2022 by Elsevier B.V.
All other material © 2022 by Brittany Correia Chapman.
All rights reserved.

Modified with permission
Masters/Doctoral Thesis LaTeX Template
Version 2.5 (8/27/2017)
<http://www.LaTeXTemplates.com>
Creative Commons License CC BY-NC-SA 3.0

To my family and friends, who believed in me even when I did not. To Ian, who inspires me everyday. And to Eleanor, Callie, and Arthur, who have been exemplary work buddies and Very Good animals. Except for Callie, who almost succeeded in deleting most of this document.

Acknowledgements

I would like to start by thanking my advisor, Dr. Detlef Heck, who has been nothing but encouraging and supporting during my time in the lab. His genuine enthusiasm for science is something I hope to carry with me throughout my career. I would also like to thank Dr. Yu Liu for his patience and all the time he spent with me learning surgeries, and Heck Lab members past and present for making lab a fun place to be day in and day out.

I would like to acknowledge and thank my committee: Dr. John Boughter, Dr. Max Fletcher, Dr. Megan Mulligan, and Dr. Shalini Narayana for their insight and support throughout this journey. Additionally, I would like to acknowledge the College of Graduate Health Sciences and the Neuroscience Institute, who have both provided support for my fellowship and for travel to share this work.

Finally, I would like to thank Ian Chapman, Martin Raymond, and Jane Brown. Forged from the fires of Brookhaven Bar and Grill, we emerged one of the greatest trivia teams ever assembled. Being part of team Professor Dr. Wittenborg a.k.a. The Regretful Ghost of Ser Pounce a.k.a. Scrooge's Dead Friend a.k.a. Origi Scored a Dole a.k.a. Thor's Hammer Fjallbo a.k.a. Joe Manchin's Sea Mansion a.k.a. Pierre Delecto a.k.a Fun Uncle Daemon was an honor of a lifetime. Constantly being around a group of friends and fellow graduate students with such an infectious love for learning was more than I could have hoped for during my time here.

Abstract

Brittany Correia Chapman

*Cerebellar Coordination of Neuronal
and Behavioral Rhythms*

Long known for its role in motor control, it is increasingly clear that the cerebellum is also involved in numerous cognitive and affective behaviors. Though the neuronal mechanism for the role of the cerebellum in cognition is still unclear, there is a consensus that it involves cerebellar interactions with the cerebral cortex. Recent studies suggest that the cerebellum monitors, and possibly coordinates, the precise phase alignment or coherence of neuronal oscillations in cerebral cortical areas. Here, we asked how loss of cerebellar function affects respiratory rhythms and the interactions of local field potential (LFP) oscillations between the lobulus simplex (LS) in the cerebellum, medial prefrontal cortex (mPFC), and dorsal CA1 (dCA1) using multisite *in vivo* extracellular recordings in freely moving mice. We compared a mouse model of cerebellar ataxia and their littermate controls. The ataxic mice were designed to have a genetically induced loss of Purkinje cell neurotransmission, resulting in an expected repertoire of cerebellar motor deficits. Here we asked whether these mice also have neurophysiological defects that are indicative of cognitive circuit dysfunction. We quantified respiratory interval regularity and rhythmicity, power spectra of LFP oscillations in each structure, the magnitudes of coherence of oscillations and Granger causality between each pair of structures using a nonparametric spectral method, and the phase amplitude coupling (PAC) of LFP oscillations within and between each structure. Resting-state coherence of gamma oscillations between LS and mPFC was significantly increased in ataxic mice relative to their controls. Ataxic animals also showed significantly larger Granger causality from the mPFC to cerebellar LS in gamma frequencies compared to littermate controls. Significant PAC within LS was observed at very high gamma frequencies. Our findings reveal that Purkinje cell neurotransmission is required for normal functional interactions between the cerebellum and cerebral cortex and between cerebral cortical areas involved in cognitive functions, suggesting an involvement of the cerebellum in the modulation or coordination of functional communication between brain areas.

Contents

1	Introduction	1
1.1	Oscillations in the Brain	1
1.2	Coherence and Brain Activity	2
1.3	Cerebellar Coordination of Cortical Rhythms	2
1.4	Project Overview	3
2	The Cerebellum as a Coordinator of Respiratory Rhythms	4
2.1	Respiration, Brain Activity, and Cognition	5
2.2	Neuronal Mechanisms of Respiratory Modulation of Brain Activity	8
2.3	Loss of Cerebellar Function Selectively Affects Rhythmicity of Eupneic Breathing	11
2.3.1	Methods	11
	Animals	11
	Measurements of Respiratory Behavior	12
	Artificial Modulation of Respiratory Interval Sequences	12
2.3.2	Results	14
2.3.3	Discussion	14
3	Loss of Purkinje Cell Neurotransmission Affects Cerebellar-Prefrontal but Not Cerebellar-Hippocampal Functional Connectivity	18
3.1	Introduction	18
3.1.1	SWM and the Cerebellum	19
3.1.2	Coherence and SWM	20
3.1.3	The Cerebellum and Coherence	21
3.2	Methods	22
3.2.1	Animals	22
3.2.2	Surgery	22
3.2.3	Electrophysiology	24
3.2.4	Power, Coherence, and Granger Causality Analysis of LFP Data	25
3.2.5	Statistical Analysis	26
3.2.6	Histology	26
3.3	Results	26
3.3.1	Loss of Purkinje Cell Transmission Increased mPFC-LS Coherence	27

3.3.2	Loss of Purkinje Cell Transmission Increased Granger Causality from mPFC to LS	31
3.4	Discussion	32
4	Very High Frequency Phase Amplitude Coupling in the Cerebellar Cortex Is Altered by Loss of Purkinje Cell Neurotransmission	35
4.1	Introduction	35
4.2	Methods	36
4.2.1	Animals	36
4.2.2	Surgery	37
4.2.3	Electrophysiology	37
4.2.4	PAC Calculations	38
4.2.5	Statistical Analyses	38
4.2.6	Considering Waveform Shape	39
4.2.7	Histology	39
4.3	Results	39
4.3.1	Evaluation of PAC in a Mouse Model of Cerebellar Ataxia	39
4.3.2	Evaluation of PAC in B6 Mice	43
4.4	Discussion	44
5	Summary and Conclusions	47
	List of References	49
	Vita	69

List of Figures

2.1	Mouse respiratory behavior was measured using a custom-made plethysmograph chamber	13
2.2	Comparison of the CV2 (intrinsic rhythmicity) of respiratory behavior	15
2.3	Prolonging the duration of a subset of respiratory intervals to mimic breathing-swallowing coordination in MU mice increased the CV2 to CT values	16
3.1	Animal model and schematic of recording strategy with histology and raw data examples	23
3.2	Average power of LFP oscillations in <i>L7 Cre; VGAT^{flox/flox}</i> (red) and <i>VGAT^{flox/flox}</i> animals (blue)	28
3.3	Average coherence of oscillations between mPFC and LS	29
3.4	Histogram of time-resolved mPFC-LS coherence values in low gamma (30-60 Hz) and high gamma (80-100 Hz) frequency bands	30
3.5	Average Granger causality of oscillations from mPFC to LS	31
3.6	Illustration of a mouse brain showing a proposed circuit of how LS is influencing the functional connectivity of cerebrocerebellar interactions	33
4.1	Representative example of high frequency PAC in the cerebellum	40
4.2	Spectrograms of PAC in <i>L7 Cre; VGAT^{flox/flox}</i> and <i>VGAT^{flox/flox}</i> mice	41
4.3	Top quartile significant PAC	42
4.4	Fraction of C57BL/6J animals with significant PAC	43
4.5	Average unfiltered LS LFP aligned to the phase of 80-100 Hz LS LFP	46

List of Abbreviations

AP	Anterior-Posterior Axis
ASD	Autism Spectrum Disorder
BC	Bimodality Coefficient
COPD	Chronic Obstructive Pulmonary Disease
CT	Control
CV	Coefficient of Variation
CV2	Coefficient of Variation 2
dCA1	Dorsal Hippocampal CA1
DCN	Deep Cerebellar Nuclei
GABA	Gamma-aminobutyric Acid
fMRI	Functional Magnetic Resonance Imaging
iEEG	Intracranial Electroencephalogram
LC	Locus Coeruleus
LFP	Local Field Potential
LS	Lobulus Simplex
MEG	Magnetoencephalography
MI	Modulation Index
ML	Medial-Lateral Axis
mPFC	Medial Prefrontal Cortex
MRI	Magnetic Resonance Imaging
MU	Mutant
NS	Not Significant
PAC	Phase Amplitude Coupling
PC	Purkinje Cell
PCB	Printed Circuit Board
PL	Prelimbic Area
PN	Pontine Nuclei
preBötC	preBötzinger Complex
RE	Nucleus Reuniens
SWM	Spatial Working Memory
VAL	Ventral Anterior-lateral Complex
VGAT	Vesicular GABA Transporter
VM	Ventral Medial Nucleus
VPL	Ventral Posterolateral Nucleus

VPM Ventral Posteromedial Nucleus

Chapter 1

Introduction

1.1 Oscillations in the Brain

An oscillation in the simplest terms can be defined as periodic upward and downward deflections in a time series. Oscillatory activity is a ubiquitous feature in the nervous system. Oscillations can occur on time scales ranging from milliseconds (e.g. 120+ Hz hippocampal sharp wave ripples) to hours (e.g. circadian rhythms) and spatial scales ranging from single neurons (e.g. membrane potential oscillations (Llinás, 1988)) to hundreds and thousands of neurons (e.g. local field potentials (LFPs)). LFPs mostly reflect the sum of neuronal activity in the form of synaptic currents from large populations of excitatory and inhibitory synapses as measured by electrodes inserted into the brain. This population activity reflected in the LFP includes fluctuations in the extracellular matrix due to individual synaptic currents, voltage-dependent membrane oscillations, spike afterpotentials, and calcium spikes (Buzsáki, 2002). The immediate functional relevance for local oscillations in the brain is that they reflect changes in neuronal excitability and therefore they provide a measure of the probability of an individual neuron being able to elicit an action potential, or “spike”.

If an individual neuron receives an excitatory signal from another neuron while in a high excitability state (relatively depolarized membrane potential), it is more likely to be able to fire an action potential itself in response to that stimulus. If however that same neuron received that excitatory signal when its membrane potential was in a relatively hyperpolarized state (low excitability), then its own probability of firing an action potential in response to the input is much lower. With this in mind, it is clear, and has been confirmed experimentally, that oscillations can play a major role in modulating spike activity (Benchenane, Tiesinga, and Battaglia, 2011). The next step is to therefore explore mechanisms and structures that can in turn modulate neuronal oscillations as those would directly influence spike activity and thus brain function.

1.2 Coherence and Brain Activity

Technical advances in the field over the past decade now make it possible to collect high density spike and LFP data from multiple areas of the brain at one time while an animal is awake and able to behave naturalistically. One obvious benefit of this is that researchers can now look more closely at the interactions between the spike activity of individual neurons and LFP oscillations, and between LFP oscillations from multiple areas, over long periods of time and while an animal is asked to perform various behaviors. One way to relate two oscillatory signals to each other is to measure the coherence between them. Coherence is a quantitative measure that ranges between 0 and 1 that reflects the phase stability of two sinusoidal signals. For example, two oscillations at a certain frequency that are phase locked would have a coherence value of 1, while two signals at a certain frequency that were constantly varying their phase relationship would have a coherence value of 0. It is important to note that high coherence values do not necessarily imply that two signals have identical phases.

The idea that coherence could be a key mechanism for facilitating communication between groups of neurons was first proposed by Pascal Fries in 2005, who dubbed it the “communication through coherence” hypothesis (Fries, 2005). According to Fries, groups of neurons, each which generate their own oscillations, can only effectively communicate with each other if they have overlapping “windows for communication”. The substrate to generate these windows are the neuronal oscillations themselves, with maximal communication between groups being achieved when the “sending” group of neurons transmits information to the “receiving” group of neurons when the “receiving” group is at peak excitability in its oscillatory cycle. Therefore, states of high coherence between neuronal groups represent periods of effective neuronal communication. Fries formed his hypothesis in the context of visual attention wherein groups of neurons representing an attended to item show much higher coherence between each other than groups of neurons corresponding to an unattended item. In this example, Fries hypothesized that neurons in the parietal cortex may be driving the oscillatory modulation in this behavioral task, but that does not preclude neuronal groups from other brain areas acting as modulatory drivers in other behaviors and contexts (Fries, 2005).

1.3 Cerebellar Coordination of Cortical Rhythms

There is mounting evidence from the Heck lab and others that the cerebellum can act as a modulator of oscillation phase alignments for the purpose of coordinating the coherence between brain areas. The first piece of evidence to support this hypothesis came from Popa and colleagues, who showed that chemogenic inactivation of the cerebellum disrupts gamma-band coherence between the primary sensory and motor cortices during whisking behavior (Popa, Spolidoro, Proville, Guyon, et al., 2013). More recently, additional work has been done investigating sensorimotor gamma coherence, showing that optogenetic

stimulation of Purkinje cells in Crus I/II of the cerebellum modulates gamma and theta coherence during whisking behavior (Lindeman, Hong, Kros, Mejias, et al., 2021).

Our lab sought to build upon these findings within the context of mounting evidence that the cerebellum also plays a functional role in non-motor tasks (see Buckner (2013) for a review). Recording from head-fixed mice, we found that Purkinje cell spike activity in the right lobulus simplex (LS) and Crus I stored information about the phases of LFP activity across multiple frequency bands in the prelimbic area and dorsal hippocampus, as well as the phase differences between these structures (McAfee, Y. Liu, Sillitoe, and D. H. Heck, 2019). LFP activity was monitored from these two structures because they are known to oscillate coherently during a spatial working memory task (Bahner, Demanuele, Schweiger, Gerchen, et al., 2015; Benchenane, Tiesinga, and Battaglia, 2011; Gordon, 2011; M. W. Jones and Wilson, 2005; Spellman, Rigotti, Ahmari, Fusi, et al., 2015; Yamamoto, Suh, Takeuchi, and Tonegawa, 2014), and cerebellar spike activity was recorded from in LS and Crus I due to the involvement of both areas in working memory (Ashida, Cerminara, R. J. Edwards, Apps, et al., 2019). An additional recent study from our group shows that optogenetic stimulation of Purkinje cells in the LS leads to increased prefrontal-hippocampal broadband coherence and altered spatial working memory performance (Y. Liu, McAfee, Van Der Heijden, Dhamala, et al., 2022). For an extended discussion on this topic, see Chapter 3.

1.4 Project Overview

The focus of the remaining chapters will be on describing the various roles the cerebellum can have on modulating oscillations at the neuronal and behavioral level. The next chapter starts with a review of literature describing the role that respiration has on modulating brain activity, followed by experimental evidence that the cerebellar cortex is required for normal breathing rhythmicity. Chapter 3 expands on the recently published work that the cerebellum modulates the coherence between the hippocampus and prelimbic area during spatial working memory and evaluates the functional connectivity between these structures while the animal is at rest. Chapter 4 further dissects this circuit and evaluates the phase amplitude coupling, another mechanism for neuronal communication via oscillatory activity, within and between these structures. Finally, I will draw conclusions from this work in Chapter 5 and discuss various ways to build upon this work.

Chapter 2

The Cerebellum as a Coordinator of Respiratory Rhythms¹

The influence of respiration on perception, cognition, and affect is relatively well-documented. For example, it is widely acknowledged that the conscious control of respiration affects heart rate variability and blood pressure, which in turn leads to changes in brain activity (Rau, Pauli, Brody, Elbert, et al., 1993), stress reduction, and the regulation of emotional and cognitive processes (Arch and Craske, 2006; Grossman and Christensen, 2008; Paul, Elam, and Verhulst, 2007). These findings suggest that the exchange of oxygen for carbon dioxide, the key function of respiration, is one route of influence of respiration on brain activity, cognition, and affect. However, recent studies in animals and humans have shown that respiration influences rhythmic brain activity in multiple frequency bands and possibly across all brain areas and - at the behavioral level - sensory, affective, and cognitive functions via respiration-locked neuronal activity driven by two major sources. Evidence suggests that this influence is primarily driven by respiration-related sensory inputs and inputs from brain stem pattern generators to subcortical structures. The observable consequence of this influence is a rhythmic modulation of brain activity at the frequency of the breath and a modulation of power of higher frequency oscillations, including gamma band oscillations, which are widely recognized for their association with cognitive processes (D. H. Heck, McAfee, Y. Liu, Babajani-Feremi, et al., 2016; J. Ito, Roy, Y. Liu, Cao, et al., 2014).

Neuronal oscillations occur in a variety of frequencies and show dynamic patterns of phase synchronization, or coherence, between different brain areas. Dynamic patterns of synchronization are implicated in affective and cognitive brain functions whereas atypical oscillation and coherence patterns are associated with affective, neurodevelopmental, and cognitive disorders. Here we review the rapidly growing literature linking respiration to brain activity and function. We discuss whether and how these new findings might inform our understanding of the role of respiration in affective disorders, such as panic attacks, or

¹Portions of chapter (from the beginning through 2.2) from previously published article; reprinted from final submission with permission from Elsevier B.V. Detlef H. Heck, Brittany L. Correia, Mia B. Fox, Yu Liu, et al. (2022). "Recent insights into respiratory modulation of brain activity offer new perspectives on cognition and emotion". In: *Biological Psychology* 170. Section: 108316. ISSN: 03010511. DOI: [10.1016/j.biopsycho.2022.108316](https://doi.org/10.1016/j.biopsycho.2022.108316).

neurodevelopmental disorders affecting social and cognitive skills such as autism spectrum disorders (ASD). We also review literature on cognitive deficits in chronic obstructive pulmonary disease (COPD), discuss whether those findings support a possible causal link between respiratory and cognitive deficits, and consider the difference between nasal and oral breathing in the context of clarifying the link between respiration and brain activity and function.

We will also consider the possible influence of respiration on the brain's functional connectome and review relevant literature. The functional connectome is described in terms of temporal correlation of activity between structures, indicating functional connectivity independent of the presence of anatomical connections (A. M. Aertsen and Gerstein, 1985; D. J. Kim, Bolbecker, Howell, Rass, et al., 2013). Respiration-locked activity from the olfactory bulb and likely other sensory inputs provide a rhythmic stimulus that drives neuronal oscillations in many brain areas. Artificial brain stimulation has been shown to reorganize the brain's functional connectome (Huang, Hajnal, Entz, Fabo, et al., 2019), suggesting that brain stimulation by respiration-locked sensory inputs might influence the functional connectome.

2.1 Respiration, Brain Activity, and Cognition

Since the first report of respiratory modulation of delta and gamma oscillations in a non-olfactory part of the mouse neocortex (J. Ito, Roy, Y. Liu, Cao, et al., 2014), a rapidly growing number of publications confirmed the initial findings in both animals and humans. Studies in humans revealed that, as a functional consequence of respiratory modulation of brain activity, cognitive and affective functions are modulated by the respiratory rhythm (Arshamian, Iravani, Majid, and Lundstrom, 2018; Grund, Al, Pabst, Dabbagh, et al., 2022; Johannknecht and Kayser, 2022; Nakamura, Fukunaga, and Oku, 2018; Perl, Ravia, Robinson, Eisen, et al., 2019; Zelano, Jiang, Zhou, Arora, et al., 2016); for a recent review see D. H. Heck, Kozma, and Kay (2019).

In an important study by Zelano, Jiang, Zhou, Arora, et al. (2016), participants were exposed to photographs of faces expressing either fear or surprise for a brief duration (100 ms). Participants detected fearful faces more quickly during nasal inspiration than expiration. Moreover, the respiratory phase also appeared to have an effect on retrieval accuracy. Participants were presented with 180 pictures of different everyday objects. In a memory retrieval session, participants were presented pictures from the original set plus pictures they had not seen before. Results showed that retrieval accuracy was significantly higher for images presented during the inspiration phase in the retrieval session. It is important to highlight that nasal respiration and hence the activation of the olfactory bulb played a special role in this study. When participants in the Zelano study were breathing through the mouth, reaction times to both types of faces increased significantly, but there was no longer a difference in detection time between inhalation and exhalation. In the second experiment, respiratory modulation of memory only occurred when participants

were breathing through the nose. These results are consistent with the original findings by J. Ito, Roy, Y. Liu, Cao, et al. (2014), which showed that respiration, via sensory inputs from the olfactory bulb, modulates neuronal oscillations in the delta and gamma frequency bands in the neocortex of awake mice. The authors carefully dissected the role of the olfactory bulb and highlighted respiration-locked delta oscillations in the whisker barrel cortex (an area of the neocortex not involved in olfactory processing). In the same area, the authors showed that the power of gamma oscillations was modulated in phase with respiration, highlighting that both respiration-locked delta oscillations and respiration-locked power modulation of gamma oscillations required an intact olfactory bulb (J. Ito, Roy, Y. Liu, Cao, et al., 2014). In turn, when the olfactory bulb was stimulated electrically with a rhythmically applied current, cortical rhythms were entrained to the stimulus rhythm applied to the bulb (J. Ito, Roy, Y. Liu, Cao, et al., 2014).

More recent studies provide additional evidence for respiratory modulation of brain function. Grund, Al, Pabst, Dabbagh, et al. (2022) investigated the combined influence of heartbeat and the breathing cycle on conscious sensory perception in humans by asking participants to report perceiving a near-threshold tactile stimulus of the index finger. The detection of near-threshold stimuli was more likely during the diastolic than systolic period of the heartbeat. Analysis of the respiratory cycle revealed that correctly detected stimuli closely clustered in time around inspiration onset, a finding consistent with the suggestion that inspiration onset or possibly the transition from expiration to inspiration is tuning the sensory system to optimize the processing of incoming information (Perl, Ravia, Robinson, Eisen, et al., 2019).

Active alignment of respiration to a task context was also observed by Johannknecht and Kayser (2022), who subjected participants to five different sensory detection and discrimination tasks and a short-term memory tasks. The analysis of task performance in relation to the respiratory cycle showed that participants tended to align their respiratory cycle to the timing of stimuli and their own response times. At the same time, the analysis of reaction times and response accuracy showed that reaction times were significantly modulated with the respiratory cycle, while there was no change in response accuracy.

Providing a potential neuronal mechanism underlying the influence of respiration on memory (D. H. Heck, Kozma, and Kay, 2019; Zelano, Jiang, Zhou, Arora, et al., 2016), a study in mice showed that hippocampal sharp wave ripples, a brief high-frequency oscillation characteristic for the hippocampus, are phase locked to respiration (Y. Liu, McAfee, and D. H. Heck, 2017). Sharp wave ripples are believed to be crucial for memory consolidation and recall (Buzsaki, 2015), a view that is supported by several studies showing a critical involvement of sharp wave ripples in memory consolidation and retrieval in mice (Malvache, Reichinnek, Villette, Haimerl, et al., 2016; Nicole, Hadzibegovic, Gajda, Bontempi, et al., 2016; Ven, Trouche, McNamara, Allen, et al., 2016), rats (Jadhav, Kemere, German, and Frank, 2012; Maingret, Girardeau, Todorova, Goutierre, et al., 2016; Papale, Zielinski, Frank, Jadhav, et al., 2016; Pfeiffer and Foster, 2015; A. C. Singer, Carr, Karlsson,

and Frank, 2013), and non-human primates (Leonard and Hoffman, 2017; Logothetis, Eschenko, Murayama, Augath, et al., 2012; Ramirez-Villegas, Logothetis, and Besserve, 2015). For an in-depth review of the link between respiration and memory see D. H. Heck, Kozma, and Kay (2019).

A recent fMRI study investigated whether the reduction of “default mode network” activity observed during performance of a word memory task (Greicius, Supekar, Menon, and Dougherty, 2009) may be linked to stimulus-induced changes in respiratory behavior (Huijbers, Pennartz, Beldzik, Domagalik, et al., 2014). Focusing on the relationship between changes in respiration and stimulus presentation, the authors calculated the average stimulus-aligned respiratory signal measured with an MRI compatible air-filled belt around the waist. Analysis of a stimulus-aligned average of the respiratory signal revealed that presentations of word stimuli were followed by a trough at 2 s post-stimulus and a peak at 4 s, indicating a stimulus triggered alignment of respiration patterns. We are using the descriptors “trough” and “peak” here because the authors do not specify whether troughs and peaks correspond to exhale or inhale. A subsequent analysis of respiratory phase aligned to stimulus presentation confirms that respiratory phase is locked to stimulus presentation. In addition, the authors show that the post-stimulus respiratory trough-peak modulation and the respiratory phase locking were significantly higher for correctly remembered words compared to forgotten words. The authors then asked participants to perform the task while holding their breath for 20 s during the presentation of word stimuli. Comparison with the control or “breathing” condition showed that a memory task related silencing of the default mode network activity only occurred during the control condition with participants allowed to breathe. These findings suggest a link between the amplitude and phase of respiratory movements in response to an external stimulus and successful cognitive performance as well as default mode network activity. The authors take their findings to “indicate a region-specific interaction between respiration and the fMRI signal associated with successful task performance” (Huijbers, Pennartz, Beldzik, Domagalik, et al., 2014).

Nakamura and colleagues (Nakamura, Fukunaga, and Oku, 2018) investigated the link between cognitive functioning and phase transition during a retrieval process, showing that phase transition in the respiratory cycle can modulate cognitive performance. In a delayed visual recognition task, a cue was presented in respiratory phase-locked (phased) or regularly paced (non-phased) presentation paradigms. When the retrieval process encompassed the expiratory-to-inspiratory transition, participants performing the task in the phase-locked presentation condition exhibited increased response time and reduced accuracy. However, when the retrieval process encompassed the inspiratory-to-expiratory transition, there were no significant changes in response time or accuracy.

Oral and nasal breathing do not always display the same patterns of influence on cognitive function. In a recent study by Perl, Ravia, Robinson, Eisen, et al. (2019), four different cognitive tests were used to study respiratory modulation of cognitive performance. While three of these turned out to be dependent on nasal breathing, a lexical task was not.

Nevertheless, nasal breathing seems to play a special role in human cognitive function. Arshamian, Iravani, Majid, and Lundstrom (2018) conducted a study investigating a possible influence of long-term breathing patterns on cognition function, using olfactory memory as a test. Specifically, the team asked whether long-term breathing (for one hour) either exclusively through the mouth or nose would influence memory consolidation, i.e. the process of transferring memory content from short-term to long-term storage. Healthy adult participants were asked to memorize 12 odors, followed by an hour of resting passively without sleeping (consolidation phase) during which they either breathed through their nose or mouth. Participants were then presented with a sequence of 24 odors, consisting of the 12 familiar and 12 new odors and asked to identify the familiar ones. The results showed that odor recognition memory was significantly increased after nasal respiration during the consolidation phase, compared with oral respiration. These findings provide the first experimental evidence that long-term respiratory behavior, in this case mouth vs. nose breathing, may affect cognitive function. However, since the paradigm used olfactory memory, the memory forming pathway and the pathway conveying respiratory modulation of brain activity were the same. It remains to be seen whether similar results would be obtained if the memory task is based on a non-olfactory sensory modality.

2.2 Neuronal Mechanisms of Respiratory Modulation of Brain Activity

The studies discussed thus far provide support for the idea that respiration has a direct influence on perceptual and cognitive processes, most likely via sensory inputs that are phase-locked to breathing. Experimental evidence from animal studies identified respiration-locked activity in the olfactory bulb as a main neuronal driving force for brain-breath coupling (J. Ito, Roy, Y. Liu, Cao, et al., 2014; Y. Liu, McAfee, and D. H. Heck, 2017). In humans the difference between oral and nasal breathing on cognitive processing supports the notion that olfactory bulb activity plays a crucial role in the coupling of brain activity and function to the breath (Arshamian, Iravani, Majid, and Lundstrom, 2018; Perl, Ravia, Robinson, Eisen, et al., 2019; Zelano, Jiang, Zhou, Arora, et al., 2016). Provided that the gas-exchange functions of nasal and oral respiration are likely to be similar, the current assumption is that the different effects of nasal and oral breathing on cognitive functions and brain activity are linked to respiration-locked sensory inputs. However, strengthening the case for a causal influence of respiratory activity on cognition would benefit from identifying the underlying mechanism responsible for the influence. This can be accomplished through a closer examination of the neocortical, oscillatory activity involved in cognition.

Local field potential (LFP) oscillations reflect the synaptic input to the area of observation (Buzsaki, Anastassiou, and Koch, 2012). This rhythmically modulated synaptic activity influences the output of the receiving local neurons in the form of the timing and frequency

of action potentials (also called “spikes”), which are transient electrical signals that carry information between connected neurons (Buzsaki, Anastassiou, and Koch, 2012).

Simultaneous measurements of LFPs and action potentials in the cortex showed that action potentials are synchronized to oscillations in the LFP signal (Eckhorn and Obermueller, 1993; Gray, Konig, Engel, and W. Singer, 1989; Jacobs, M. J. Kahana, Ekstrom, and Fried, 2007; Murthy and Fetz, 1996; Nase, W. Singer, Monyer, and Engel, 2003). Spikes typically coincide with the negative phase of LFP oscillations, which correspond to the synaptic influx of positively charged ions into the dendrite of a cell. The negative phase generally reflects increased excitatory synaptic input and thus increased probability of spike activity in the postsynaptic cells (Buzsaki, Anastassiou, and Koch, 2012). Oscillations of LFPs temporally organize spike probability or spike synchrony between different parts of the brain, as a means to enhance neuronal communication between task-related parts of the brain for the duration of the task performance (Fries, 2005; Fries, 2015; Womelsdorf, Schoffelen, Oostenveld, W. Singer, et al., 2007). Neural oscillations in the LFP signal are thus functionally highly relevant as they directly influence neuronal communication. Investigating the influence of respiration on neuronal oscillations thus helps understand the link between respiratory rhythm and neuronal communication in the brain (D. H. Heck, McAfee, Y. Liu, Babajani-Feremi, et al., 2016; Kluger, Balestrieri, Busch, and Gross, 2021; Rojas-Libano, Wimmer Del Solar, Aguilar-Rivera, Montefusco-Siegmund, et al., 2018).

The temporal organization of action potentials, especially synchrony in spike activity in response to synaptic inputs has been implicated in cognitive processing, which requires the transmission of information through the synchronous firing of action potentials in large groups of neurons (Diesmann, Gewaltig, and A. Aertsen, 1999; Uhlhaas, Pipa, Lima, Melloni, et al., 2009). There is experimental evidence for a link between cognitive functions and synchronized spike activity. In rats, selectively preventing neurons in a brain area from generating spikes by using locally applied toxin results in the elimination of the function of the relevant brain area (e.g., McLaughlin and See (2003) and Wesierska, Dockery, and Fenton (2005)). In primates, prefrontal cortical neurons synchronize their spike firing during the performance of a task requiring a context-dependent decision to either respond to a signal with a movement (“go” condition) or to ignore the signal (“no-go” condition) (Vaadia, Haalman, Abeles, Bergman, et al., 1995).

Importantly for our purposes, oscillatory neocortical activity in the gamma (30–100 Hz) frequency range is tightly linked to the performance of specific cognitive tasks like decision making (Beshel, N. Kopell, and Kay, 2007; Siegel, Engel, and Donner, 2011), problem solving (Sheth, Sandkuhler, and Bhattacharya, 2009), memory formation (Osipova, Takashima, Oostenveld, Fernandez, et al., 2006; Sederberg, Schulze-Bonhage, Madsen, Bromfield, et al., 2007; Vugt, Schulze-Bonhage, Litt, Brandt, et al., 2010) and language processing (Babajani-Feremi, Rezaie, Narayana, Choudhri, et al., 2014; Crone, Hao, Hart, Boatman, et al., 2001; Towle, H. A. Yoon, Castelle, Edgar, et al., 2008). Correspondingly, deficits in the power or coherence of gamma oscillations have been linked to schizophrenia

(e.g., Furth, Mastwal, K. H. Wang, Buonanno, et al. (2013)), ASD (e.g., Brown, Gruber, Boucher, Rippon, et al. (2005)), and Alzheimer's disease (Basar, Emek-Savas, Guntekin, and Yener, 2016; Klein, Donoso, Kempner, D. Schmitz, et al., 2016; J. Wang, Fang, X. Wang, Yang, et al., 2017).

In mice, respiration directly drives delta/theta rhythms of cortical activity via sensory inputs from the olfactory bulb, but the power of gamma oscillations is also modulated with the respiratory phase (Biskamp, M. Bartos, and Sauer, 2017; J. Ito, Roy, Y. Liu, Cao, et al., 2014). These findings were confirmed in humans, with intracranial electroencephalogram (iEEG) recordings obtained from pharmaco-resistant epilepsy patients who received implants of subdural grid or intracranial depth electrodes (electrocorticogram) (Herrero, Khuvis, Yeagle, Cerf, et al., 2018; Zelano, Jiang, Zhou, Arora, et al., 2016). Zelano, Jiang, Zhou, Arora, et al. (2016) showed respiration-locked slow oscillations in the piriform cortex, hippocampus, and amygdala and that the power of delta, theta and beta oscillations in all three structures were modulated with the phase of respiration. Importantly, these respiratory modulations of neuronal oscillations were linked to nasal breathing and were not observed during oral breathing. Herrero, Khuvis, Yeagle, Cerf, et al. (2018) recorded iEEG activity in 30 cortical and limbic brain areas, including the three areas recorded by Zelano, Jiang, Zhou, Arora, et al. (2016), but also in several frontal and parietal cortical areas while patients were breathing exclusively through the nose. Respiration-locked iEEG activity was observed in all areas and, using an attention to breath task, the authors could show that the influence of respiration on brain activity increased with attention, reflected in increased breath iEEG coherence. Respiratory modulation of human brain activity can also be captured non-invasively, as recently shown by Kluger, Balestrieri, Busch, and Gross (2021), who used magnetoencephalography (MEG) to show that beta coherence in the sensorimotor cortex is modulated with the respiratory phase. In the same study, the authors also showed that conscious control of respiration reduced the average beta coherence in the sensorimotor cortex but left the respiration-locked modulation of beta power intact.

Overall, experiments in animals and humans show that respiration influences neuronal activity by driving neuronal oscillations that follow the respiratory rhythm and by modulating the power of higher frequency oscillations (including gamma), propelled by respiration-locked sensory input to the cortex from the olfactory system. While more research is needed to confirm this thesis, it is plausible that spike activity and synchrony are a key part of the neuronal mechanism that is responsible for respiratory influence on brain function. Moreover, the full story about the underlying mechanism will likely involve explaining how respiration modulates norepinephrine release.

The respiratory rhythm is generated by brainstem circuits, and brainstem projections carrying respiration-locked rhythmic spike activity have been shown to project to the thalamus. Yackle, L. A. Schwarz, Kam, Sorokin, et al. (2017) recently showed that the locus coeruleus (LC), which is the major source of norepinephrine in the mammalian brain (Aston-Jones and J. D. Cohen, 2005), receives direct inputs from the mouse preBötzinger complex

(preBötC), the primary breathing rhythm generator (Del Negro, Funk, and Feldman, 2018). Importantly, Yackle, L. A. Schwarz, Kam, Sorokin, et al. (2017) showed that the specific subpopulation of neurons in the preBötC that project to the LC regulate the balance between calm and aroused behaviors.

Taken together the above cited studies suggest that respiration rhythmically modulates LC neuronal activity and the excitability of LC neurons. This is of significance for our argument as a recent study by Zerbi and colleagues (Zerbi, Floriou-Servou, Markicevic, Vermeiren, et al., 2019) showed that the stimulation of LC results in norepinephrine release in the entire forebrain and powerfully changes the functional connectome, i.e. the spatiotemporal pattern of synchronous activity between forebrain structures. Neurocomputational work has further demonstrated that baseline modulation of LC output regulates overall neural excitability or gain, dynamically modulating the overall topology of the functional connectome (Aston-Jones and J. D. Cohen, 2005; Eldar, J. D. Cohen, and Niv, 2013; Warren, Eldar, Brink, Tona, et al., 2016). The notion that respiration might modulate cortical excitability, possibly via the LC activation received experimental support from a recent study from Kluger, Balestrieri, Busch, and Gross (2021), in which the authors employed MEG to measure cortical activity during a near-threshold sensory detection task while also monitoring respiration. This study found that respiration modulated the power of posterior alpha oscillations, which is considered a reliable indicator of cortical excitability. Thus, the projections from the preBötC to the LC as described by Yackle, L. A. Schwarz, Kam, Sorokin, et al. (2017) might represent a key neuronal substrate for respiratory modulation of cortical excitability and the functional connectome.

2.3 Loss of Cerebellar Function Selectively Affects Rhythmicity of Eupneic Breathing

2.3.1 Methods

Animals

This experiment used a total of 67 adult mice (26 female) aged 2-3 or 5-7 months. We compared two groups of mice: those with cerebellar ataxia [mutant (MU): L7Cre;VGAT^{flox/flox}, n=31] and their healthy littermates [control (CT): VGAT^{flox/flox}, n=36] that served as controls. Cerebellar ataxia in the MU animals stemmed from a selective knockout of VGAT (vesicular GABA transporter), a protein essential for vesicle docking and GABAergic transmission, in Purkinje cells (White, Arancillo, Stay, George-Jones, et al., 2014; Chaudhry, Reimer, Bellocchio, Danbolt, et al., 1998). These mice exhibit severe motor impairments and altered organization of ZebrinII patterning throughout the cerebellum (White, Arancillo, Stay, George-Jones, et al., 2014). The experimental protocols were approved by the Institutional Animal Care and Use Committee of The University of Tennessee Health Science Center.

Measurements of Respiratory Behavior

Respiratory data was collected for 30 min by placing mice in a plethysmograph made of a small glass container where mice could move freely (**Figure 2.1**). A constant flow (1 l/min) of fresh air was directed into the chamber through an opening in the lid with a second opening in the lid serving as an outlet. While the mice were in the chamber, a box was placed over the chamber to block direct light.

Inspiration movements cause the air pressure in the plethysmograph chamber to slightly increase. These pressure changes were measured with a pressure transducer (Validyne Engineering, USA). The voltage output of the transducer reflected pressure increase as a decrease in voltage. Therefore the minima of voltage troughs correspond to the end-of-inhale movements. Voltage data were digitized at 2 kHz using an analogue to digital converter (CED 1401, Cambridge Electronic Design, UK) and stored for off-line analysis using custom scripts in Matlab (Matlab R2019b). The minima of each voltage trough in the raw data were detected and the times of their occurrences were used as temporal markers of end-of-inspiration events. All data analysis was based on the resulting time series of end-of-inspiration markers.

Further analysis of different aspects of the respiratory rhythm, such as mean respiratory interval duration, coefficient of variation (CV), and intrinsic variability (CV2) were based on the end-of-inspiration times. The CV2 provides a measure of the similarity of two adjacent inter-inspiration intervals. We evaluated the CV2 of each respiratory sequence as the average of all CV2 values calculated for each interval pair, as described in (Holt, Softky, Koch, and Douglas, 1996). All further group analyses are based on the average CV2 value.

Artificial Modulation of Respiratory Interval Sequences

To mimic a proposed cerebellar-dependent extension of the duration of individual respiratory intervals, I artificially increased the duration of 10% of the intervals in the respiration sequences measured in MU mice. Specifically, in each MU respiratory sequence I increased the duration of every tenth respiratory interval by 50% of its original duration, which translated to an average increase of around 75 ms.

I determined these parameters by creating a custom simulation program in Matlab that manipulated the respiratory intervals of mutant animals at various frequencies by various lengths, then performed a 2-sample t-test on the resultant “manipulated mutant” data’s CV, CV2, and mean respiratory interval the respective parameters of the control mice. The goal of this exercise was to determine which manipulation parameters, if any, would result in the MU CV2 to become statistically indistinguishable from CT CV2 while staying within a plausible physiological range.

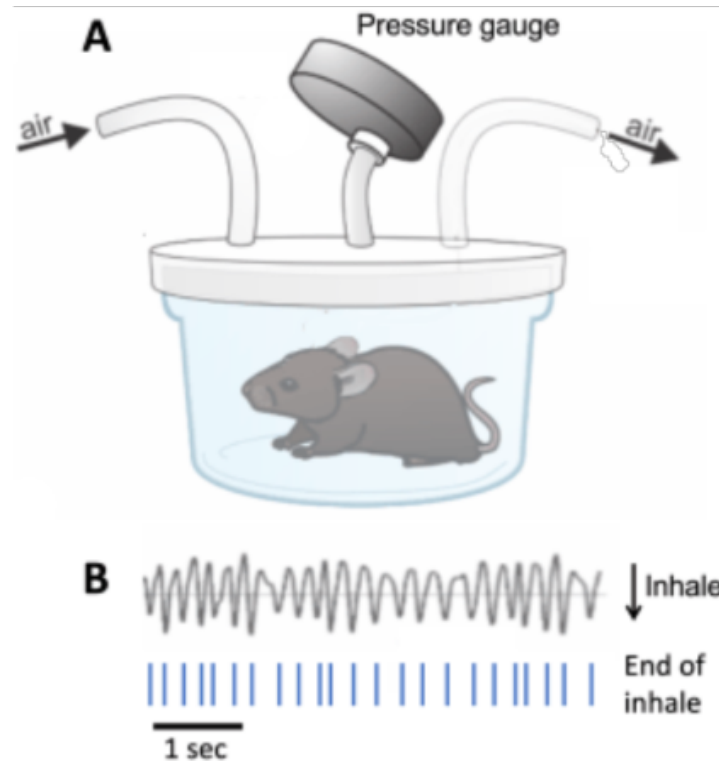


Figure 2.1: Mouse respiratory behavior was measured using a custom-made plethysmograph chamber. A) Pressure inside the chamber was measured with a pressure transducer (Validyne Engineering, USA). Inhalation movements increase the pressure inside the chamber, resulting in decreases in voltage. **B)** Raw voltage output from the pressure transducer reflecting respiration-related pressure changes. Inhalation-related increases in pressure are reflected as decreases in voltage. Troughs in the voltage signal reflect the end of inhale times, which were marked and used as temporal alignments for further analysis of the respiratory rhythm. Reprinted from final submission with open access permission. Y. Liu, S. Qi, F. Thomas, B. L. Correia, et al. (Apr. 13, 2020). "Loss of cerebellar function selectively affects intrinsic rhythmicity of eupneic breathing". In: *Biol Open* 9.4. Edition: 20200413. ISSN: 2046-6390 (Print) 2046-6390 (Linking). DOI: [10.1242/bio.048785](https://doi.org/10.1242/bio.048785). URL: <https://www.ncbi.nlm.nih.gov/pubmed/32086251>

2.3.2 Results

To measure spontaneous respiratory behavior, mice were placed in a plethysmograph chamber where they could move freely (**Figure 2.1**). Spontaneous respiration was monitored for 30 minutes and compared between MU mice and their CT littermates. Male and female mice of both genotypes were divided into two age groups, 2–3 or 5–7 months old, corresponding approximately to the transition from adolescents/young adults to mature adults in human development (Flurkey and Harrison, 2007).

The CV measures variability based on the distribution of intervals across the entire observation time. Brief but reoccurring changes in rhythmicity cause no change in the CV, so long as the overall interval distribution remains the same or similar. In 1996, Holt et al. introduced a novel measure of variability, the CV2, specifically designed to detect brief, reoccurring changes in rhythmicity, which they called ‘intrinsic rhythmicity’ (Holt, Softky, Koch, and Douglas, 1996).

The overall variability of the respiratory rhythm, quantified as the coefficient of variation of the inter-inhalation interval distribution ($CV = \text{standard deviation of interval distribution} / \text{mean of interval duration}$) was, like the mean interval duration, dependent on age ($p < 0.001$, with lower values for younger mice), but not on sex ($p = 0.70$). Also in analogy to the mean interval duration above, we could not find a difference between MU mice and their CT littermates with respect to CV ($p = 0.95$, adjusted for age).

Comparison of the CV2 of respiratory behavior in CT and MU mice revealed a lower CV2 in MU mice compared to the CT littermates ($p < 0.001$), when adjusting for age ($p < 0.001$) and sex ($p = 0.048$, **Figure 2.2**). While the CV2 increased with age in the control mice ($p < 0.001$), it did not change substantially with age in MU mice ($p = 0.16$, **Figure 2.2**). When the two genotypes were combined, the interaction effect between age and genotype was not significant ($p = 0.27$); something that would be expected if the age/CV2 relationship holds for only one of the two genotypes.

The reduced CV2 in MU mice suggests that the difference in the respiratory sequences in MU and CT mice is based on the temporal modulation of a subset of individual respiratory intervals. In mutant mice, those modulations seem to be less pronounced, resulting in a smaller CV2 value, reflecting reduced intrinsic variability. To address our hypothesis that the difference in CV2 indeed could be explained by modulating the duration of a subset of respiratory intervals, we mimicked in our collected data an extension of the duration of every tenth interval in the respiratory sequence of MU mice by 50%, corresponding to an average of about 75 ms (**Figure 2.3**). By so doing, rendered the CV2 values of the respiratory sequence of MU mice comparable to that of CT mice.

2.3.3 Discussion

While the cerebellum has previously been shown as a part of the neural circuitry involved in strained breathing, such as during hypercapnia or hypoxia (P. M. Macey, Woo, K. E.

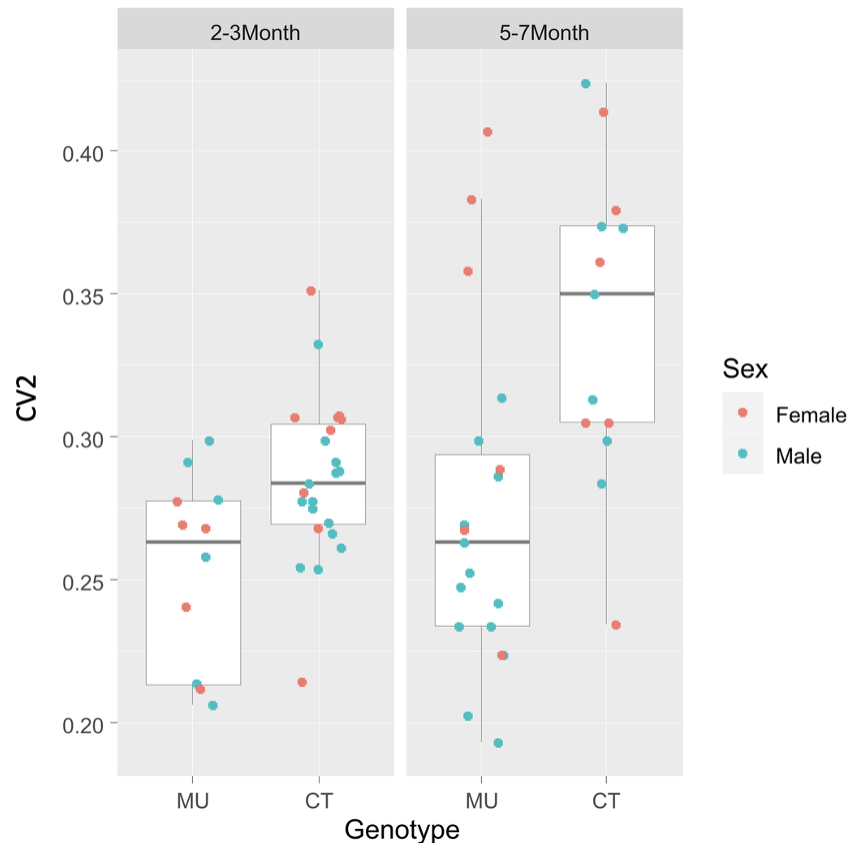


Figure 2.2: Comparison of the CV2 (intrinsic rhythmicity) of respiratory behavior. The CV2 is lower in the MU mice compared to their CT littermates (left versus right box in each panel; $p < 0.001$) when adjusting for age ($p < 0.001$) and sex ($p = 0.048$). In addition, the CV2 was significantly higher in older compared to younger CT mice ($p < 0.001$ in the CT subgroup), but possibly remained unchanged across age in the MU mice ($p = 0.16$ in the MU subgroup). However, in the combined data, the interaction effect between age and genotype is not statistically significant ($p = 0.19$); something that would be expected if the age-CV2 relationship holds for only one of the two genotypes. Reprinted from final submission with open access permission. Y. Liu, S. Qi, F. Thomas, B. L. Correia, et al. (Apr. 13, 2020). “Loss of cerebellar function selectively affects intrinsic rhythmicity of eupneic breathing”. In: *Biol Open* 9.4. Edition: 20200413. ISSN: 2046-6390 (Print) 2046-6390 (Linking). DOI: [10.1242/bio.048785](https://doi.org/10.1242/bio.048785). URL: <https://www.ncbi.nlm.nih.gov/pubmed/32086251>

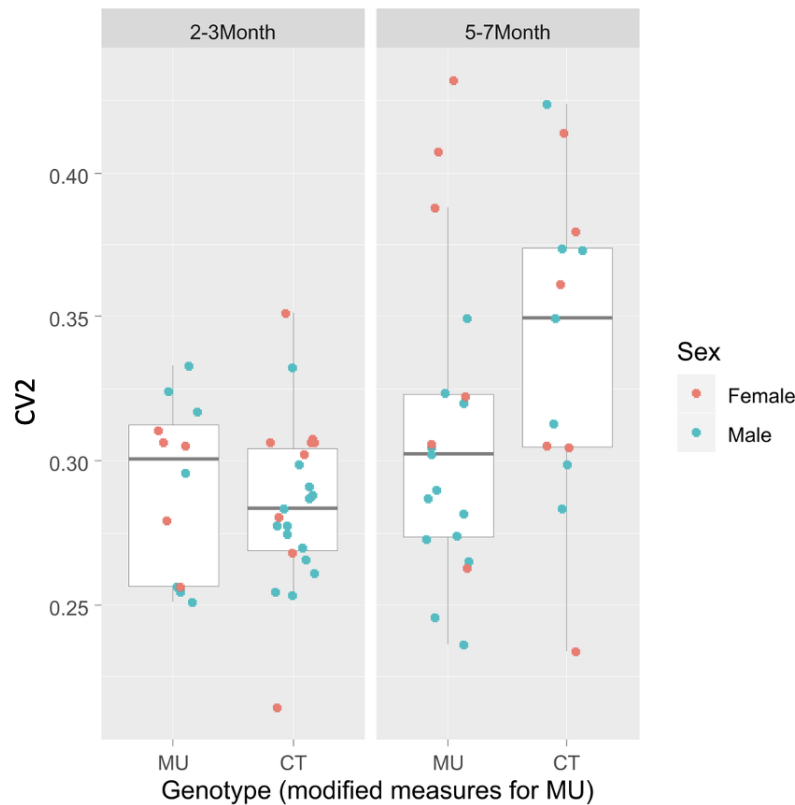


Figure 2.3: Prolonging the duration of a subset of respiratory intervals to mimic breathing-swallowing coordination in MU mice increased the CV2 to CT values. Using the same analytical approach as in the original respiratory sequence measured in MU mice, one would now conclude that the genotype is not statistically significant ($p = 0.31$; age remains significant with $p < 0.001$). The respiratory sequences of MU mice were modified *in silico* by extending the duration of every tenth interval by 50%, as described in the Methods section. Reprinted from final submission with open access permission. Y. Liu, S. Qi, F. Thomas, B. L. Correia, et al. (Apr. 13, 2020). "Loss of cerebellar function selectively affects intrinsic rhythmicity of eupneic breathing". In: *Biol Open* 9.4. Edition: 20200413. ISSN: 2046-6390 (Print) 2046-6390 (Linking). DOI: [10.1242/bio.048785](https://doi.org/10.1242/bio.048785). URL: <https://www.ncbi.nlm.nih.gov/pubmed/32086251>

Macey, Keens, et al., 2005; Parsons, Egan, Liotti, Brannan, et al., 2001), no studies have thus far shown the cerebellum's involvement in spontaneous or "normal" breathing (Ebert, Hefter, Dohle, and Freund, 1995; Moruzzi, 1940; Heijden and Zoghbi, 2018; Xu and Frazier, 2002; Xu, Owen, and Frazier, 1995). This study supports previous findings that a loss of cerebellar function does not affect the average respiratory rate or the CV of eupneic respiration in mice. However, analysis of the CV2 shows that MU mice have significantly lower intrinsic variability than their littermate controls. CV2 analysis is a powerful way to detect this phenomenon because it is sensitive to brief changes in rhythmicity, such as regular or irregular repeated changes in interval length (Holt, Softky, Koch, and Douglas, 1996). These findings suggest that the loss of cerebellar output corresponds with a loss of modulation of certain respiratory intervals.

The biological purpose of cerebellar modulation of select respiratory intervals is unknown. However, a possible function could be the proper temporal coordination of breathing with swallowing movements (Hardemark Cedborg, Sundman, Boden, Hedstrom, et al., 2009). Inappropriate temporal coordination of swallowing with respiration can lead to dysphagia, increasing the risk of aspiration pneumonia (Yagi, Oku, Nagami, Yamagata, et al., 2017). Dysphagia is a common symptom in patients with cerebellar disease (Ramio-Torrentia, Gomez, and Genis, 2006) and a potential anatomical substrate for a cerebellar coordination of brain stem pattern generators controlling breathing and other orofacial movements exists in form of extensive reciprocal connections between the cerebellum and brain stem (Asanuma, Thach, and E. G. Jones, 1983; Teune, Burg, Moer, Voogd, et al., 2000; Whiteside and Snider, 1953). Coordinating breathing with swallowing is essentially a timing problem, which fits well with the widely accepted role of the cerebellum in timing and temporal coordination of sensorimotor activity (Braitenberg, 1961; Ivry, Spencer, Zelaznik, and Diedrichsen, 2002; Mauk and Buonomano, 2004).

While our findings would be consistent with a proposed cerebellar role in the coordination of breathing with orofacial movements (Bryant, Boughter, Gong, LeDoux, et al., 2010; Lu, Cao, Tokita, D. H. Heck, et al., 2013), additional experiments are needed to fully address this. For example, additional recordings of both respiration and swallowing using a larger sample of animals would be beneficial. Similarly, to address the observed age-related differences in CV2, collection of longitudinal respiration data could elucidate how this measure changes over time.

Chapter 3

Loss of Purkinje Cell Neurotransmission Affects Cerebellar-Prefrontal but Not Cerebellar-Hippocampal Functional Connectivity

3.1 Introduction

The cerebellum and its reciprocal connections with the cerebral cortex have traditionally been viewed in the context of temporal coordination of sensorimotor control (Braitenberg, 1967; Braitenberg, D. Heck, and Sultan, 1997; D'Angelo and De Zeeuw, 2009; De Zeeuw and Yeo, 2005; Ivry and Keele, 1989; Ivry, Spencer, Zelaznik, and Diedrichsen, 2002; Johansson, Jirenhed, Rasmussen, Zucca, et al., 2014; Onuki, Van Someren, De Zeeuw, and Van der Werf, 2015; Perrett, Ruiz, and Mauk, 1993; Person and Raman, 2012; Salman, 2002; Spoelstra, Schweighofer, and Arbib, 2000; Timmann, Watts, and Hore, 1999). However, in the past several years, there has been an increased interest in understanding the role of the cerebellum in cognitive functions (Buckner, 2013; M. Ito, 2008; Strick, Dum, and Fiez, 2009), including spatial working memory (SWM) (Courtney, Ungerleider, Keil, and Haxby, 1996; Goodlett, Hamre, and West, 1992; Y. Liu, McAfee, Van Der Heijden, Dhamala, et al., 2022; Molinari, Grammaldo, and Petrosini, 1997; Tomlinson, Davis, and Bracewell, 2013; Tomlinson, Davis, Morgan, and Bracewell, 2014). Anatomical and imaging studies provide evidence for connections between the cerebellum and neocortical areas essential for cognitive functions (Buckner, 2013; M. Ito, 2008; Strick, Dum, and Fiez, 2009) and cerebellar neuropathology has been implicated in cognitive disorders such as autism, schizophrenia, dementia and Alzheimer's disease (Andreasen and Pierson, 2008; E. B. Becker and Stoodley, 2013; Courchesne, 1997; Fatemi, Aldinger, Ashwood, Bauman, et al., 2012; Palmen, Engeland, Hof, and C. Schmitz, 2004; Picard, Amado, Mouchet-Mages, Olie, et al., 2008; Schmahmann, 2016). Thus, in order to progress towards a complete understanding of normal cognitive brain function and of the neuropathology of mental illnesses, it is essential to understand the neuronal mechanisms that comprise the cerebellar role in cognition.

3.1.1 SWM and the Cerebellum

SWM is a cognitive function readily tractable in mice that involves the ability to temporarily retain and manipulate spatial information in memory while maneuvering in the environment. This behavior requires the integrity of both the medial prefrontal cortex (mPFC) and the dorsal hippocampal CA1 (dCA1) (Gordon, 2011; Spellman, Rigotti, Ahmari, Fusi, et al., 2015), two structures which have indirect reciprocal connections with the cerebellum (Ikai, Takada, and Mizuno, 1994; Lisman and Grace, 2005; Middleton and Strick, 2001; Newman and Reza, 1979; Onuki, Van Someren, De Zeeuw, and Van der Werf, 2015; Rogers, Dickson, D. H. Heck, Goldowitz, et al., 2011; Strick, Dum, and Fiez, 2009; Watabe-Uchida, Zhu, Ogawa, Vamanrao, et al., 2012; Watson, N. Becker, Apps, and M. W. Jones, 2014; Yu and Krook-Magnuson, 2015). Normal SWM also requires an intact cerebellum (Courtney, Ungerleider, Keil, and Haxby, 1996; Goodlett, Hamre, and West, 1992; Y. Liu, McAfee, Van Der Heijden, Dhamala, et al., 2022; Molinari, Grammaldo, and Petrosini, 1997; Tomlinson, Davis, and Bracewell, 2013; Tomlinson, Davis, Morgan, and Bracewell, 2014) and imaging studies in humans have shown that various cerebellar sites show increased activity during working memory tasks (Awh, John Jonides, Edward E. Smith, Eric H. Schumacher, et al., 2016; Desmond, Gabrieli, Wagner, Ginier, et al., 1997; Fiez, Raife, Balota, J. P. Schwarz, et al., 1996; Grasby, Frith, Friston, Simpson, et al., 1994; Igloi, Doeller, Paradis, Benchenane, et al., 2015; J. Jonides, E. H. Schumacher, E. E. Smith, Lauber, et al., 1997; Paulesu, Frith, and Frackowiak, 1993). Cerebellar substructures implicated in SWM with the largest overlap across studies are the right anterior cerebellar hemisphere lobules VI and VII (Desmond, Gabrieli, Wagner, Ginier, et al., 1997; Igloi, Doeller, Paradis, Benchenane, et al., 2015), which corresponds to lobulus simplex (LS), Crus I/II in rodents (Apps and Hawkes, 2009). Additionally, preliminary data from our lab using a model of cerebellar ataxia (*L7 Cre; VGAT^{flox/flox}*) shows that ataxic mice have a significant deficit in SWM performance compared to their litter-mate controls as measured by rates of spontaneous alternation in a cross-maze task. In this model, release of GABA from Purkinje cell synapses is selectively suppressed, a manipulation that eliminates cerebellar cortical output to the deep cerebellar nuclei (White, Arancillo, Stay, George-Jones, et al., 2014).

Recent work from our lab has shown causal evidence that LS is involved in SWM. Optogenetic stimulation of LS significantly impairs SWM performance in a cross-maze task, and decreases mPFC-dCA1 coherence at moments of decision making (Y. Liu, McAfee, Van Der Heijden, Dhamala, et al., 2022). It is hypothesized that the cerebellum plays a critical role in controlling the functional connectivity between the mPFC and dCA1 during SWM decision-making by controlling the coherence of neuronal oscillations between the two structures. Within the framework of our hypothesis, loss of cerebellar control of mPFC-dCA1 coherence disrupts mPFC-dCA1 functional connectivity and causes SWM deficits.

3.1.2 Coherence and SWM

The mPFC and dorsal hippocampus are reciprocally connected via multisynaptic pathways (Barbas and Blatt, 1995; Conde, Maire-Lepoivre, Audinat, and Crepel, 1995; Hoover and Vertes, 2007; Rajasethupathy, Sankaran, Marshel, C. K. Kim, et al., 2015) and are both key structures for SWM in rodents (Lee and Kesner, 2003a; Lee and Kesner, 2003b; Spellman, Rigotti, Ahmari, Fusi, et al., 2015) and humans (Bahner, Demanuele, Schweiger, Gerchen, et al., 2015). Lesion studies in rodents have shown that SWM requires the integrity of both the mPFC and hippocampus (Churchwell and Kesner, 2011; Kesner and Churchwell, 2011; T. Yoon, Okada, Jung, and J. J. Kim, 2008). A prominent neuronal signature of their joint involvement in SWM in rodents is an increase in the coherence of theta and gamma oscillations between mPFC and hippocampus at the time of decision-making (Bahner, Demanuele, Schweiger, Gerchen, et al., 2015; Benchenane, Tiesinga, and Battaglia, 2011; Gordon, 2011; M. W. Jones and Wilson, 2005; Spellman, Rigotti, Ahmari, Fusi, et al., 2015; Yamamoto, Suh, Takeuchi, and Tonegawa, 2014). These oscillations have functional relevance as they often control spike timing (Benchenane, Tiesinga, and Battaglia, 2011), which is of critical importance and the basis for the “communication-through-coherence” hypothesis described below (Fries, 2005). These same experiments also showed that the increase in coherence is higher for correct than for incorrect choices (Gordon, 2011; M. W. Jones and Wilson, 2005; Spellman, Rigotti, Ahmari, Fusi, et al., 2015), suggesting that this decision-related coherence is critical to SWM decision-making (Spellman, Rigotti, Ahmari, Fusi, et al., 2015).

Coherence is a quantitative measure of the stability of the phase relationship or the phase-locking of two oscillations with similar frequencies. Coherence can take on values between 0 and 1, and is independent of oscillation power or amplitude. Two oscillations with a perfectly stable phase relationship over time would have a coherence of 1, irrespective of whether there is a phase delay or advance between the oscillations, as long as the delay is stable. Coherence is 0 if the phase relationship constantly varies over time.

In the nervous system, oscillations are a common occurrence in the local field potential (LFP), a population signal that largely reflects synaptic activity (Friston, Bastos, Pinotsis, and Litvak, 2015). LFP oscillations in two connected brain areas can transition in and out of coherence dependent on behavioral context (e.g. Spellman, Rigotti, Ahmari, Fusi, et al. (2015)). Temporary increases in coherence are interpreted as temporary increases in the functional connectivity between the two structures (Bastos, Vezoli, and Fries, 2015; Fries, 2015). In SWM tests, coherence between the mPFC and dCA1 increases for a few seconds, time-locked to the moment of decision-making (Benchenane, Tiesinga, and Battaglia, 2011; Gordon, 2011; M. W. Jones and Wilson, 2005; Spellman, Rigotti, Ahmari, Fusi, et al., 2015; Yamamoto, Suh, Takeuchi, and Tonegawa, 2014) and coherence magnitude differentiates between correct and incorrect decisions: coherence increases to higher values during correct compared to incorrect decisions (Gordon, 2011; M. W. Jones and Wilson, 2005; Spellman, Rigotti, Ahmari, Fusi, et al., 2015). Decision-related coherence increases between the mPFC

and dCA1 are considered crucial for normal SWM performance (Spellman, Rigotti, Ahmari, Fusi, et al., 2015).

Following the arguments of Fries and colleagues (Fries, 2005), we interpret the transient increase in coherence during SWM as a period of increased “functional connectivity” between two structures (Bastos, Vezoli, and Fries, 2015; Fries, 2005; Fries, 2015). Oscillations in the LFP reflect rhythmic fluctuations of synaptic input activity (Buzsaki, Anastassiou, and Koch, 2012; Friston, Bastos, Pinotsis, and Litvak, 2015). This translates to rhythmic fluctuations of neuronal excitability. Periods of increased excitability represent “windows of opportunity,” during which a neuron is more likely to respond to synaptic input from a connected structure by generating an action potential. Periods of high excitability typically correspond to the negative phase of LFP oscillations recorded at dendritic sites (Buzsaki, Anastassiou, and Koch, 2012; Gray, Konig, Engel, and W. Singer, 1989; Jacobs, M. J. Kahana, Ekstrom, and Fried, 2007; Murthy and Fetz, 1996).

Two connected structures can thus optimize their neuronal communication or “functional connectivity” if they align the phases of their oscillations such, that spikes arriving from one structure will arrive at the other structure during the negative phase of the oscillation, i.e. when excitability is highest. Fries called this mechanism “communication-through-coherence” (Fries, 2005). It allows structures to establish transient, task-dependent increases in functional connectivity, which end again when the task is completed (Bastos, Vezoli, and Fries, 2015; Fries, 2005). How the magnitude or the timing of coherence of oscillations between two brain structures is controlled remains unknown, but the cerebellum has been proposed a candidate to perform this function (McAfee, Y. Liu, Sillitoe, and D. H. Heck, 2021).

3.1.3 The Cerebellum and Coherence

The hypothesis described in McAfee, Y. Liu, Sillitoe, and D. H. Heck (2021) assigns the cerebellum the task of temporal coordination of neuronal communication between the mPFC and dCA1. Our hypothesis states that the cerebellum performs similar neuronal computations for sensorimotor and cognitive tasks, which would explain why the gross neuronal circuitry of the cerebellar cortex is largely homogeneous, irrespective of whether a particular area primarily connects to motor or non-motor areas of the neocortex. Recent evidence supporting the hypothesis that the cerebellum acts as a coordinator of communication by modulating the coherence of neuronal oscillations has shown that the cerebellum can influence SWM and modulate SWM decision-related increases in mPFC-dCA1 coherence (Y. Liu, McAfee, Van Der Heijden, Dhamala, et al., 2022). This phenomenon has also been observed in a more traditional sensorimotor context, where the cerebellum has been shown to modulate gamma coherence between the sensory and motor cortices during whisking behavior (Lindeman, Hong, Kros, Mejias, et al., 2021; Popa, Spolidoro, Proville, Guyon, et al., 2013).

Optical stimulation of Purkinje cells (PCs) in the LS leads to increased mPFC-dCA1 coherence in several frequency bands and the same stimulus applied during SWM decision making in freely moving mice significantly alters SWM performance (Y. Liu, McAfee, Van Der Heijden, Dhamala, et al., 2022). Additionally, PCs in LS and Crus I/II have been shown to preferentially respond to phase and phase differences of local field potential oscillations across multiple frequencies in the mPFC and dCA1 (McAfee, Y. Liu, Sillitoe, and D. H. Heck, 2019), providing additional support for the role of LS and Crus I in SWM circuitry. Taken together, these studies suggest that LS is one of the key cerebellar cortical areas involved in cerebellar modulation of mPFC-dCA1 coherence during SWM decision making behaviors. What is less clear, however, is what the functional connectivity of this circuit looks like during periods when it is not involved in SWM behaviors and how it would be affected by cerebellar dysfunction. Here, we are using the *L7 Cre; VGAT^{flox/flox}* mouse model of cerebellar ataxia (Figure 3.1A) and *in vivo* multi-site electrophysiology to test the hypothesis that output from the cerebellar cortex is required for normal oscillatory interactions between the cerebellum, mPFC, and dCA1.

3.2 Methods

3.2.1 Animals

A total of 13 adult mice were used in this study. *L7 Cre; VGAT^{flox/flox}* ($n = 7$) conditional mutant mice were compared to *VGAT^{flox/flox}* ($n = 6$) control litter-mates of either sex throughout the study. Mice were aged 4-5 months before experiments began. Mice were housed in a climate-controlled mouse colony at the University of Tennessee Health Science Center animal facilities with 12-h light/dark cycles in standard cages with access to food and water *ad libitum*. All animal procedures were performed in accordance with the National Institute of Health Guide for the Care and Use of Laboratory Animals. Experimental protocols were approved by the Institutional Animal Care and Use Committee at the University of Tennessee Health Science Center.

3.2.2 Surgery

Mice were surgically prepared for electrophysiological recordings in the mPFC, dCA1, and LS for free exploration of a homecage environment. Surgical anesthesia was initiated by exposing mice to 3% isoflurane in oxygen in an induction chamber. Anesthesia was maintained with 1–2% isoflurane in oxygen during surgery using an Ohio isoflurane vaporizer (Highland Medical Equipment, Deerfield, IL, USA). Body temperature was maintained at 37–38 °C with a servo-controlled heat blanket (FHC, Bowdoinham, ME, USA) monitored by a rectal thermometer. At the beginning of each surgery, after mice were anesthetized, but before the first incision, mice received a single subcutaneous injection of the analgesic Meloxicam SR (4 mg/kg, 0.06 ml) to alleviate pain. Three small burr holes were made into the skull bone overlying the left mPFC (AP 1.5 mm; ML 0.5 mm), the left

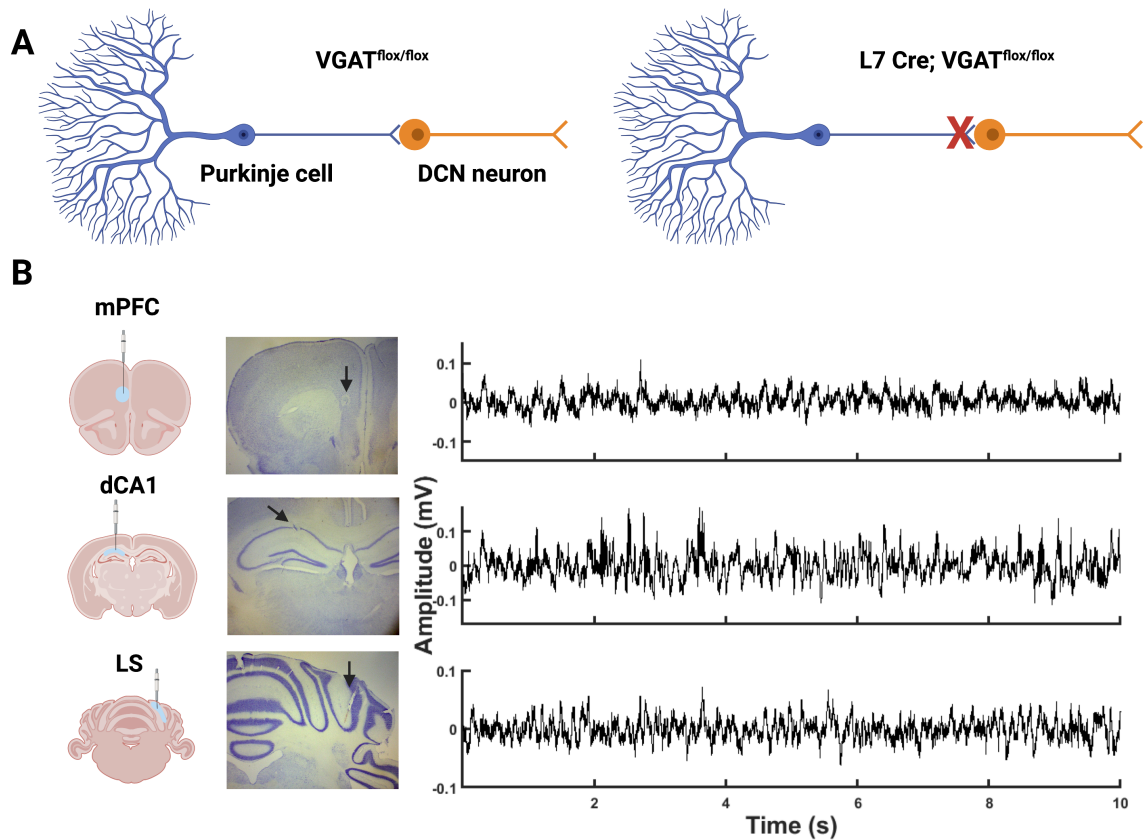


Figure 3.1: Animal model and schematic of recording strategy with histology and raw data examples. **A)** Schematic of *L7 Cre; VGAT^{flox/flox}* knockout mouse (right) their litter-mate controls (left) at the cellular level. VGAT knockout animals lose GABAergic synaptic transmission from Purkinje cells to their primary targets: neurons of the deep cerebellar nuclei. **B)** From left to right: illustration of recording sites, histological confirmation of recording sites by electrolytic lesion, and raw LFP data example from (top to bottom) mPFC, dCA1, and LS.

hippocampus (AP 2.0 mm; ML 1.5 mm), and the right cerebellum (AP -6.0; ML 1.8) using a dental drill (Microtorque II, RAM Products, Inc., USA), leaving the underlying dura intact. All coordinates were relative to Bregma.

For 9 of the animals, two extracellular recording electrodes (glass insulated tungsten/-platinum; 80- μ m diameter; impedance: 3.5–5.0 M Ω) attached to a custom-made micro-drive were centered over the mPFC, dCA1, and LS skull openings and the micro-drives were fixed to the skull using acrylic cement. The six electrodes, a reference wire, and a ground wire were then connected to a 20-pin micro-connector (Omnetics Connector Corp.). The micro-drives, head-post, and micro-connector were embedded in dental cement and anchored to the skull bone using three small skull screws. Of those three screws, one on the right side (AP - 1 mm; ML 3 mm) was connected with the reference wire, and one on the left side (AP - 4 mm; ML 4 mm) was connected to ground.

For 4 of the animals, a different recording system was used. For these experiments, four recording tetrodes (NiCr alloy; 12- μ m diameter; 1.2-1.5 M Ω) were bundled in a guiding tube and implanted into each respective recording site for a total of 16 data channels per site. The tetrodes were advanced to depths of 1.5 mm, 1.2 mm, and 0.8 mm for the mPFC, dCA1, and LS recording sites, respectively. The tetrodes were hand-spun and soldered onto a custom printed circuit board (PCB) chip, which was connected to an amplifier and secured in a custom 3D printed head cap. Both the tetrodes and head-cap were fixed to the skull using acrylic cement and anchored by two skull screws which also connected to ground and reference wires. For both recording strategies, a post-surgical recovery period of 7-10 days was allowed before electrophysiological experiments began.

3.2.3 Electrophysiology

Electrophysiological recordings were conducted with extracellular recording electrodes either attached to a custom-made micro-drive (glass insulated tungsten/platinum; 80- μ m diameter; impedance: 3.5–5.0 M Ω , Thomas Recording, GmbH, Germany), or as part of a custom-made high-density tetrode array (NiCr alloy; 12- μ m diameter; 1.2-1.5 M Ω). For the 9 animals with a micro-drive, two electrodes, separated by 0.25 mm, were placed in the mPFC, dCA1, and LS. All six electrodes were connected to a 20-pin micro-connector (Omnetics Connector Corporation). During recording sessions, a wireless head stage (W2100-HS16, Multichannel Systems, Germany) was plugged into the micro-connector. To reduce weight, the battery was kept off the head stage, and power was supplied by connecting the battery and head stage via two flexible thin wires (2 m, 40 AWG solid nickel). Electrophysiological recordings were performed on five consecutive days. On the first day, electrodes were manually advanced into the left mPFC, left dCA1, and right LS while the animals were in their home-cage with the micro-drive. The occurrence of sharp-wave ripples (SWR) was used to determine electrode tip placement in dCA1 (**Figure 3.1B**) (Buzsaki, 2015). On subsequent days, recordings were performed continually while the mice freely explored in their home-cage for 30 minutes. Recordings were agnostic of whether the animal was

actively exploring its environment or if it was stationary. Electrode positions were only altered in the dCA1 if SWR signals were lost. Broadband voltage signals (0.1-8 kHz) were digitized at 20kHz and saved to a hard disk (W2100-HS16, Multichannel Systems, Germany). LFPs were band-pass filtered offline at 0.1-200 Hz and down-sampled to 2-kHz using Spike2 (Cambridge Electronic Design Limited, UK).

A largely equivalent recording strategy was used for the four animals that received tetrode implants. During surgery, bundles of four tetrodes threaded through guiding tubes were advanced and buried in acrylic cement to their final recording depths, which were 1.5 mm in mPFC, 1.2 mm in dCA1, and 0.8 mm in LS. All tetrodes were soldered to a custom-made PCB prior to surgery, which was connected to a head-stage and amplifier (HS-640, White Matter Systems, USA) and placed within a 3D-printed head-cap to be secured onto the animal's skull by acrylic cement during surgery. During the recording sessions with implanted tetrodes, the head-stage was connected to the data acquisition system (eCube Server, White Matter Systems, USA) via a commutator cable. Animals were given one day of habituation in a novel home-cage environment before recordings began for the subsequent 5 days for 30 minutes a day. Again, recordings were agnostic of whether the animal was actively exploring its environment or if it was stationary. Broadband voltage signals (0.1-8 KHz) were digitized at 15kHz and saved to a hard disk (White Matter Systems, USA). LFPs were band-pass filtered offline at 0.1-200 Hz and down-sampled to 2-kHz using Matlab (Matlab R2019b). After completion of the final day of the experiment, recording sites were marked by small electrolytic lesions (10- μ A DC; 10 s) and verified anatomically (Figure 3.1A) for both recording strategies.

3.2.4 Power, Coherence, and Granger Causality Analysis of LFP Data

Raw electrophysiological data were first processed to remove power-line interference (60 Hz and 120 Hz and 180 Hz harmonics) using a spectrum interpolation method (Leske and Dalal, 2019; Mewett, Reynolds, and Nazeran, 2004). Data were then low-pass filtered to create LFPs for further analysis (cutoff frequency: 200 Hz). Periods of noisy data, such as when there was excess movement by the animal, were removed from the data set. One signal each in the mPFC, dCA1, and LS was selected for further analysis. Signal selection was based on a lack of artifact or line noise in the data, the clear presence of SWRs in dCA1, and the presence of spike activity observed in the raw data for the mPFC and LS signals. All LFP data were normalized by removing the mean prior to further analysis. Baseline power, coherence, and Granger causality were calculated using a non-parametric spectral method programmed by custom scripts in Matlab (Matlab R2019b). For time-resolved coherence analysis, coherence was calculated in 2 second intervals with a 200 ms sliding window. To evaluate the shape of the distribution of time-resolved coherence values, skewness and kurtosis were calculated using their corresponding functions in Matlab, and the Warren Sarle's bimodality coefficient (BC) was calculated using the Bimodality Coefficient Calculation with an open source Matlab package (Zhivomirov, 2021). All measures used were calculated for each frequency

tested (1-200 Hz) in 1 Hz steps and later averaged into eight separate frequency bands for further analysis.

3.2.5 Statistical Analysis

Average power, which is a function of oscillation amplitude, coherence, which measures the phase stability of two signals over time, and Granger causality, which evaluates to what extent two signals predict each other, was calculated for each brain structure (for power) or between each combination of two brain structures (for coherence and Granger causality). Each of these measures were initially tested for statistical significance on a frequency-by-frequency basis, i.e. a separate test was performed in 1 Hz steps. Initially, a two-sample F-test for equal variances was performed on all analysis measures to determine if the data came from normal distributions with the same variance (Matlab R2019b; function code: *vartest2*). Results from this test showed that the data were not normally distributed with equal variance, so non-parametric statistical tests were used moving forward. The Wilcoxon rank sum test (Matlab R2019b; function code: *ranksum*) was used to compare average power, coherence, and Granger causality measures between strains at each frequency, and also between strains once data were averaged into frequency bands. The BC calculated from distributions of time-resolved coherence, which has a range of zero to one, is a function of skewness and kurtosis where a value greater than 5/9 indicates that the data come from a bimodal or multimodal distribution. There were no statistical differences in any measure between mice that were implanted with extracellular recording electrodes adjusted with a micro-drive and mice that received fixed tetrode implants, suggesting that the data collected from these two recording strategies could be combined.

3.2.6 Histology

At the end of the experiments, animals were deeply anesthetized with an intraperitoneal injection of a Ketamine/Xylazine mixture (100 mg/kg / 10 mg/kg) and intracardially perfused with 0.9% NaCl followed by a 4% para-formaldehyde solution. Brains were removed from the skull and post-fixed in 4% para-formaldehyde solution for a minimum of 24 hours. Fixed brains were then sections at 60 μ m, mounted onto glass slides, and Nissl stained. Light microscopy was used to localize electrolytic lesions and verify the correct placement of the recording electrode tip in the mPFC, dCA1, and LS (**Figure 3.1B**).

3.3 Results

I evaluated the functional connectivity between mPFC, dCA1, and LS by analyzing the power, coherence, and Granger causality of LFP oscillations in a mouse model of cerebellar ataxia compared to its healthy litter-mate controls. Ataxic animals lacked the VGAT protein in cerebellar Purkinje cells, which is essential for vesicle docking. Therefore, these cells were not able to engage in chemical neurotransmission to their primary target neurons in

the deep cerebellar nuclei (DCN), functionally disconnecting the cerebellar cortex from the cerebellar output neurons. This mutation effectively eliminated the influence of the cerebellar cortex on neuronal activity in the cerebral cortex. As expected, this mutation led to profound motor deficits, which have been well documented (White, Arancillo, Stay, George-Jones, et al., 2014). However, the effects of this mutation had not yet been evaluated in the context of cerebrocerebellar communication and the cerebellar role in coordinating interactions between higher order brain areas, which is the purpose of the present study.

Mice had extracellular recording electrodes implanted into the left mPFC, left dCA1, and right LS, which all recorded LFP signals. All recording sites were confirmed post-hoc by the presence of electrolytic lesions, which were made on the final recording day (**Figure 3.1B**). Of the recording sites from each structure, the signal that showed the strongest SWR activity in the dCA1, and clean signals that exhibited spike activity in its high frequency components in the mPFC and LS were selected for further analysis. Evaluation of the average power of oscillations in mPFC on a frequency-by-frequency basis showed that there was a significant increase in power from 115-125 Hz in ataxic animals ($p < 0.05$, **Figure 3.2A**). However, when data was averaged into frequency bands, this region of significance did not hold up in the high frequency (100-130 Hz) band ($p = 0.052$, **Figure 3.2B**). There were no significant differences in power in the dCA1 and LS signals between ataxic and control animals at any frequency (Fig. **Figure 3.2C,D**), suggesting that the influence of the cerebellar cortex of this circuit does not affect the amplitude of their oscillations.

3.3.1 Loss of Purkinje Cell Transmission Increased mPFC-LS Coherence

I conducted a baseline and time-resolved analysis of coherence of mPFC-dCA1, dCA1-LS, and mPFC-LS LFP activity for neuronal oscillations between 4 and 200 Hz divided into eight commonly used frequency bands: theta (4-8 Hz), alpha (8-12 Hz), beta (12-30 Hz), low gamma (30-60 Hz), mid gamma (60-80 Hz), high gamma (80-100 Hz), high frequency (100-130 Hz), and very high frequency (130-200 Hz). Baseline coherence reflects an average coherence measurement taken across a 30-minute recording session where a mouse was able to freely explore a homecage environment. While there were no significant differences in average coherence of mPFC-dCA1 or dCA1-LS activity, ataxic animals showed significantly higher mPFC-LS coherence at several frequency in the low and mid gamma bands (26, 31-51, 53-56, 64-65, 67-72, 74, 76-79, 84, 89, 93, and 103 Hz) when analyzing coherence on a frequency-by-frequency basis ($p < 0.05$, **Figure 3.3A**). When grouping these values into their corresponding frequency bands, low gamma mPFC-LS coherence in ataxic animals remained significantly higher than in their litter-mate controls ($p < 0.05$), while the effect was no longer significant in the mid gamma frequency band (**Figure 3.3B**).

To better understand the dynamics of the differences found in mPFC-LS gamma coherence, I performed a time-resolved coherence analysis (i.e. if the observed average differences were due to an increase or decrease in very high coherence values, a mean shift in the entire distribution, or another factor). To quantify this, I sorted all values into

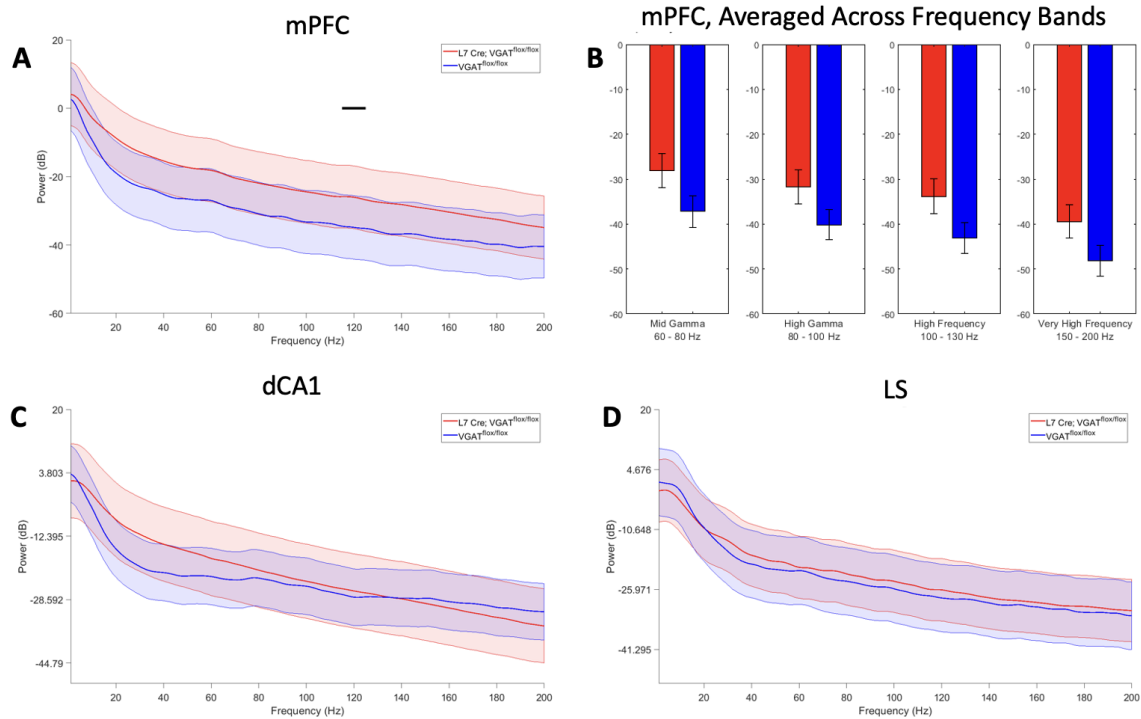


Figure 3.2: Average power of LFP oscillations in *L7 Cre; VGAT^{flox/flox}* (red) and *VGAT^{flox/flox}* animals (blue). A) Average power in mPFC is significantly different between *L7 Cre; VGAT^{flox/flox}* and *VGAT^{flox/flox}* animals from 115—125 Hz. B) Power in mPFC averaged into frequency bands. Not significant (NS) in any band between *L7 Cre; VGAT^{flox/flox}* and *VGAT^{flox/flox}* animals. C) Average power in dCA1 and D) LS, NS between *L7 Cre; VGAT^{flox/flox}* and *VGAT^{flox/flox}* animals at any frequency.

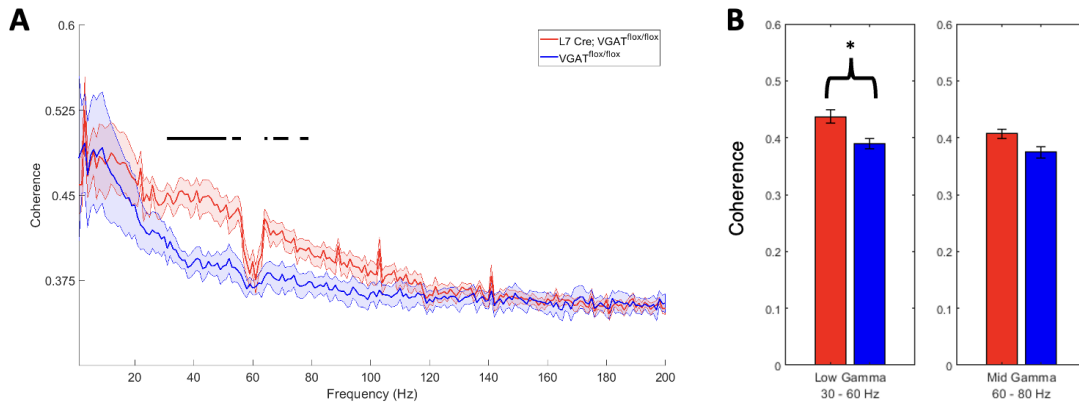


Figure 3.3: Average coherence of oscillations between mPFC and LS. A)

Average coherence of oscillations between mPFC and LS is significantly different between *L7 Cre; VGAT^{flox/flox}* and *VGAT^{flox/flox}* animals at 26 Hz, from 31-51 Hz, 53-56 Hz, 64-65 Hz, 67-72 Hz, at 74 Hz, from 76-79 Hz, and at 84, 89, 93, and 103 Hz. **B)** Coherence between mPFC and LS averaged across the low gamma band (30-60 Hz) is significantly different between *L7 Cre; VGAT^{flox/flox}* and *VGAT^{flox/flox}* animals but not when averaged across the mid gamma band (60-80 Hz) or any other frequency band.

their respective frequency bands, and calculated the BC, skewness, and kurtosis of their distributions. BC is a value ranging from zero to one and tests whether a distribution is multimodal or not. BC values great than 5/9 are considered to reflect multimodal distributions. If multimodality is confirmed, further inspection is required to determine whether the distribution is truly bimodal. There were no significant difference between ataxic and control animals in BC, skewness, or kurtosis in the time-resolved coherence distributions in any frequency band, including the low gamma band where a difference in average coherence was seen (**Figure 3.4A**). However, ataxic animals had a significantly higher maximal mPFC-LS coherence value in the high gamma (80-100 Hz) band ($p < 0.05$, **Figure 3.4B**). Additionally, all BC values were less than 5/9, indicating that all time-resolved coherence distributions were unimodal. Taken together, these data show that the observed differences in average mPFC-LS coherence seen in the low gamma band are due to a rightward shift of the distribution or due to a longer tail at the high-value end of the distribution of coherence values in ataxic animals which lack output from the cerebellar cortex.

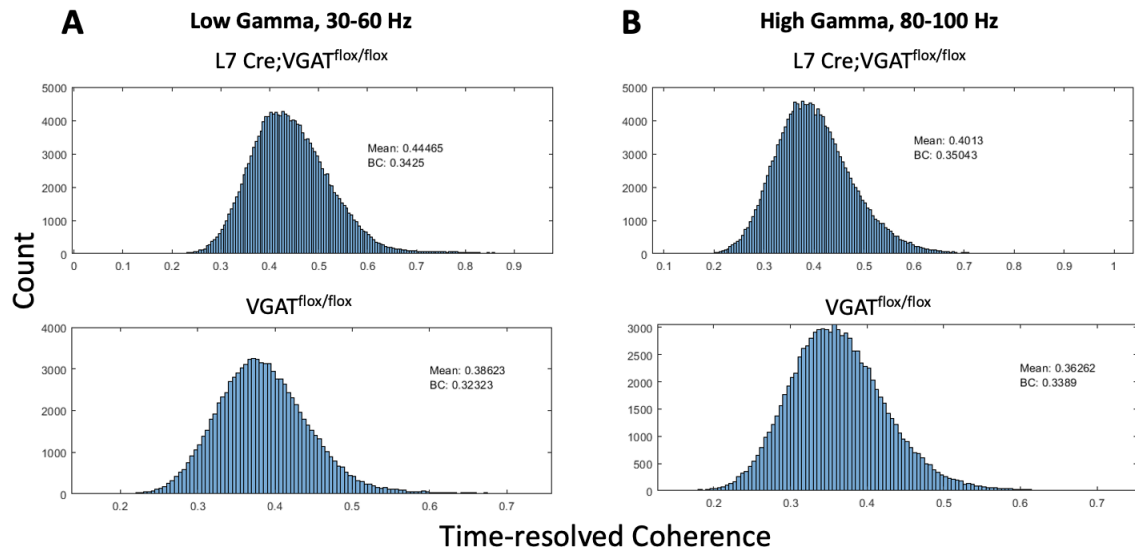


Figure 3.4: Histogram of time-resolved mPFC-LS coherence values in low gamma (30-60 Hz) and high gamma (80-100 Hz) frequency bands. A) Significant differences in average coherence between *L7 Cre; VGAT^{flox/flox}* and *VGAT^{flox/flox}* animals in low gamma frequencies are due to a rightward shift in the mean of the distribution of coherence values. BC < 0.55 in both conditions, indicating that the distribution of coherence values remained unimodal. There were no differences in skewness or kurtosis of coherence distribution of coherence in low gamma frequencies. **B)** While there were no significant differences in average coherence, skewness, or kurtosis in time-resolved coherence, significantly higher maximal coherence values were observed in *L7 Cre; VGAT^{flox/flox}* animals ($p < 0.05$).

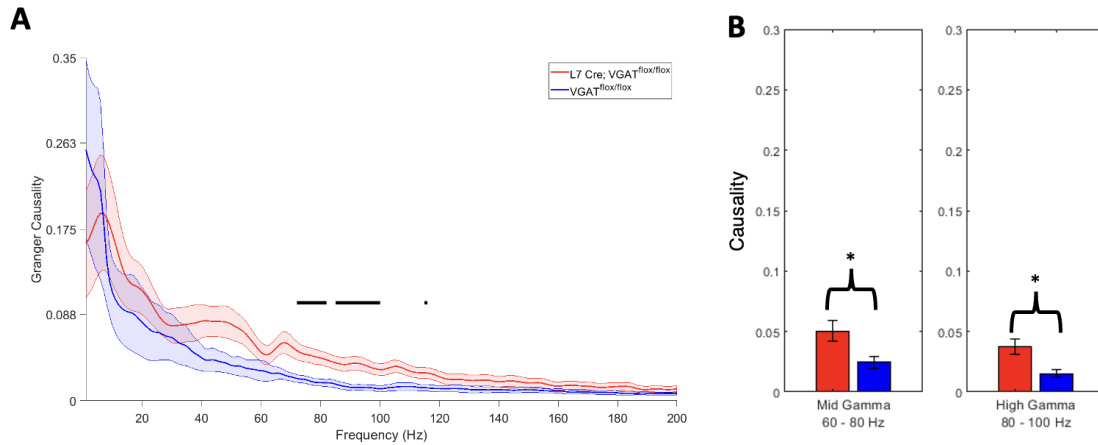


Figure 3.5: Average Granger causality of oscillations from mPFC to LS. A) Average Granger causality of from mPFC to LS is significantly different between *L7 Cre; VGAT^{flox/flox}* and *VGAT^{flox/flox}* animals at 69 Hz, from 72-82 Hz, 85-100 Hz, and 115-117 Hz. **B)** Granger causality from mPFC to LS averaged across the mid gamma band (60-80 Hz) and high gamma band (80-100 Hz) is significantly different between *L7 Cre; VGAT^{flox/flox}* and *VGAT^{flox/flox}* animals but not when averaged across any other frequency band.

3.3.2 Loss of Purkinje Cell Transmission Increased Granger Causality from mPFC to LS

Diving deeper into the relationship between mPFC and LS oscillations in this paradigm, I next applied Granger causality analysis to the LFP data to learn more about the directionality of the relationship between these two signals. In simple terms, this methods asks whether the information in two signals evolving over time, *A* and *B*, can predict future values of one another based on their own past values better than their own past values can predict their own future values (i.e. variable *A* Granger-causes variable *B* if predictions of the value of *B* based on its own past values and on the past values of *A* are better than predictions of *B* based only on *B*'s own past values). I applied the non-parametric version of this analysis to test to what extent the LFP's from mPFC Granger-caused the LFP's in LS and vice versa, and whether these causality values across frequencies differed between ataxic animals and their litter-mate controls. I found that ataxic animals had significantly higher Granger causality from mPFC to LS in gamma frequencies (69, 72-82, 85-100, and 115-117 Hz) than litter-mate controls (**Figure 3.5A**) when testing on a frequency-by-frequency basis ($p < 0.05$). When averaging across frequency bands, the observed increase in causality remained, with significant differences between strains being found in the mid gamma (60-80 Hz) band and

high gamma (80-100 Hz) band ($p < 0.05$, **Figure 3.5B**). There were no significant differences in Granger causality between ataxic and control animals from LS to mPFC, nor between mPFC and dCA1, and LS and dCA1.

3.4 Discussion

The data shown above builds upon previous experiments and reviews from our group to suggest a functional role for cerebellar LS in the coordination of communication between mPFC and dCA1, two areas that interact dynamically during SWM tasks. In baseline conditions where an animal is not asked to perform any specific behavior, the removal of GABAergic output from Purkinje cells in the cerebellar cortex significantly alters coherence between mPFC and LS. More specifically, Granger causality analysis shows that the disruption in this pathway in our mouse model of cerebellar ataxia seems to be in the mPFC \rightarrow LS direction, rather than the reverse. We did not see any changes in mPFC-dCA1 interactions, which seems contrary to our hypothesis based on a recently published study that shows mPFC-dCA1 coherence and task performance changes with optogenetic manipulation of Purkinje cells in a SWM task (Y. Liu, McAfee, Van Der Heijden, Dhamala, et al., 2022). However, mice in this study were not engaged in a SWM task and the cerebellar deficit was global, affecting the entire cerebellar cortex. In our previous study, we disrupted cerebellar activity locally in just LS (Y. Liu, McAfee, Van Der Heijden, Dhamala, et al., 2022). We also did not find any differences in dCA1-LS connectivity. This points to the possibility that the cerebellar manipulation of mPFC-dCA1 coherence occurs by the cerebellum setting the phase in the mPFC (via the thalamus), and not in the dCA1.

While these findings were initially unexpected, for the reasons described below they nevertheless fit with emerging ideas about the control of functional connectivity in cerebrocerebellar interactions (McAfee, Y. Liu, Sillitoe, and D. H. Heck, 2021) and thalamocortical interactions, which may also have a role in coordinating the coherence of forebrain structures (Nakajima and Halassa, 2017). The most notable difference between Y. Liu, McAfee, Van Der Heijden, Dhamala, et al. (2022) and the present study is that the LFP data collected here was sampled during periods of both rest and free exploration of a homecage environment, rather than during a SWM task. Y. Liu, McAfee, Van Der Heijden, Dhamala, et al. (2022) demonstrated transient mPFC-dCA1 coherence changes in a task specific manner and did not evaluate coherence for extended periods of time or outside the context of their SWM task. This study supports those findings in that it suggests that the cerebellar modulation of mPFC-dCA1 coherence during spontaneous behavior in the home cage differs from coherence modulation in the context of SWM behavior. While we do have a general idea of the mPFC-dCA1-LS circuit (**Figure 3.6**), detailed anatomical evidence of what specific pathways is required to facilitate information sharing between cerebellar LS and mPFC is lacking.

Tracing studies available through the Allen Brain Atlas Mouse Connectivity database may shed light on anatomical pathways for the cerebellum to modulate communication

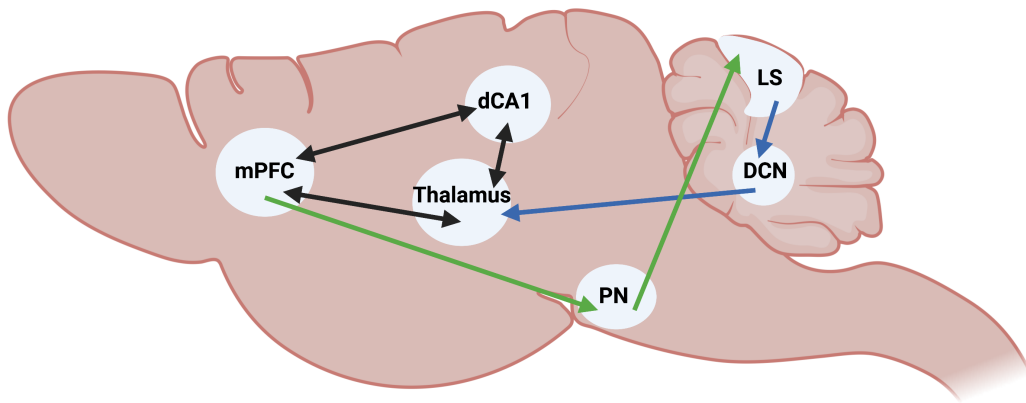


Figure 3.6: Illustration of a mouse brain showing a proposed circuit of how LS is influencing the functional connectivity of cerebrocerebellar interactions. Green arrows indicate known pathways of how information is received by LS, with the bulk of neocortical information passing first through the pontine nuclei (PN). Blue arrows show the most likely output pathways out of the cerebellum. Though proposed, no monosynaptic connections have been found between the DCN and hippocampus (Yu and Krook-Magnuson, 2015). Black arrows indicate reciprocal multi-synaptic pathways connecting prefrontal and hippocampal areas with each other and with the thalamus. Created with BioRender.com.

in cerebral cortical areas. In one experiment, anterograde tracer injected into the right interposed nucleus of the DCN (the target structure for Purkinje cells in LS) mapped projections to several contralateral nuclei in the thalamus, including the ventral anterior-lateral complex (VAL), ventral medial nucleus (VM), ventral posterolateral nucleus (VPL), and ventral posteromedial nucleus (VPM) (Harris, Mihalas, Hirokawa, Whitesell, et al., 2019; Oh, Harris, Ng, Winslow, et al., 2014). Of these targets, VM may be one of the most promising, as it itself projects to the prelimbic area (PL) of the mPFC and to the nucleus reuniens (RE) of the thalamus, among many other forebrain structures (Harris, Mihalas, Hirokawa, Whitesell, et al., 2019; Oh, Harris, Ng, Winslow, et al., 2014). Evidence suggests that RE has been shown to coordinate neural oscillations between frontal areas and the hippocampus during SWM (Dolleman-van der Weel, Griffin, H. T. Ito, Shapiro, et al., 2019; Griffin, 2021; Vertes, Hoover, Szigeti-Buck, and Leranath, 2007), making it a key candidate for involvement in this circuit.

It is becoming increasingly clear that the thalamus is involved in more than sensory integration and as a relay. For example, anatomically, thalamic output to the cortex is quite variable, with few thalamic circuits innervating just a single cortical target (Clasca, Rubio-Garrido, and Jabaudon, 2012; Kuramoto, Pan, Furuta, Tanaka, et al., 2017). Additionally, many thalamic circuits receive convergence of inputs from a single or multiple cortical regions, which is at odds with the idea that the thalamus exists merely as a topographic relay (Rovo, Ulbert, and Acsady, 2012). Reciprocal communication between the neocortex and various thalamic nuclei is within itself a potential mechanism for the modulation of functional connectivity in a task specific manner (Nakajima and Halassa, 2017), and operates in tandem with the hypothesis that the cerebellum acts as a temporal coordinator of forebrain oscillations.

This study shows the novel finding that, in addition to the cerebellum having the capacity to modulate the coherence of oscillations between two areas during a relevant behavioral task, output from the cerebellar cortex appears to keep functionally connected brain areas at a homeostasis that is disrupted with a loss of Purkinje cell output. There are several future directions extending from this study, including further exploring disruption of this circuit during SWM behavior. Additionally, more work needs to be done mapping the anatomical projections relevant to this circuit, with a particular focus on identifying the thalamic nuclei most involved on relaying cerebellar output to forebrain structures and how this circuit may be disrupted in cognitive disorders known to involve the cerebellum, such as autism, schizophrenia, and Alzheimer's Disease. Finally, transient activation or inhibition of components of this circuit via optogenetic manipulations to induce coherence changes may help to further elucidate this mechanism.

Chapter 4

Very High Frequency Phase Amplitude Coupling in the Cerebellar Cortex Is Altered by Loss of Purkinje Cell Neurotransmission

The following chapter builds off the work of Chapter 3, which found elevated mPFC-LS coherence and mPFC \rightarrow LS Granger causality in mice that lacked output from the cerebellar cortex. No changes in power, coherence, or Granger causality were observed in the dCA1-LS axis, or between mPFC and dCA1. To further explore how silencing Purkinje cells alters functional connectivity in this circuit, I developed and implemented a phase amplitude coupling (PAC) algorithm for this dataset. In simple terms, PAC evaluates the extent to which the amplitude of higher frequency oscillations is modulated by the phase of lower frequency oscillations. To augment my findings and to explore PAC at higher frequencies, I added additional data from four C57BL/6J animals. This chapter reports the novel finding of very high frequency PAC within the cerebellar cortex.

4.1 Introduction

Oscillations are a key component to many biological systems, and the nervous system is no exception. Neuronal oscillations are the product of the interactions of large populations of neurons, and arise from the interdependent nature of the varying timing and power of different subunits in the brain, whether they be individual neurons, nuclei, or full brain networks. These neuronal oscillations, which occur on timescales ranging from milliseconds to hours, reflect changes in neuronal excitability and are a powerful mechanism to organize and modulate the activity of individual neurons. The previous chapter centers and builds upon the recently published works of Y. Liu, McAfee, Van Der Heijden, Dhamala, et al. (2022) and McAfee, Y. Liu, Sillitoe, and D. H. Heck (2021), which provide evidence for the hypothesis that the cerebellum is an active player in cognition by coordinating the communication between cortical structures through the modulation of coherence of their neuronal oscillations. However, the coordination of coherence is not the only mechanism for manipulating functional connectivity by modulating neuronal oscillations. Cross-frequency

coupling, wherein neuronal oscillations of different frequencies interact with each other, is also a critical way to synchronize neuronal activity.

One form of cross-frequency coupling is PAC, which describes the amplitude of a higher frequency oscillation being modulated by the phase of a lower frequency oscillation. This phenomenon was first observed within the CA1 subfield of the rat hippocampus, where LFP recordings revealed that the amplitude of gamma oscillations varied with the phase of the theta frequency (Bragin, Jando, Nadasdy, Hetke, et al., 1995). This well supported finding is now considered the archetypical example of neuronal PAC (Belluscio, Mizuseki, Schmidt, Kempter, et al., 2012; Colgin, 2015; Schack, Vath, Petsche, Geissler, et al., 2002; Meij, M. Kahana, and Maris, 2012; Zhong, Ciatipis, Wolfenstetter, Jessberger, et al., 2017). PAC is thought to be generated through reciprocal connections of excitatory and inhibitory neuronal populations receiving driving oscillatory input (A. C. Onslow, R. Bogacz, and M. W. Jones, 2011; A. B. L. Tort, A. C. E. Onslow, Matthew W. Jones, and Rafal Bogacz, 2014), a hypothesis that has been supported experimentally in the context of hippocampal PAC (Wulff, Ponomarenko, Marlene Bartos, Korotkova, et al., 2009).

Due in part to the ubiquity of the neuronal architecture thought to be required to generate PAC, PAC has also been observed within and between many other brain areas, including between the hippocampus and neocortical areas (Sirota, Montgomery, Fujisawa, Isomura, et al., 2008), between the olfactory bulb and neocortical areas (J. Ito, Roy, Y. Liu, Cao, et al., 2014; Zhong, Ciatipis, Wolfenstetter, Jessberger, et al., 2017), between the somatosensory cortex and the striatum (Nicolai, Engler, Sharott, Engel, et al., 2014), and within the human medial prefrontal cortex (M. X. Cohen, Elger, and Fell, 2008). It is also clear that PAC has functional relevance, with several studies describing PAC during different phases of behavioral tasks (M. X. Cohen, Elger, and Fell, 2008; Farrokhi, Tafakori, and Daliri, 2022; Shearkhani and Takehara-Nishiuchi, 2013; A. B. Tort, Komorowski, Manns, N. J. Kopell, et al., 2009). See Ryan T. Canolty and Knight (2010) for a review. Changes in PAC have also been observed in diseases such as Parkinson's disease (Hemptinne, Ryapolova-Webb, Air, Garcia, et al., 2013) and Alzheimer's disease (Bazzigaluppi, Beckett, Koletar, Lai, et al., 2018; Zhang, Zhong, Brankack, Weyer, et al., 2016). The present study seeks to understand whether PAC exists within the cerebellar cortex, and if PAC within and between mPFC, dCA1, and LS is altered by the loss of Purkinje cell output from the cerebellar cortex while mice are freely exploring a homecage environment. To date, there have been no reports of PAC existing within the cerebellum, or between the cerebellar cortex and other regions of the brain.

4.2 Methods

4.2.1 Animals

See Chapter 3 Section 2.1 for a detailed description of animals used in the present study. In addition to the 13 *L7 Cre; VGAT^{flox/flox}* mice and their litter-mate controls from Chapter

3, data from 4 C57BL/6J (JAX # 000664) were added to this analysis to serve as additional controls.

4.2.2 Surgery

See [Chapter 3 Section 2.2](#) for a detailed description of the surgical procedures used for the 13 *L7 Cre; VGAT^{flox/flox}* mice and their littermate controls. The 4 additional B6 animals added to this dataset received fixed tetrode implants. For these experiments, four recording tetrodes (NiCr alloy; 12- μ m diameter; 1.2-1.5 M Ω) were bundled in a guiding tube and implanted into each respective recording site for a total of 16 data channels per site. The tetrodes were advanced to depths of 1.5 mm, 1.2 mm, and 0.8 mm for the mPFC, dCA1, and LS recording sites, respectively. The tetrodes were hand-spun and soldered onto a custom PCB chip, which was connected to an amplifier and secured in a custom 3D printed head cap. Both the tetrodes and headcap were fixed to the skull using acrylic cement and anchored by two skull screws which also connected to ground and reference wires. For both recording strategies, a postsurgical recovery period of 7-10 days was allowed before electrophysiological experiments began.

4.2.3 Electrophysiology

For a complete description of electrophysiological recordings conducted in the 13 *L7 Cre; VGAT^{flox/flox}* and their litter-mate controls, please see [Chapter 3 Section 2.3](#). Data collection for the 4 B6 animals proceeded identically as previously described in Chapter 3, with the key difference that LFPs were band-pass filtered offline at 0.1-450 Hz, rather than maximally at 200 Hz as previously done. This was done to explore PAC at frequencies beyond 200 Hz. Re-filtering and extending the LFP signal to 450 Hz was not possible for the 13 *L7 Cre; VGAT^{flox/flox}* mice and their litter-mate controls due to hardware limitations. 450 Hz is considered an acceptable cutoff range for LFP filtering as seen in recent studies (Buzsaki, 2015).

Raw electrophysiological data were first processed to remove power-line interference (60 Hz and 120 Hz and 180 Hz harmonics) using a spectrum interpolation method (Leske and Dalal, 2019; Mewett, Reynolds, and Nazeran, 2004). Periods of noisy data, such as when there was excess movement by the animal, were removed from the data set. One signal each in the mPFC, dCA1, and LS was selected for further analysis. Signal selection was based on a lack of artifact or line noise in the data, the clear presence of SWRs in dCA1, and the presence of spike activity observed in the raw data for the mPFC and LS signals. The longest continuous segment of LFP data (i.e. the longest artifact-free stretch of data) for each animal was used for group analysis. All LFP data were normalized by removing the mean prior to further analysis.

4.2.4 PAC Calculations

PAC was calculated using the modulation index (MI) method (R. T. Canolty, E. Edwards, Dalal, Soltani, et al., 2006) using the open-source function package “Matlab toolbox for estimating Phase Amplitude Coupling” as first published in A. C. Onslow, R. Bogacz, and M. W. Jones (2011). MI was selected over the envelope-to-signal correlation and cross frequency coupling methods based on raw data signal quality and length (A. C. Onslow, R. Bogacz, and M. W. Jones, 2011). Using the MI method, PAC was calculated within (mPFC_{ph}-mPFC_{amp}, dCA1_{ph}-dCA1_{amp}, LS_{ph}-LS_{amp}) and between each structure (mPFC_{ph}-dCA1_{amp}, dCA1_{ph}-mPFC_{amp}, dCA1_{ph}-LS_{amp}, LS_{ph}-dCA1_{amp}, mPFC_{ph}-LS_{amp}, LS_{ph}-mPFC_{amp}) at 5 Hz phase and amplitude intervals starting at 1 Hz and extending to the cutoff filter for that LFP signal (200 Hz for the 13 *L7 Cre; VGAT^{flox/flox}* mice and 450 Hz for the 4 B6 mice).

4.2.5 Statistical Analyses

Significance of individual PAC values was determined using a bootstrapping method in which the temporal relationship was destroyed between the test phase and test amplitude LFP signals by randomly shuffling the phase and then recalculating PAC, and repeating this process 50 times. If the resulting PAC value exceeded the 95% confidence interval of the bootstrap distribution, that value was considered statistically significant. A Bonferroni correction for multiple comparisons was applied to tests within each animal.

Not all animals showed PAC in their LFP activities. Thus, as a first step I determined what fraction of animals displayed statistically significant PAC (as determined above) at each phase-amplitude combination. Next, I sorted these fractions into quartiles. Phase-amplitude frequency combinations whose fraction of animals that displayed statistically significant PAC in the top quartile were included for group analysis.

For example, if this procedure were implemented on a group of 6 animals where only animal 1 displayed significant PAC at a given phase-amplitude frequency combination and 5 animals displayed significant PAC at a different phase-amplitude frequency combination, the latter phase-amplitude frequency combination would be far more likely to be included in group analysis for areas of significant PAC because a fraction of 5/6 animals with significant PAC would fall into a higher quartile than a fraction of 1/6 animals with significant PAC.

Focusing exclusively on whether a PAC value was considered significant based on its own shuffled data proved more revealing than comparing PAC values directly between *L7 Cre; VGAT^{flox/flox}* and *VGAT^{flox/flox}* mice using an independent samples t-test. Using this method, no phase-amplitude frequency combinations were found to be significantly different at the $p < 0.05$ level, even prior to a correction for multiple comparisons (data not shown).

4.2.6 Considering Waveform Shape

Many studies have shown that non-sinusoidal oscillations can artificially increase estimations of PAC (see Cole and Voytek (2017) for a review). This was of particular concern to us given that we are reporting broadband, high frequency PAC in the cerebellum, a topic on which there is little to no existing literature. To determine whether the evaluation of PAC in these data was biased by the presence of non-sinusoidal oscillations, I conducted an analysis to determine whether this data showed systemic deviation from the sinus at a given frequency in 4 B6 mice. For this test, I band-passed unfiltered raw data (down sampled to 2000 Hz) at 80-100 Hz, which was a range of phase frequencies that often generated significant LS PAC in B6 animals. Then, I created time stamps of instances of a particular phase (I chose $-\pi/2$) in that filtered signal. Next, I found the average waveform amplitude of the unfiltered raw data aligned to these timestamps and visually compared it against a standard sine wave to screen for the presence of obvious deviations of the average observed waveform from sinusoidal waveforms.

4.2.7 Histology

See Chapter 3 Section 2.6 for a detailed description of how tissue was processed for this study.

4.3 Results

This study reports the novel finding of high frequency PAC in the cerebellum, as well as findings confirming previous reports of PAC within dCA1 and mPFC (Bragin, Jando, Nadasdy, Hetke, et al., 1995; M. X. Cohen, Elger, and Fell, 2008; Sirota, Montgomery, Fujisawa, Isomura, et al., 2008). See Figure 4.1 for an example of how the amplitude of oscillations in LS at very high frequencies (300-350 Hz) is modulated by the phase of LS gamma oscillations (60-80 Hz) in a representative B6 animal. PAC was also calculated for LFP's between each pair of structures recorded from both ataxic, control, and B6 animals, but no significant phase-amplitude frequency combinations were found (data not shown). This negative result was not necessarily unexpected, as the structures recorded from at present are 1) not being asked to interact with each other as they might during a relevant behavioral task and 2) not monosynaptically connected.

4.3.1 Evaluation of PAC in a Mouse Model of Cerebellar Ataxia

Analysis of PAC within the dorsal hippocampus of both ataxic (*L7 Cre; VGAT^{flox/flox}*) mice and their littermate (*VGAT^{flox/flox}*) control mice revealed significant gamma amplitude coupling to theta phase, which is consistent with previous studies (Belluscio, Mizuseki, Schmidt, Kempter, et al., 2012; Bragin, Jando, Nadasdy, Hetke, et al., 1995; Colgin, 2015; Schack, Vath, Petsche, Geissler, et al., 2002; Meij, M. Kahana, and Maris, 2012; Zhong, Ciatipis, Wolfenstetter, Jessberger, et al., 2017) (Figure 4.2A,B, left panel). To directly

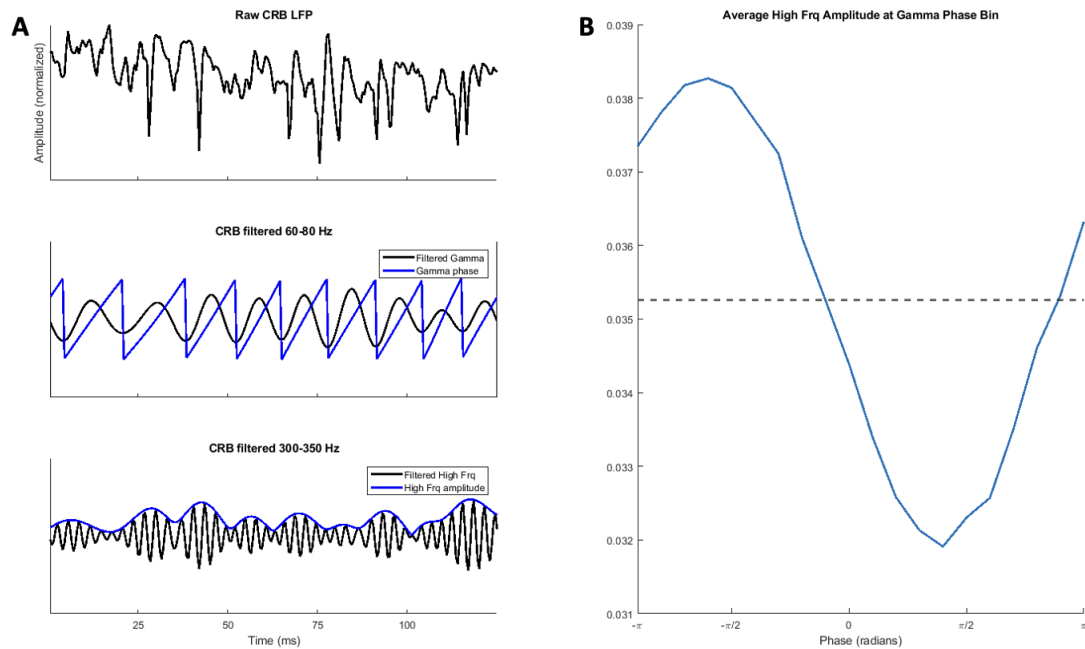


Figure 4.1: Representative example of high frequency PAC in the cerebellum. **A)** Example of how PAC is calculated. From the raw LFP signal (top), data is filtered into a lower (middle) and higher (bottom) frequency component. The Hilbert transform is applied to each signal to extract its respective phase (middle) and amplitude (bottom) information. **B)** Amplitude of filtered 300-350 Hz oscillations in LS plotted against the phase of 60-80 Hz oscillations in LS, clearly showing PAC at these phase-amplitude frequency combinations. Dashed black line represents the average waveform amplitude.

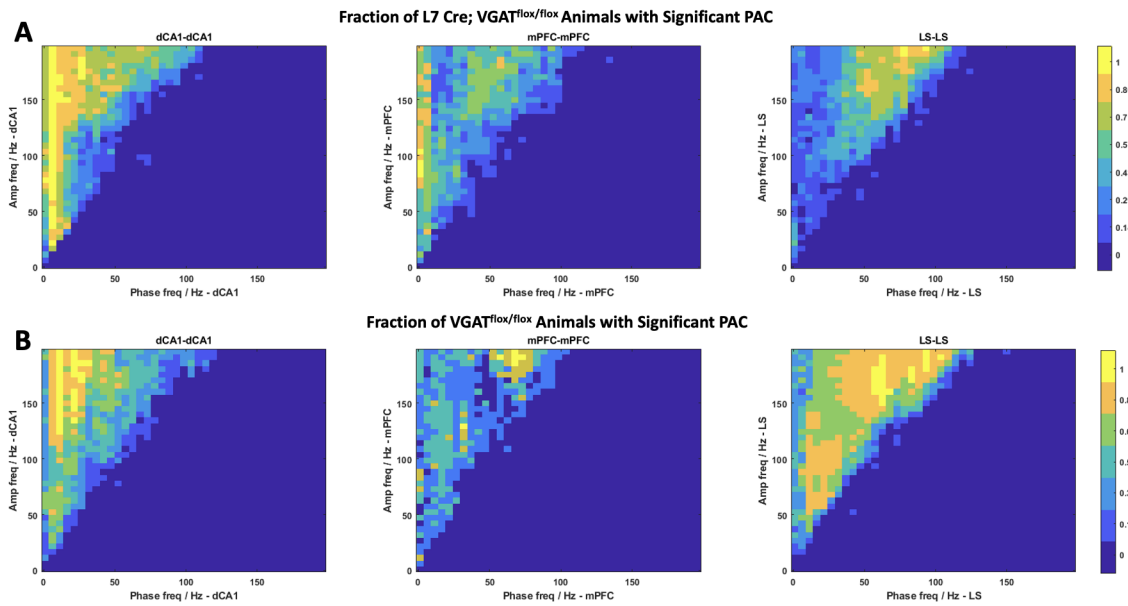


Figure 4.2: Spectrograms of PAC in *L7 Cre; VGAT^{flox/flox}* and *VGAT^{flox/flox}* mice. A) Fraction of *L7 Cre; VGAT^{flox/flox}* animals with significant PAC within dCA1 (left), mPFC (middle), and LS (right). B) Same as A) but showing PAC for *VGAT^{flox/flox}* control animals.

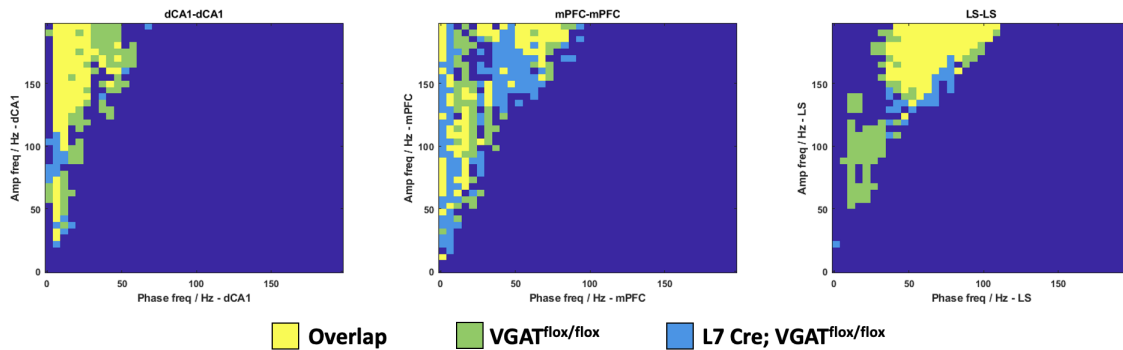


Figure 4.3: Top quartile significant PAC. Overlay of the top quartile of significant PAC of **A** and **B** from **Figure 4.2** for dCA1 (left), mPFC (middle), and LS (right).

compare the phase-amplitude frequency combinations that show significant PAC between *L7 Cre; VGAT^{flox/flox}* ataxic mice and *VGAT^{flox/flox}* control mice, I filtered the values of the heatmaps shown in **Figure 4.2** so that they only showed significant PAC if the fraction of animals with significant PAC at any given phase-amplitude frequency combination was in the top quartile of fraction values. This allowed me to compare the phase-amplitude frequency “hot spots” more effectively from the PAC heatmaps generated in **Figure 4.2**. The resulting quartile filtering can be seen in **Figure 4.3**, where I show PAC spectrograms that plot the phase-amplitude frequencies whose fraction were in the top quartile of all fraction values. This method allowed me to directly compare the “most significant” regions of PAC on the spectrogram between *L7 Cre; VGAT^{flox/flox}* ataxic mice and *VGAT^{flox/flox}* control mice. This procedure shows consistency in significant regions of dCA1 PAC between ataxic and control mice (**Figure 4.3, left panel**).

Significant phase-amplitude pairings within mPFC were less obvious in both ataxic and control mice, with pockets of significant PAC appearing in the delta phase/gamma amplitude range. 5/7 ataxic animals also showed significant mPFC PAC in a cluster of phase-amplitude frequency combinations centered in the low gamma phase/high gamma amplitude range (**Figure 4.2A, middle panel**). Interestingly, regions of significant PAC in the littermate control group were generally more inconsistent, with fewer large regions of significant PAC. However, the trends seen in the ataxic animals were generally replicated in the controls, as seen in the plot of overlapping footprints for mPFC PAC (**Figure 4.3, middle panel**).

Within the cerebellar cortex, significant PAC was observed between gamma (50-100 Hz) phase and the amplitude of very high frequency oscillations (130-200 Hz). This phenomenon was observed for both ataxic and control animals, with 100% of animals, regardless of genotype, exhibiting significant PAC at these high phase-amplitude frequency

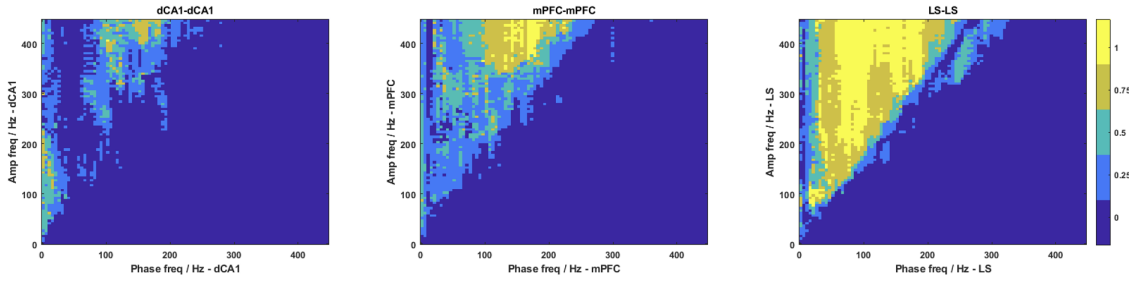


Figure 4.4: Fraction of C57BL/6J animals with significant PAC. Fraction of C57BL/6J animals with significant PAC within dCA1 (left), mPFC (middle), and LS (right).

combinations. In addition to the gamma-high frequency coupling in both ataxic and control animals, there was another significant cluster of LS PAC ranging from 15-30 Hz in the phase frequency range and 50-150 Hz in the amplitude frequency range. This beta-gamma/high frequency PAC was only observed in $VGAT^{flox/flox}$ littermate controls, as shown by the plot of overlapping footprints for LS PAC (**Figure 4.3, right panel**) There were no areas of significant PAC in ataxic or control mice when looking at PAC between structures (mPFC_{ph}-dCA1_{amp}, dCA1_{ph}-mPFC_{amp}, dCA1_{ph}-LS_{amp}, LS_{ph}-dCA1_{amp}, mPFC_{ph}-LS_{amp}, LS_{ph}-mPFC_{amp}).

4.3.2 Evaluation of PAC in B6 Mice

To explore whether these observed PAC findings, especially within the cerebellum, are unique to this mouse model, I repeated this analysis on four B6 animals. As $VGAT^{flox/flox}$ mice are bred on a B6 background, the null hypothesis here is that there will be no observed differences in PAC between $VGAT^{flox/flox}$ mice and B6 mice. Due to minor differences in the tools used for data collection from these animals, I had more control over the filtering parameters to translate raw electrophysiological data into LFP signal. To take advantage of this, I extended the upper bounds of the LFP filtering cutoff to 450 Hz to primarily see if there was an upper boundary to the amplitude frequency of LS PAC observed in $L7 Cre; VGAT^{flox/flox}$ mice and their littermate controls.

Within-structure PAC findings closely correspond to PAC observed in ataxic animals and their littermate controls. In dCA1 PAC, B6 animals consistently show canonical theta-gamma PAC (**Figure 4.4, left panel**). Similar to the earlier mPFC PAC analysis, there is no clear and consistent significant PAC within frequencies below 200 Hz among B6 mice (**Figure 4.4, middle panel**). The dCA1 and mPFC PAC spectrogram plots both show significant PAC in the 100-200 Hz phase frequencies and 350-450 Hz amplitude frequencies. These areas of significance could be artifacts from spiking activity in these structures (see Discussion). Evaluation of LS PAC in B6 animals supports the finding of very high frequency

PAC observed in *L7 Cre; VGAT^{flox/flox}* and *VGAT^{flox/flox}* mice (**Figure 4.4, right panel**). B6 animals also show significant beta-gamma/high frequency LS PAC, which corresponds with a PAC hot spot found at 15-30 Hz in the phase domain and 60-130 Hz in the amplitude domain in *VGAT^{flox/flox}* mice but not *L7 Cre; VGAT^{flox/flox}* mice (**Figure 4.3, right panel**), providing further evidence to suggest that beta-gamma/high frequency LS PAC requires intact Purkinje cell output. Similar to the findings from ataxic and control mice, there was no significant PAC in B6 mice when evaluating PAC between structures (mPFC_{ph}-dCA1_{amp}, dCA1_{ph}-mPFC_{amp}, dCA1_{ph}-LS_{amp}, LS_{ph}-dCA1_{amp}, mPFC_{ph}-LS_{amp}, LS_{ph}-mPFC_{amp}).

4.4 Discussion

This study builds on the findings of Chapter 3 and evaluates the PAC of LFP signals within and between left mPFC, left dCA1, and right LS in the *L7 Cre; VGAT^{flox/flox}* model of cerebellar ataxia where Purkinje cell inhibitory output is eliminated, healthy littermate controls (*VGAT^{flox/flox}*), and B6 mice. These three structures were chosen due to evidence showing that Purkinje cell spiking activity in LS stores phase information and phase differences between mPFC and dCA1 (McAfee, Y. Liu, Sillitoe, and D. H. Heck, 2019), and new causal evidence showing that these three structures are involved in spatial working memory (Y. Liu, McAfee, Van Der Heijden, Dhamala, et al., 2022). Chapter 3 evaluated the baseline functional connectivity between these three structures and found that coherence between left mPFC and right LS was significantly increased in the low gamma frequency band (30-60 Hz) in ataxic mice relative to their littermate controls. Additionally, Chapter 3 found an increase in mPFC → LS Granger causality in the mid gamma (60-80 Hz) and high gamma (80-100 Hz) bands in ataxic mice. This work provides additional evidence to support the hypothesis that the cerebellum can act to coordinate cerebro-cortical oscillatory activity through the modulation of coherence between structures (McAfee, Y. Liu, Sillitoe, and D. H. Heck, 2021). In this study, we wanted to see whether PAC, another mechanism to coordinate neuronal oscillations, could be contributing to this circuit.

Here, we report the novel finding of significant PAC within the LS of the cerebellum at very high frequencies in animals that lack Purkinje cell output and their littermate controls. While both mutant and control animals exhibited very high frequency LS PAC (phase of 50-100 Hz oscillations coupled to amplitude of 120-200 Hz oscillations), significant LS PAC was also observed in the 15-30 Hz in the phase frequency range and 50-150 Hz in the amplitude frequency range in control animals but not in ataxic animals, suggesting that PAC in those frequency ranges requires intact Purkinje cell synaptic transmission. A previous study has shown that *L7 Cre; VGAT^{flox/flox}* mutant mice exhibit altered Purkinje cell firing patterns in vivo relative to control *VGAT^{flox/flox}* mice. More specifically, *L7 Cre; VGAT^{flox/flox}* mutant mice show a significant increase in Purkinje cell simple spike regularity (as measured by the coefficient of variation (CV) of spike times) and a significant decrease in complex spike firing frequency relative to *VGAT^{flox/flox}* littermate controls (White, Arancillo, Stay, George-Jones, et al., 2014). These findings, paired with the altered LS PAC findings

found at present, are likely due to the cerebellar cortico-nucleo-olivary circuit (Libster and Yarom, 2013), a tri-synaptic feedback loop from Purkinje cells to cerebellar nuclei neurons to inferior olive neurons, which in turn project back to Purkinje cells via climbing fibers.

In the *L7 Cre; VGAT^{flox/flox}* mutant mice and *VGAT^{flox/flox}* control mice, PAC analysis was performed up to 200 Hz, with significant PAC within LS being found at the upper bounds of frequencies I was able to test with this data. To determine the upper frequency boundary of PAC and in order to evaluate whether our earlier findings with 0.1-200 Hz bandpass filtered LFPs were not an artifact of animal strain, I analyzed LFP data with the upper bound of its bandpass filter at 450 Hz (Buzsaki, 2015) from four B6 animals to evaluate PAC at even higher frequencies. Findings from this analysis support the finding of significant very high frequency (amplitude of 130-200 Hz oscillations coupled to the phase of 50-100 Hz oscillations) LS PAC found in *L7 Cre; VGAT^{flox/flox}* mutant mice and *VGAT^{flox/flox}* control mice. Similarly, B6 animals displayed significant PAC in LS in the 15-30 Hz in the phase frequency range and 50-150 Hz in the amplitude frequency range. This matches the LS PAC findings in *VGAT^{flox/flox}* control mice and suggests that LS PAC observed in this phase-amplitude frequency range requires intact Purkinje cell synaptic transmission in contribution to the cortico-nucleo-olivary feedback circuit.

Analysis of LS PAC in B6 animals up to 450 Hz showed that there was no obvious “upper frequency boundary” to significant phase-amplitude frequency combinations. Extending the LFP frequency range up to 450 Hz also revealed significant mPFC PAC at very high phase-amplitude frequency combinations (100-200 Hz in the phase frequency range and 300-450 Hz in the amplitude frequency range). A similar, but less consistent pattern was seen in dCA1 PAC (Figure 4.4). That all three within-structure PAC comparisons showed significant PAC in these extremely high phase-amplitude frequency combinations suggests that some spike information may be present in the LFP signal at these frequencies, and that we could be inadvertently measuring a form of spike-field coherence in amplitude frequency ranges beyond 300 Hz. Thus, we primarily emphasize our LS PAC findings that exist below 300 Hz.

Although the existence of PAC in the rodent cerebellum has never been reported, much less in very high phase-amplitude frequency combinations, multiple lines of evidence suggest that our findings are real rather than an artifact related to multiplexing (Cole and Voytek, 2017). Firstly, modulation of high frequency LFP activity in and of itself is not a completely novel finding in the cerebellum. For example, in a mouse model of Alzheimer’s Disease, a peak in the power spectrum of at 245 Hz was observed in LFP recordings in the Purkinje cell layer that was not seen in control animals (Cheron, Ristori, Marquez-Ruiz, Cebolla, et al., 2022). Additionally, that we saw differences in the range of phase-amplitude frequency combinations where significant LS PAC was observed (see Figure 4.3, right panel) between *L7 Cre; VGAT^{flox/flox}* mutant mice and *VGAT^{flox/flox}* control mice suggests that our findings have a physiological basis. Visual inspection of filtered LS LFP data (Figure 4.1A) paired with a plot of high frequency amplitude against gamma phase clearly shows that

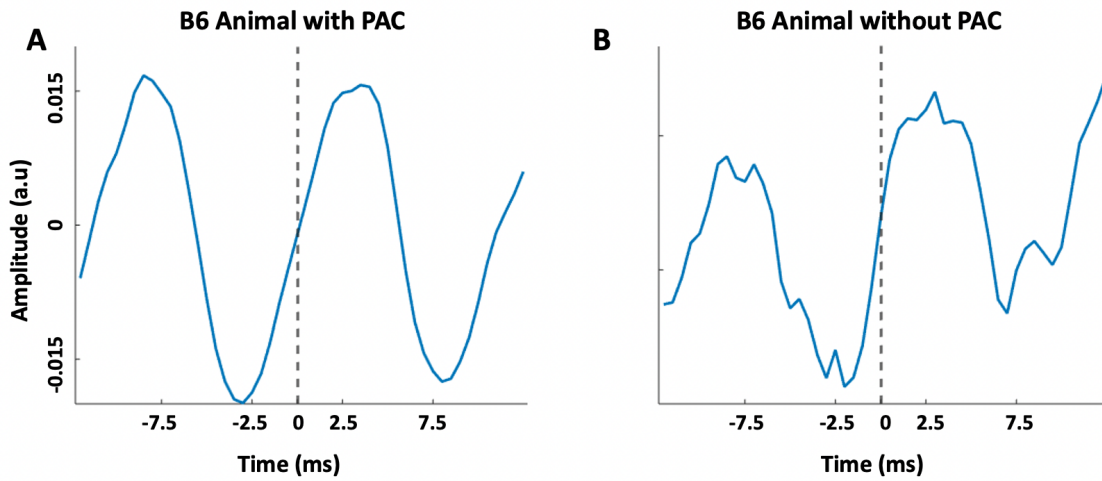


Figure 4.5: Average unfiltered LS LFP aligned to the phase of 80-100 Hz LS LFP. A) A representative B6 animal with broadband significant PAC at 80-100 Hz phase frequencies. **B)** A representative B6 animal without broadband significant PAC at 80-100 Hz phase frequencies.

the amplitude of very high frequency oscillations is modulated by gamma phase (**Figure 4.1B**). While it is possible that the PAC results reported here could be biased by the presence of non-sinusoidal oscillations or multiplexing (Cole and Voytek, 2017), **Figure 4.5** shows that raw, unfiltered LS LFP data averaged and temporally aligned to the phase of 80-100 Hz band-passed LS oscillations does not show signs of high frequency components and hence no obvious deviation from a sinusoidal waveform. Additionally, we do not believe these factors are driving our results because we do not see PAC at delta or theta phase frequencies, which can be indicative of multiplexing (Cole and Voytek, 2017).

To conclude, this study reports the novel finding of significant PAC within the LS of the mouse cerebellum in *L7 Cre; VGAT^{fllox/flox}* mutant mice, *VGAT^{fllox/flox}* control mice, and in B6 mice at very high phase-amplitude frequency combinations. That the phase-amplitude frequency combinations of significant LS PAC in *L7 Cre; VGAT^{fllox/flox}* mutant mice and *VGAT^{fllox/flox}* control mice are overlapping in some parts of the PAC spectrogram (i.e. for amplitudes at 130-200 Hz modulated by phases at 50-100 Hz) but not others (i.e. for amplitudes at 50-150 Hz modulated by phases at 15-30 Hz) suggest that an intact cerebellar cortico-nucleo-olivary circuit is necessary for the presence of beta-gamma/high frequency PAC within LS. Given the novelty of this finding, follow up experiments are required to determine the ubiquity of PAC within other lobules in the cerebellar cortex, and to determine the functional role of PAC in the cerebellum. In this regard, evaluation of PAC during behavior may prove promising.

Chapter 5

Summary and Conclusions

The purpose of this project was to better understand the ways that the pathways and mechanisms used by the cerebellum influence neuronal and behavioral rhythms through the coordination of neuronal oscillations.

Chapter 1 introduces why the study of neuronal oscillations is important within the context of their ability to influence spike probabilities. It introduces the “communication through coherence” hypothesis that much of the work presented here is based around. It also provides a brief literature review of evidence showing that the cerebellum is more involved than previously thought in coordinating the communication between brain structures. Finally, Chapter 1 provides a roadmap for this body of work exploring how the cerebellum acts to manipulate neuronal oscillations in a variety of contexts.

Chapter 2 synthesizes a recently published literature review (Detlef H. Heck, Brittany L. Correia, Fox, Yu Liu, et al., 2022) on the role of respiratory modulation of brain activity on emotion and cognition with recently published experimental work (Y. Liu, Qi, Thomas, B. L. Correia, et al., 2020) showing that loss of Purkinje cell transmission has a significant effect on respiratory intrinsic rhythmicity. Here I developed an *in silico* manipulation to demonstrate that artificially lengthening every tenth respiratory interval by 50% in mutant animals removes the significant differences in CV2 initially observed between mutant ataxic and littermate control animals. With these results in mind, we proposed that the cerebellum could play a role in coordinating respiration with swallowing, which coincides with our finding of significantly increased CV2 in healthy control mice. Further work could be done to expand this project, including recording respiratory activity during a variety of different naturalistic behaviors, along with manipulating cerebellar output with more spatial and temporal (i.e. chemogenetic or optogenetic) precision to determine which lobules of the cerebellum most contribute to this process and on what time course.

Chapter 3 builds upon previously published work in the Heck lab (McAfee, Y. Liu, Sillitoe, and D. H. Heck, 2019; Y. Liu, McAfee, Van Der Heijden, Dhamala, et al., 2022) to evaluate the functional connectivity of a spatial working memory circuit of a mouse model of cerebellar ataxia. This chapter uses the same cerebellar ataxia model as Chapter 2 where mutant animals lose Purkinje cell transmission to the deep cerebellar nuclei. This chapter

analyzes the average coherence and Granger causality between the right LS, left mPFC, and left dCA1, as well as the average power of oscillations within these structures while an animal is freely exploring a homecage environment. I found that mPFC-LS coherence was significantly increased at gamma frequencies in mutant animals, as well as Granger causality from mPFC to LS at similar frequencies. These findings point to the cerebellar cortex being able to keep functionally connected brain areas at an oscillatory homeostasis that is disrupted with a loss of Purkinje cell output.

Chapter 4 is a natural extension of Chapter 3 in that it applies PAC analysis to this same data set (with the addition of 4 WT animals) to evaluate potential differences in the cross-frequency or nested coupling of oscillations due to a loss of Purkinje cell output. In addition to providing supporting evidence of canonical theta-gamma PAC within dCA1, this chapter reports the novel finding of significant high frequency PAC (between gamma (50-100 Hz) phase and very high frequency (130-200 Hz) amplitude) within LS in both ataxic and control animals. This finding was corroborated when the PAC for similarly collected data was evaluated in four WT animals. I found a cluster of significant beta-gamma PAC within LS in control and WT animals that was not observed in ataxic animals, suggesting that the cerebellar cortico-nucleo-olivary circuit may be responsible for generating PAC within the cerebellar cortex at these phase and amplitude frequency combinations.

Taken together, these experiments and analyses presented here suggest a role for the cerebellum in coordinating behavioral and neuronal rhythms and bring us closer to elucidating the neuronal mechanisms of cerebrocerebellar functional connectivity with a broader understanding of the cerebellum beyond the context of motor coordination.

List of References

- Aertsen, A. M. and G. L. Gerstein (Aug. 12, 1985). "Evaluation of neuronal connectivity: sensitivity of cross-correlation". In: *Brain Res* 340.2, pp. 341–54. ISSN: 0006-8993 (Print) 0006-8993 (Linking). DOI: [10.1016/0006-8993\(85\)90931-x](https://doi.org/10.1016/0006-8993(85)90931-x). URL: <https://www.ncbi.nlm.nih.gov/pubmed/4027655>.
- Andreasen, N. C. and R. Pierson (July 15, 2008). "The role of the cerebellum in schizophrenia". In: *Biol Psychiatry* 64.2. Edition: 20080408, pp. 81–8. ISSN: 1873-2402 (Electronic) 0006-3223 (Linking). DOI: [10.1016/j.biopsych.2008.01.003](https://doi.org/10.1016/j.biopsych.2008.01.003). URL: <https://www.ncbi.nlm.nih.gov/pubmed/18395701>.
- Apps, R. and R. Hawkes (Sept. 2009). "Cerebellar cortical organization: a one-map hypothesis". In: *Nat Rev Neurosci* 10.9, pp. 670–81. ISSN: 1471-0048 (Electronic) 1471-003X (Linking). DOI: [10.1038/nrn2698](https://doi.org/10.1038/nrn2698). URL: <https://www.ncbi.nlm.nih.gov/pubmed/19693030>.
- Arch, J. J. and M. G. Craske (Dec. 2006). "Mechanisms of mindfulness: emotion regulation following a focused breathing induction". In: *Behav Res Ther* 44.12. Edition: 20060207, pp. 1849–58. ISSN: 0005-7967 (Print) 0005-7967 (Linking). DOI: [10.1016/j.brat.2005.12.007](https://doi.org/10.1016/j.brat.2005.12.007). URL: <https://www.ncbi.nlm.nih.gov/pubmed/16460668>.
- Arshamian, A. et al. (Nov. 28, 2018). "Respiration Modulates Olfactory Memory Consolidation in Humans". In: *J Neurosci* 38.48. Edition: 20181022, pp. 10286–10294. ISSN: 1529-2401 (Electronic) 0270-6474 (Linking). DOI: [10.1523/JNEUROSCI.3360-17.2018](https://doi.org/10.1523/JNEUROSCI.3360-17.2018). URL: <https://www.ncbi.nlm.nih.gov/pubmed/30348674>.
- Asanuma, C., W. T. Thach, and E. G. Jones (May 1983). "Brainstem and spinal projections of the deep cerebellar nuclei in the monkey, with observations on the brainstem projections of the dorsal column nuclei". In: *Brain Res* 286.3, pp. 299–322. ISSN: 0006-8993 (Print) 0006-8993 (Linking). DOI: [10.1016/0165-0173\(83\)90017-6](https://doi.org/10.1016/0165-0173(83)90017-6). URL: <https://www.ncbi.nlm.nih.gov/pubmed/6189563>.
- Ashida, R. et al. (Nov. 1, 2019). "Sensorimotor, language, and working memory representation within the human cerebellum". In: *Hum Brain Mapp* 40.16. Edition: 20190730, pp. 4732–4747. ISSN: 1097-0193 (Electronic) 1065-9471 (Linking). DOI: [10.1002/hbm.24733](https://doi.org/10.1002/hbm.24733). URL: <https://www.ncbi.nlm.nih.gov/pubmed/31361075>.
- Aston-Jones, G. and J. D. Cohen (2005). "An integrative theory of locus coeruleus-norepinephrine function: adaptive gain and optimal performance". In: *Annu Rev Neurosci* 28, pp. 403–50. ISSN: 0147-006X (Print) 0147-006X (Linking). DOI: [10.1146/annurev.neuro.28.061604.135709](https://doi.org/10.1146/annurev.neuro.28.061604.135709). URL: <https://www.ncbi.nlm.nih.gov/pubmed/16022602>.

- Awh, Edward et al. (2016). "Dissociation of Storage and Rehearsal in Verbal Working Memory: Evidence From Positron Emission Tomography". In: *Psychological Science* 7.1. Section: 25, pp. 25–31. ISSN: 0956-7976 1467-9280. DOI: [10.1111/j.1467-9280.1996.tb00662.x](https://doi.org/10.1111/j.1467-9280.1996.tb00662.x).
- Babajani-Feremi, A. et al. (Dec. 17, 2014). "Variation in the topography of the speech production cortex verified by cortical stimulation and high gamma activity". In: *Neuroreport* 25.18, pp. 1411–7. ISSN: 1473-558X (Electronic) 0959-4965 (Linking). DOI: [10.1097/WNR.0000000000000276](https://doi.org/10.1097/WNR.0000000000000276). URL: <https://www.ncbi.nlm.nih.gov/pubmed/25371284>.
- Bahner, F. et al. (June 2015). "Hippocampal-dorsolateral prefrontal coupling as a species-conserved cognitive mechanism: a human translational imaging study". In: *Neuropsychopharmacology* 40.7. Edition: 20150112, pp. 1674–81. ISSN: 1740-634X (Electronic) 0893-133X (Linking). DOI: [10.1038/npp.2015.13](https://doi.org/10.1038/npp.2015.13). URL: <https://www.ncbi.nlm.nih.gov/pubmed/25578799>.
- Barbas, H. and G. J. Blatt (1995). "Topographically specific hippocampal projections target functionally distinct prefrontal areas in the rhesus monkey". In: *Hippocampus* 5.6, pp. 511–33. ISSN: 1050-9631 (Print) 1050-9631 (Linking). DOI: [10.1002/hipo.450050604](https://doi.org/10.1002/hipo.450050604). URL: <https://www.ncbi.nlm.nih.gov/pubmed/8646279>.
- Basar, E. et al. (2016). "Delay of cognitive gamma responses in Alzheimer's disease". In: *Neuroimage Clin* 11. Edition: 20160120, pp. 106–115. ISSN: 2213-1582 (Electronic) 2213-1582 (Linking). DOI: [10.1016/j.nicl.2016.01.015](https://doi.org/10.1016/j.nicl.2016.01.015). URL: <https://www.ncbi.nlm.nih.gov/pubmed/26937378>.
- Bastos, A. M., J. Vezoli, and P. Fries (Apr. 2015). "Communication through coherence with inter-areal delays". In: *Curr Opin Neurobiol* 31. Edition: 20141120, pp. 173–80. ISSN: 1873-6882 (Electronic) 0959-4388 (Linking). DOI: [10.1016/j.conb.2014.11.001](https://doi.org/10.1016/j.conb.2014.11.001). URL: <https://www.ncbi.nlm.nih.gov/pubmed/25460074>.
- Bazzigaluppi, P. et al. (Mar. 2018). "Early-stage attenuation of phase-amplitude coupling in the hippocampus and medial prefrontal cortex in a transgenic rat model of Alzheimer's disease". In: *J Neurochem* 144.5. Edition: 20171010, pp. 669–679. ISSN: 1471-4159 (Electronic) 0022-3042 (Linking). DOI: [10.1111/jnc.14136](https://doi.org/10.1111/jnc.14136). URL: <https://www.ncbi.nlm.nih.gov/pubmed/28777881>.
- Becker, E. B. and C. J. Stoodley (2013). "Autism spectrum disorder and the cerebellum". In: *Int Rev Neurobiol* 113, pp. 1–34. ISSN: 2162-5514 (Electronic) 0074-7742 (Linking). DOI: [10.1016/B978-0-12-418700-9.00001-0](https://doi.org/10.1016/B978-0-12-418700-9.00001-0). URL: <https://www.ncbi.nlm.nih.gov/pubmed/24290381>.
- Belluscio, M. A. et al. (2012). "Cross-Frequency Phase-Phase Coupling between Theta and Gamma Oscillations in the Hippocampus". In: *Journal of Neuroscience* 32.2. Section: 423, pp. 423–435. ISSN: 0270-6474 1529-2401. DOI: [10.1523/jneurosci.4122-11.2012](https://doi.org/10.1523/jneurosci.4122-11.2012).
- Benchenane, K., P. H. Tiesinga, and F. P. Battaglia (June 2011). "Oscillations in the prefrontal cortex: a gateway to memory and attention". In: *Curr Opin Neurobiol* 21.3. Edition: 20110321, pp. 475–85. ISSN: 1873-6882 (Electronic) 0959-4388 (Linking). DOI: [10.1016/j.conb.2011.01.004](https://doi.org/10.1016/j.conb.2011.01.004). URL: <https://www.ncbi.nlm.nih.gov/pubmed/21429736>.

- Beshel, J., N. Kopell, and L. M. Kay (Aug. 1, 2007). "Olfactory bulb gamma oscillations are enhanced with task demands". In: *J Neurosci* 27.31, pp. 8358–65. ISSN: 1529-2401 (Electronic) 0270-6474 (Linking). DOI: [10.1523/JNEUROSCI.1199-07.2007](https://doi.org/10.1523/JNEUROSCI.1199-07.2007). URL: <https://www.ncbi.nlm.nih.gov/pubmed/17670982>.
- Biskamp, J., M. Bartos, and J. F. Sauer (Mar. 28, 2017). "Organization of prefrontal network activity by respiration-related oscillations". In: *Sci Rep* 7. Edition: 20170328, p. 45508. ISSN: 2045-2322 (Electronic) 2045-2322 (Linking). DOI: [10.1038/srep45508](https://doi.org/10.1038/srep45508). URL: <https://www.ncbi.nlm.nih.gov/pubmed/28349959>.
- Bragin, A. et al. (1995). "Gamma (40-100 Hz) oscillation in the hippocampus of the behaving rat". In: *The Journal of Neuroscience* 15.1. Section: 47, pp. 47–60. ISSN: 0270-6474 1529-2401. DOI: [10.1523/jneurosci.15-01-00047.1995](https://doi.org/10.1523/jneurosci.15-01-00047.1995).
- Braitenberg, V. (1961). "Functional Interpretation of Cerebellar Histology". In: *Nature* 190.4775. Section: 539, pp. 539–540. ISSN: 0028-0836 1476-4687. DOI: [10.1038/190539b0](https://doi.org/10.1038/190539b0).
- (1967). "Is the cerebellar cortex a biological clock in the millisecond range?" In: *Prog Brain Res* 25, pp. 334–46. ISSN: 0079-6123 (Print) 0079-6123 (Linking). DOI: [10.1016/S0079-6123\(08\)60971-1](https://doi.org/10.1016/S0079-6123(08)60971-1). URL: <https://www.ncbi.nlm.nih.gov/pubmed/6081778>.
- Braitenberg, V., D. Heck, and F. Sultan (June 1997). "The detection and generation of sequences as a key to cerebellar function: experiments and theory". In: *Behav Brain Sci* 20.2, 229–45, discussion 245–77. ISSN: 0140-525X (Print) 0140-525X (Linking). URL: <https://www.ncbi.nlm.nih.gov/pubmed/10096998>.
- Brown, C. et al. (June 2005). "Gamma abnormalities during perception of illusory figures in autism". In: *Cortex* 41.3, pp. 364–76. ISSN: 0010-9452 (Print) 0010-9452 (Linking). DOI: [10.1016/S0010-9452\(08\)70273-9](https://doi.org/10.1016/S0010-9452(08)70273-9). URL: <https://www.ncbi.nlm.nih.gov/pubmed/15871601>.
- Bryant, J. L. et al. (July 2010). "Cerebellar cortical output encodes temporal aspects of rhythmic licking movements and is necessary for normal licking frequency". In: *Eur J Neurosci* 32.1. Edition: 20100628, pp. 41–52. ISSN: 1460-9568 (Electronic) 0953-816X (Linking). DOI: [10.1111/j.1460-9568.2010.07244.x](https://doi.org/10.1111/j.1460-9568.2010.07244.x). URL: <https://www.ncbi.nlm.nih.gov/pubmed/20597972>.
- Buckner, R. L. (Oct. 30, 2013). "The cerebellum and cognitive function: 25 years of insight from anatomy and neuroimaging". In: *Neuron* 80.3, pp. 807–15. ISSN: 1097-4199 (Electronic) 0896-6273 (Linking). DOI: [10.1016/j.neuron.2013.10.044](https://doi.org/10.1016/j.neuron.2013.10.044). URL: <https://www.ncbi.nlm.nih.gov/pubmed/24183029>.
- Buzsaki, G. (Oct. 2015). "Hippocampal sharp wave-ripple: A cognitive biomarker for episodic memory and planning". In: *Hippocampus* 25.10, pp. 1073–188. ISSN: 1098-1063 (Electronic) 1050-9631 (Linking). DOI: [10.1002/hipo.22488](https://doi.org/10.1002/hipo.22488). URL: <https://www.ncbi.nlm.nih.gov/pubmed/26135716>.
- Buzsaki, G., C. A. Anastassiou, and C. Koch (May 18, 2012). "The origin of extracellular fields and currents—EEG, ECoG, LFP and spikes". In: *Nat Rev Neurosci* 13.6. Edition: 20120518, pp. 407–20. ISSN: 1471-0048 (Electronic) 1471-003X (Linking). DOI: [10.1038/nrn3241](https://doi.org/10.1038/nrn3241). URL: <https://www.ncbi.nlm.nih.gov/pubmed/22595786>.

- Buzsáki, György (2002). "Theta Oscillations in the Hippocampus". In: *Neuron* 33.3. Section: 325, pp. 325–340. ISSN: 08966273. DOI: [10.1016/s0896-6273\(02\)00586-x](https://doi.org/10.1016/s0896-6273(02)00586-x).
- Canolty, R. T. et al. (Sept. 15, 2006). "High gamma power is phase-locked to theta oscillations in human neocortex". In: *Science* 313.5793, pp. 1626–8. ISSN: 1095-9203 (Electronic) 0036-8075 (Linking). DOI: [10.1126/science.1128115](https://doi.org/10.1126/science.1128115). URL: <https://www.ncbi.nlm.nih.gov/pubmed/16973878>.
- Canolty, Ryan T. and Robert T. Knight (2010). "The functional role of cross-frequency coupling". In: *Trends in Cognitive Sciences* 14.11. Section: 506, pp. 506–515. ISSN: 13646613. DOI: [10.1016/j.tics.2010.09.001](https://doi.org/10.1016/j.tics.2010.09.001).
- Chaudhry, F. A. et al. (Dec. 1, 1998). "The vesicular GABA transporter, VGAT, localizes to synaptic vesicles in sets of glycinergic as well as GABAergic neurons". In: *J Neurosci* 18.23, pp. 9733–50. ISSN: 0270-6474 (Print) 0270-6474 (Linking). URL: <https://www.ncbi.nlm.nih.gov/pubmed/9822734>.
- Cheron, Guy et al. (2022). "Electrophysiological alterations of the Purkinje cells and deep cerebellar neurons in a mouse model of Alzheimer disease (electrophysiology on cerebellum of AD mice)". In: *European Journal of Neuroscience*. ISSN: 0953-816X 1460-9568. DOI: [10.1111/ejn.15621](https://doi.org/10.1111/ejn.15621).
- Churchwell, J. C. and R. P. Kesner (Dec. 1, 2011). "Hippocampal-prefrontal dynamics in spatial working memory: interactions and independent parallel processing". In: *Behav Brain Res* 225.2. Edition: 20110803, pp. 389–95. ISSN: 1872-7549 (Electronic) 0166-4328 (Linking). DOI: [10.1016/j.bbr.2011.07.045](https://doi.org/10.1016/j.bbr.2011.07.045). URL: <https://www.ncbi.nlm.nih.gov/pubmed/21839780>.
- Clasca, F., P. Rubio-Garrido, and D. Jabaudon (May 2012). "Unveiling the diversity of thalamocortical neuron subtypes". In: *Eur J Neurosci* 35.10, pp. 1524–32. ISSN: 1460-9568 (Electronic) 0953-816X (Linking). DOI: [10.1111/j.1460-9568.2012.08033.x](https://doi.org/10.1111/j.1460-9568.2012.08033.x). URL: <https://www.ncbi.nlm.nih.gov/pubmed/22606998>.
- Cohen, Michael X., Christian E. Elger, and Juergen Fell (2008). "Oscillatory Activity and Phase-Amplitude Coupling in the Human Medial Frontal Cortex during Decision Making". In: *Journal of Cognitive Neuroscience* 21.2. Section: 390, pp. 390–402. ISSN: 0898-929X 1530-8898. DOI: [10.1162/jocn.2008.21020](https://doi.org/10.1162/jocn.2008.21020).
- Cole, S. R. and B. Voytek (Feb. 2017). "Brain Oscillations and the Importance of Waveform Shape". In: *Trends Cogn Sci* 21.2. Edition: 20170104, pp. 137–149. ISSN: 1879-307X (Electronic) 1364-6613 (Linking). DOI: [10.1016/j.tics.2016.12.008](https://doi.org/10.1016/j.tics.2016.12.008). URL: <https://www.ncbi.nlm.nih.gov/pubmed/28063662>.
- Colgin, Laura Lee (2015). "Theta-gamma coupling in the entorhinal-hippocampal system". In: *Current Opinion in Neurobiology* 31. Section: 45, pp. 45–50. ISSN: 09594388. DOI: [10.1016/j.conb.2014.08.001](https://doi.org/10.1016/j.conb.2014.08.001).
- Conde, F. et al. (Feb. 20, 1995). "Afferent connections of the medial frontal cortex of the rat. II. Cortical and subcortical afferents". In: *J Comp Neurol* 352.4, pp. 567–93. ISSN: 0021-9967 (Print) 0021-9967 (Linking). DOI: [10.1002/cne.903520407](https://doi.org/10.1002/cne.903520407). URL: <https://www.ncbi.nlm.nih.gov/pubmed/7722001>.

- Courchesne, E. (Apr. 1997). "Brainstem, cerebellar and limbic neuroanatomical abnormalities in autism". In: *Curr Opin Neurobiol* 7.2, pp. 269–78. ISSN: 0959-4388 (Print) 0959-4388 (Linking). DOI: [10.1016/s0959-4388\(97\)80016-5](https://doi.org/10.1016/s0959-4388(97)80016-5). URL: <https://www.ncbi.nlm.nih.gov/pubmed/9142760>.
- Courtney, S. M. et al. (Jan. 1996). "Object and spatial visual working memory activate separate neural systems in human cortex". In: *Cereb Cortex* 6.1, pp. 39–49. ISSN: 1047-3211 (Print) 1047-3211 (Linking). DOI: [10.1093/cercor/6.1.39](https://doi.org/10.1093/cercor/6.1.39). URL: <https://www.ncbi.nlm.nih.gov/pubmed/8670637>.
- Crone, N. E. et al. (Dec. 11, 2001). "Electrocorticographic gamma activity during word production in spoken and sign language". In: *Neurology* 57.11, pp. 2045–53. ISSN: 0028-3878 (Print) 0028-3878 (Linking). DOI: [10.1212/wnl.57.11.2045](https://doi.org/10.1212/wnl.57.11.2045). URL: <https://www.ncbi.nlm.nih.gov/pubmed/11739824>.
- D'Angelo, E. and C. I. De Zeeuw (Jan. 2009). "Timing and plasticity in the cerebellum: focus on the granular layer". In: *Trends Neurosci* 32.1. Edition: 20081030, pp. 30–40. ISSN: 0166-2236 (Print) 0166-2236 (Linking). DOI: [10.1016/j.tins.2008.09.007](https://doi.org/10.1016/j.tins.2008.09.007). URL: <https://www.ncbi.nlm.nih.gov/pubmed/18977038>.
- De Zeeuw, C. I. and C. H. Yeo (Dec. 2005). "Time and tide in cerebellar memory formation". In: *Curr Opin Neurobiol* 15.6. Edition: 20051103, pp. 667–74. ISSN: 0959-4388 (Print) 0959-4388 (Linking). DOI: [10.1016/j.conb.2005.10.008](https://doi.org/10.1016/j.conb.2005.10.008). URL: <https://www.ncbi.nlm.nih.gov/pubmed/16271462>.
- Del Negro, C. A., G. D. Funk, and J. L. Feldman (June 2018). "Breathing matters". In: *Nat Rev Neurosci* 19.6, pp. 351–367. ISSN: 1471-0048 (Electronic) 1471-003X (Linking). DOI: [10.1038/s41583-018-0003-6](https://doi.org/10.1038/s41583-018-0003-6). URL: <https://www.ncbi.nlm.nih.gov/pubmed/29740175>.
- Desmond, J. E. et al. (Dec. 15, 1997). "Lobular patterns of cerebellar activation in verbal working-memory and finger-tapping tasks as revealed by functional MRI". In: *J Neurosci* 17.24, pp. 9675–85. ISSN: 0270-6474 (Print) 0270-6474 (Linking). URL: <https://www.ncbi.nlm.nih.gov/pubmed/9391022>.
- Diesmann, M., M. O. Gewaltig, and A. Aertsen (Dec. 2, 1999). "Stable propagation of synchronous spiking in cortical neural networks". In: *Nature* 402.6761, pp. 529–33. ISSN: 0028-0836 (Print) 0028-0836 (Linking). DOI: [10.1038/990101](https://doi.org/10.1038/990101). URL: <https://www.ncbi.nlm.nih.gov/pubmed/10591212>.
- Dolleman-van der Weel, M. J. et al. (July 2019). "The nucleus reuniens of the thalamus sits at the nexus of a hippocampus and medial prefrontal cortex circuit enabling memory and behavior". In: *Learn Mem* 26.7. Edition: 20190617, pp. 191–205. ISSN: 1549-5485 (Electronic) 1072-0502 (Linking). DOI: [10.1101/lm.048389.118](https://doi.org/10.1101/lm.048389.118). URL: <https://www.ncbi.nlm.nih.gov/pubmed/31209114>.
- Ebert, D. et al. (July 7, 1995). "Ataxic breathing during alternating forearm movements of various frequencies in cerebellar patients". In: *Neurosci Lett* 193.3, pp. 145–8. ISSN: 0304-3940 (Print) 0304-3940 (Linking). DOI: [10.1016/0304-3940\(95\)11674-1](https://doi.org/10.1016/0304-3940(95)11674-1). URL: <https://www.ncbi.nlm.nih.gov/pubmed/7478169>.

- Eckhorn, R. and A. Obermueller (1993). "Single neurons are differently involved in stimulus-specific oscillations in cat visual cortex". In: *Exp Brain Res* 95.1, pp. 177–82. ISSN: 0014-4819 (Print) 0014-4819 (Linking). DOI: [10.1007/BF00229667](https://doi.org/10.1007/BF00229667). URL: <https://www.ncbi.nlm.nih.gov/pubmed/8405251>.
- Eldar, E., J. D. Cohen, and Y. Niv (Aug. 2013). "The effects of neural gain on attention and learning". In: *Nat Neurosci* 16.8. Edition: 20130616, pp. 1146–53. ISSN: 1546-1726 (Electronic) 1097-6256 (Linking). DOI: [10.1038/nn.3428](https://doi.org/10.1038/nn.3428). URL: <https://www.ncbi.nlm.nih.gov/pubmed/23770566>.
- Farrokhi, A., S. Tafakori, and M. R. Daliri (Oct. 1, 2022). "Dynamic theta-modulated high frequency oscillations in rat medial prefrontal cortex during spatial working memory task". In: *Physiol Behav* 254. Edition: 20220711, p. 113912. ISSN: 1873-507X (Electronic) 0031-9384 (Linking). DOI: [10.1016/j.physbeh.2022.113912](https://doi.org/10.1016/j.physbeh.2022.113912). URL: <https://www.ncbi.nlm.nih.gov/pubmed/35835179>.
- Fatemi, S. H. et al. (Sept. 2012). "Consensus paper: pathological role of the cerebellum in autism". In: *Cerebellum* 11.3, pp. 777–807. ISSN: 1473-4230 (Electronic) 1473-4222 (Linking). DOI: [10.1007/s12311-012-0355-9](https://doi.org/10.1007/s12311-012-0355-9). URL: <https://www.ncbi.nlm.nih.gov/pubmed/22370873>.
- Fiez, J. A. et al. (Jan. 15, 1996). "A positron emission tomography study of the short-term maintenance of verbal information". In: *J Neurosci* 16.2, pp. 808–22. ISSN: 0270-6474 (Print) 0270-6474 (Linking). URL: <https://www.ncbi.nlm.nih.gov/pubmed/8551361>.
- Flurkey, K and DE Harrison (2007). *The mouse in aging research*. Burlington: American College Laboratory Animal Medicine.
- Fries, P. (Oct. 2005). "A mechanism for cognitive dynamics: neuronal communication through neuronal coherence". In: *Trends Cogn Sci* 9.10, pp. 474–80. ISSN: 1364-6613 (Print) 1364-6613 (Linking). DOI: [10.1016/j.tics.2005.08.011](https://doi.org/10.1016/j.tics.2005.08.011). URL: <https://www.ncbi.nlm.nih.gov/pubmed/16150631>.
- (Oct. 7, 2015). "Rhythms for Cognition: Communication through Coherence". In: *Neuron* 88.1, pp. 220–35. ISSN: 1097-4199 (Electronic) 0896-6273 (Linking). DOI: [10.1016/j.neuron.2015.09.034](https://doi.org/10.1016/j.neuron.2015.09.034). URL: <https://www.ncbi.nlm.nih.gov/pubmed/26447583>.
- Friston, K. J. et al. (Apr. 2015). "LFP and oscillations-what do they tell us?" In: *Curr Opin Neurobiol* 31. Edition: 20140730, pp. 1–6. ISSN: 1873-6882 (Electronic) 0959-4388 (Linking). DOI: [10.1016/j.conb.2014.05.004](https://doi.org/10.1016/j.conb.2014.05.004). URL: <https://www.ncbi.nlm.nih.gov/pubmed/25079053>.
- Furth, K. E. et al. (2013). "Dopamine, cognitive function, and gamma oscillations: role of D4 receptors". In: *Front Cell Neurosci* 7. Edition: 20130702, p. 102. ISSN: 1662-5102 (Print) 1662-5102 (Linking). DOI: [10.3389/fncel.2013.00102](https://doi.org/10.3389/fncel.2013.00102). URL: <https://www.ncbi.nlm.nih.gov/pubmed/23847468>.
- Goodlett, C. R., K. M. Hamre, and J. R. West (Apr. 10, 1992). "Dissociation of spatial navigation and visual guidance performance in Purkinje cell degeneration (pcd) mutant mice". In: *Behav Brain Res* 47.2, pp. 129–41. ISSN: 0166-4328 (Print) 0166-4328 (Linking). DOI: [10.1016/s0166-4328\(05\)80119-6](https://doi.org/10.1016/s0166-4328(05)80119-6). URL: <https://www.ncbi.nlm.nih.gov/pubmed/1590945>.

- Gordon, J. A. (June 2011). "Oscillations and hippocampal-prefrontal synchrony". In: *Curr Opin Neurobiol* 21.3. Edition: 20110404, pp. 486–91. ISSN: 1873-6882 (Electronic) 0959-4388 (Linking). DOI: [10.1016/j.conb.2011.02.012](https://doi.org/10.1016/j.conb.2011.02.012). URL: <https://www.ncbi.nlm.nih.gov/pubmed/21470846>.
- Grasby, P. M. et al. (Dec. 1994). "A graded task approach to the functional mapping of brain areas implicated in auditory-verbal memory". In: *Brain* 117 (Pt 6), pp. 1271–82. ISSN: 0006-8950 (Print) 0006-8950 (Linking). DOI: [10.1093/brain/117.6.1271](https://doi.org/10.1093/brain/117.6.1271). URL: <https://www.ncbi.nlm.nih.gov/pubmed/7820565>.
- Gray, C. M. et al. (Mar. 23, 1989). "Oscillatory responses in cat visual cortex exhibit inter-columnar synchronization which reflects global stimulus properties". In: *Nature* 338.6213, pp. 334–7. ISSN: 0028-0836 (Print) 0028-0836 (Linking). DOI: [10.1038/338334a0](https://doi.org/10.1038/338334a0). URL: <https://www.ncbi.nlm.nih.gov/pubmed/2922061>.
- Greicius, M. D. et al. (Jan. 2009). "Resting-state functional connectivity reflects structural connectivity in the default mode network". In: *Cereb Cortex* 19.1. Edition: 20080409, pp. 72–8. ISSN: 1460-2199 (Electronic) 1047-3211 (Linking). DOI: [10.1093/cercor/bhn059](https://doi.org/10.1093/cercor/bhn059). URL: <https://www.ncbi.nlm.nih.gov/pubmed/18403396>.
- Griffin, A. L. (Sept. 2021). "The nucleus reuniens orchestrates prefrontal-hippocampal synchrony during spatial working memory". In: *Neurosci Biobehav Rev* 128. Edition: 20210701, pp. 415–420. ISSN: 1873-7528 (Electronic) 0149-7634 (Linking). DOI: [10.1016/j.neubiorev.2021.05.033](https://doi.org/10.1016/j.neubiorev.2021.05.033). URL: <https://www.ncbi.nlm.nih.gov/pubmed/34217746>.
- Grossman, Dave and Loren W. Christensen (2008). *On combat : the psychology and physiology of deadly conflict in war and in peace*. Third edition. Illinois: Warrior Science Pub. xxiv, 403 pages : illustrations. ISBN: 9780964920545 (paperback).
- Grund, M. et al. (Jan. 26, 2022). "Respiration, Heartbeat, and Conscious Tactile Perception". In: *J Neurosci* 42.4. Edition: 20211201, pp. 643–656. ISSN: 1529-2401 (Electronic) 0270-6474 (Linking). DOI: [10.1523/JNEUROSCI.0592-21.2021](https://doi.org/10.1523/JNEUROSCI.0592-21.2021). URL: <https://www.ncbi.nlm.nih.gov/pubmed/34853084>.
- Hardemark Cedborg, A. I. et al. (Apr. 2009). "Co-ordination of spontaneous swallowing with respiratory airflow and diaphragmatic and abdominal muscle activity in healthy adult humans". In: *Exp Physiol* 94.4. Edition: 20090112, pp. 459–68. ISSN: 1469-445X (Electronic) 0958-0670 (Linking). DOI: [10.1113/expphysiol.2008.045724](https://doi.org/10.1113/expphysiol.2008.045724). URL: <https://www.ncbi.nlm.nih.gov/pubmed/19139059>.
- Harris, Julie A. et al. (2019). "Hierarchical organization of cortical and thalamic connectivity". In: *Nature* 575.7781. Section: 195, pp. 195–202. ISSN: 0028-0836 1476-4687. DOI: [10.1038/s41586-019-1716-z](https://doi.org/10.1038/s41586-019-1716-z).
- Heck, D. H., R. Kozma, and L. M. Kay (Aug. 1, 2019). "The rhythm of memory: how breathing shapes memory function". In: *J Neurophysiol* 122.2. Edition: 20190619, pp. 563–571. ISSN: 1522-1598 (Electronic) 0022-3077 (Linking). DOI: [10.1152/jn.00200.2019](https://doi.org/10.1152/jn.00200.2019). URL: <https://www.ncbi.nlm.nih.gov/pubmed/31215344>.

- Heck, D. H. et al. (2016). "Breathing as a Fundamental Rhythm of Brain Function". In: *Front Neural Circuits* 10. Edition: 20170112, p. 115. ISSN: 1662-5110 (Electronic) 1662-5110 (Linking). DOI: [10.3389/fncir.2016.00115](https://doi.org/10.3389/fncir.2016.00115). URL: <https://www.ncbi.nlm.nih.gov/pubmed/28127277>.
- Heck, Detlef H. et al. (2022). "Recent insights into respiratory modulation of brain activity offer new perspectives on cognition and emotion". In: *Biological Psychology* 170. Section: 108316. ISSN: 03010511. DOI: [10.1016/j.biopsycho.2022.108316](https://doi.org/10.1016/j.biopsycho.2022.108316).
- Heijden, M. E. van der and H. Y. Zoghbi (July 4, 2018). "Loss of Atoh1 from neurons regulating hypoxic and hypercapnic chemoresponses causes neonatal respiratory failure in mice". In: *Elife* 7. Edition: 20180704. ISSN: 2050-084X (Electronic) 2050-084X (Linking). DOI: [10.7554/eLife.38455](https://doi.org/10.7554/eLife.38455). URL: <https://www.ncbi.nlm.nih.gov/pubmed/29972353>.
- Hemptinne, Coralie de et al. (2013). "Exaggerated phase–amplitude coupling in the primary motor cortex in Parkinson disease". In: *Proceedings of the National Academy of Sciences* 110.12. Section: 4780, pp. 4780–4785. ISSN: 0027-8424 1091-6490. DOI: [10.1073/pnas.1214546110](https://doi.org/10.1073/pnas.1214546110).
- Herrero, J. L. et al. (Jan. 1, 2018). "Breathing above the brain stem: volitional control and attentional modulation in humans". In: *J Neurophysiol* 119.1. Edition: 20170927, pp. 145–159. ISSN: 1522-1598 (Electronic) 0022-3077 (Linking). DOI: [10.1152/jn.00551.2017](https://doi.org/10.1152/jn.00551.2017). URL: <https://www.ncbi.nlm.nih.gov/pubmed/28954895>.
- Holt, G. R. et al. (May 1996). "Comparison of discharge variability in vitro and in vivo in cat visual cortex neurons". In: *J Neurophysiol* 75.5, pp. 1806–14. ISSN: 0022-3077 (Print) 0022-3077 (Linking). DOI: [10.1152/jn.1996.75.5.1806](https://doi.org/10.1152/jn.1996.75.5.1806). URL: <https://www.ncbi.nlm.nih.gov/pubmed/8734581>.
- Hoover, W. B. and R. P. Vertes (Sept. 2007). "Anatomical analysis of afferent projections to the medial prefrontal cortex in the rat". In: *Brain Struct Funct* 212.2. Edition: 20070727, pp. 149–79. ISSN: 1863-2653 (Print) 1863-2653 (Linking). DOI: [10.1007/s00429-007-0150-4](https://doi.org/10.1007/s00429-007-0150-4). URL: <https://www.ncbi.nlm.nih.gov/pubmed/17717690>.
- Huang, Y. et al. (July 31, 2019). "Intracortical Dynamics Underlying Repetitive Stimulation Predicts Changes in Network Connectivity". In: *J Neurosci* 39.31. Edition: 20190610, pp. 6122–6135. ISSN: 1529-2401 (Electronic) 0270-6474 (Linking). DOI: [10.1523/JNEUROSCI.0535-19.2019](https://doi.org/10.1523/JNEUROSCI.0535-19.2019). URL: <https://www.ncbi.nlm.nih.gov/pubmed/31182638>.
- Huijbers, W. et al. (Sept. 2014). "Respiration phase-locks to fast stimulus presentations: implications for the interpretation of posterior midline "deactivations"". In: *Hum Brain Mapp* 35.9. Edition: 20140416, pp. 4932–43. ISSN: 1097-0193 (Electronic) 1065-9471 (Linking). DOI: [10.1002/hbm.22523](https://doi.org/10.1002/hbm.22523). URL: <https://www.ncbi.nlm.nih.gov/pubmed/24737724>.
- Igloi, K. et al. (Nov. 2015). "Interaction Between Hippocampus and Cerebellum Crus I in Sequence-Based but not Place-Based Navigation". In: *Cereb Cortex* 25.11. Edition: 20140619, pp. 4146–54. ISSN: 1460-2199 (Electronic) 1047-3211 (Linking). DOI: [10.1093/cercor/bhu132](https://doi.org/10.1093/cercor/bhu132). URL: <https://www.ncbi.nlm.nih.gov/pubmed/24947462>.
- Ikai, Y., M. Takada, and N. Mizuno (Aug. 1994). "Single neurons in the ventral tegmental area that project to both the cerebral and cerebellar cortical areas by way of axon collaterals". In: *Neuroscience* 61.4, pp. 925–34. ISSN: 0306-4522 (Print) 0306-4522 (Linking). DOI: [10.1016/0306-4522\(94\)90413-8](https://doi.org/10.1016/0306-4522(94)90413-8). URL: <https://www.ncbi.nlm.nih.gov/pubmed/7838388>.

- Ito, J. et al. (Apr. 1, 2014). "Whisker barrel cortex delta oscillations and gamma power in the awake mouse are linked to respiration". In: *Nat Commun* 5. Edition: 20140401, p. 3572. ISSN: 2041-1723 (Electronic) 2041-1723 (Linking). DOI: [10.1038/ncomms4572](https://doi.org/10.1038/ncomms4572). URL: <https://www.ncbi.nlm.nih.gov/pubmed/24686563>.
- Ito, M. (Apr. 2008). "Control of mental activities by internal models in the cerebellum". In: *Nat Rev Neurosci* 9.4, pp. 304–13. ISSN: 1471-0048 (Electronic) 1471-003X (Linking). DOI: [10.1038/nrn2332](https://doi.org/10.1038/nrn2332). URL: <https://www.ncbi.nlm.nih.gov/pubmed/18319727>.
- Ivry, R. B. and S. W. Keele (1989). "Timing functions of the cerebellum". In: *J Cogn Neurosci* 1.2, pp. 136–52. ISSN: 0898-929X (Print) 0898-929X (Linking). DOI: [10.1162/jocn.1989.1.2.136](https://doi.org/10.1162/jocn.1989.1.2.136). URL: <https://www.ncbi.nlm.nih.gov/pubmed/23968462>.
- Ivry, R. B. et al. (Dec. 2002). "The cerebellum and event timing". In: *Ann N Y Acad Sci* 978, pp. 302–17. ISSN: 0077-8923 (Print) 0077-8923 (Linking). DOI: [10.1111/j.1749-6632.2002.tb07576.x](https://doi.org/10.1111/j.1749-6632.2002.tb07576.x). URL: <https://www.ncbi.nlm.nih.gov/pubmed/12582062>.
- Jacobs, J. et al. (Apr. 4, 2007). "Brain oscillations control timing of single-neuron activity in humans". In: *J Neurosci* 27.14, pp. 3839–44. ISSN: 1529-2401 (Electronic) 0270-6474 (Linking). DOI: [10.1523/JNEUROSCI.4636-06.2007](https://doi.org/10.1523/JNEUROSCI.4636-06.2007). URL: <https://www.ncbi.nlm.nih.gov/pubmed/17409248>.
- Jadhav, S. P. et al. (June 15, 2012). "Awake hippocampal sharp-wave ripples support spatial memory". In: *Science* 336.6087. Edition: 20120503, pp. 1454–8. ISSN: 1095-9203 (Electronic) 0036-8075 (Linking). DOI: [10.1126/science.1217230](https://doi.org/10.1126/science.1217230). URL: <https://www.ncbi.nlm.nih.gov/pubmed/22555434>.
- Johannknecht, M. and C. Kayser (Feb. 16, 2022). "The influence of the respiratory cycle on reaction times in sensory-cognitive paradigms". In: *Sci Rep* 12.1. Edition: 20220216, p. 2586. ISSN: 2045-2322 (Electronic) 2045-2322 (Linking). DOI: [10.1038/s41598-022-06364-8](https://doi.org/10.1038/s41598-022-06364-8). URL: <https://www.ncbi.nlm.nih.gov/pubmed/35173204>.
- Johansson, F. et al. (Oct. 14, 2014). "Memory trace and timing mechanism localized to cerebellar Purkinje cells". In: *Proc Natl Acad Sci U S A* 111.41. Edition: 20140929, pp. 14930–4. ISSN: 1091-6490 (Electronic) 0027-8424 (Linking). DOI: [10.1073/pnas.1415371111](https://doi.org/10.1073/pnas.1415371111). URL: <https://www.ncbi.nlm.nih.gov/pubmed/25267641>.
- Jones, M. W. and M. A. Wilson (Dec. 2005). "Theta rhythms coordinate hippocampal-prefrontal interactions in a spatial memory task". In: *PLoS Biol* 3.12. Edition: 20051115, e402. ISSN: 1545-7885 (Electronic) 1544-9173 (Linking). DOI: [10.1371/journal.pbio.0030402](https://doi.org/10.1371/journal.pbio.0030402). URL: <https://www.ncbi.nlm.nih.gov/pubmed/16279838>.
- Jonides, J. et al. (July 1997). "Verbal Working Memory Load Affects Regional Brain Activation as Measured by PET". In: *J Cogn Neurosci* 9.4, pp. 462–75. ISSN: 0898-929X (Print) 0898-929X (Linking). DOI: [10.1162/jocn.1997.9.4.462](https://doi.org/10.1162/jocn.1997.9.4.462). URL: <https://www.ncbi.nlm.nih.gov/pubmed/23968211>.
- Kesner, R. P. and J. C. Churchwell (Oct. 2011). "An analysis of rat prefrontal cortex in mediating executive function". In: *Neurobiol Learn Mem* 96.3. Edition: 20110809, pp. 417–31. ISSN: 1095-9564 (Electronic) 1074-7427 (Linking). DOI: [10.1016/j.nlm.2011.07.002](https://doi.org/10.1016/j.nlm.2011.07.002). URL: <https://www.ncbi.nlm.nih.gov/pubmed/21855643>.

- Kim, D. J. et al. (2013). "Disturbed resting state EEG synchronization in bipolar disorder: A graph-theoretic analysis". In: *Neuroimage Clin* 2. Edition: 20130322, pp. 414–23. ISSN: 2213-1582 (Print) 2213-1582 (Linking). DOI: [10.1016/j.nicl.2013.03.007](https://doi.org/10.1016/j.nicl.2013.03.007). URL: <https://www.ncbi.nlm.nih.gov/pubmed/24179795>.
- Klein, A. S. et al. (2016). "Early Cortical Changes in Gamma Oscillations in Alzheimer's Disease". In: *Front Syst Neurosci* 10. Edition: 20161026, p. 83. ISSN: 1662-5137 (Print) 1662-5137 (Linking). DOI: [10.3389/fnsys.2016.00083](https://doi.org/10.3389/fnsys.2016.00083). URL: <https://www.ncbi.nlm.nih.gov/pubmed/27833535>.
- Kluger, D. S. et al. (Dec. 14, 2021). "Respiration aligns perception with neural excitability". In: *Elife* 10. Edition: 20211214. ISSN: 2050-084X (Electronic) 2050-084X (Linking). DOI: [10.7554/eLife.70907](https://doi.org/10.7554/eLife.70907). URL: <https://www.ncbi.nlm.nih.gov/pubmed/34904567>.
- Kuramoto, E. et al. (Jan. 1, 2017). "Individual mediodorsal thalamic neurons project to multiple areas of the rat prefrontal cortex: A single neuron-tracing study using virus vectors". In: *J Comp Neurol* 525.1. Edition: 20160714, pp. 166–185. ISSN: 1096-9861 (Electronic) 0021-9967 (Linking). DOI: [10.1002/cne.24054](https://doi.org/10.1002/cne.24054). URL: <https://www.ncbi.nlm.nih.gov/pubmed/27275581>.
- Lee, I. and R. P. Kesner (Oct. 2003a). "Differential roles of dorsal hippocampal subregions in spatial working memory with short versus intermediate delay". In: *Behav Neurosci* 117.5, pp. 1044–53. ISSN: 0735-7044 (Print) 0735-7044 (Linking). DOI: [10.1037/0735-7044.117.5.1044](https://doi.org/10.1037/0735-7044.117.5.1044). URL: <https://www.ncbi.nlm.nih.gov/pubmed/14570553>.
- (Feb. 15, 2003b). "Time-dependent relationship between the dorsal hippocampus and the prefrontal cortex in spatial memory". In: *J Neurosci* 23.4, pp. 1517–23. ISSN: 1529-2401 (Electronic) 0270-6474 (Linking). URL: <https://www.ncbi.nlm.nih.gov/pubmed/12598640>.
- Leonard, T. K. and K. L. Hoffman (Jan. 23, 2017). "Sharp-Wave Ripples in Primates Are Enhanced near Remembered Visual Objects". In: *Curr Biol* 27.2. Edition: 20161229, pp. 257–262. ISSN: 1879-0445 (Electronic) 0960-9822 (Linking). DOI: [10.1016/j.cub.2016.11.027](https://doi.org/10.1016/j.cub.2016.11.027). URL: <https://www.ncbi.nlm.nih.gov/pubmed/28041797>.
- Leske, S. and S. S. Dalal (Apr. 1, 2019). "Reducing power line noise in EEG and MEG data via spectrum interpolation". In: *Neuroimage* 189. Edition: 20190111, pp. 763–776. ISSN: 1095-9572 (Electronic) 1053-8119 (Linking). DOI: [10.1016/j.neuroimage.2019.01.026](https://doi.org/10.1016/j.neuroimage.2019.01.026). URL: <https://www.ncbi.nlm.nih.gov/pubmed/30639330>.
- Libster, A. M. and Y. Yarom (2013). "In and out of the loop: external and internal modulation of the olivo-cerebellar loop". In: *Front Neural Circuits* 7. Edition: 20130419, p. 73. ISSN: 1662-5110 (Print) 1662-5110 (Linking). DOI: [10.3389/fncir.2013.00073](https://doi.org/10.3389/fncir.2013.00073). URL: <https://www.ncbi.nlm.nih.gov/pubmed/23626524>.
- Lindeman, S. et al. (Jan. 12, 2021). "Cerebellar Purkinje cells can differentially modulate coherence between sensory and motor cortex depending on region and behavior". In: *Proc Natl Acad Sci U S A* 118.2. ISSN: 1091-6490 (Electronic) 0027-8424 (Linking). DOI: [10.1073/pnas.2015292118](https://doi.org/10.1073/pnas.2015292118). URL: <https://www.ncbi.nlm.nih.gov/pubmed/33443203>.

- Lisman, J. E. and A. A. Grace (June 2, 2005). "The hippocampal-VTA loop: controlling the entry of information into long-term memory". In: *Neuron* 46.5, pp. 703–13. ISSN: 0896-6273 (Print) 0896-6273 (Linking). DOI: [10.1016/j.neuron.2005.05.002](https://doi.org/10.1016/j.neuron.2005.05.002). URL: <https://www.ncbi.nlm.nih.gov/pubmed/15924857>.
- Liu, Y., S. S. McAfee, and D. H. Heck (Aug. 21, 2017). "Hippocampal sharp-wave ripples in awake mice are entrained by respiration". In: *Sci Rep* 7.1. Edition: 20170821, p. 8950. ISSN: 2045-2322 (Electronic) 2045-2322 (Linking). DOI: [10.1038/s41598-017-09511-8](https://doi.org/10.1038/s41598-017-09511-8). URL: <https://www.ncbi.nlm.nih.gov/pubmed/28827599>.
- Liu, Y. et al. (Apr. 13, 2020). "Loss of cerebellar function selectively affects intrinsic rhythmicity of eupneic breathing". In: *Biol Open* 9.4. Edition: 20200413. ISSN: 2046-6390 (Print) 2046-6390 (Linking). DOI: [10.1242/bio.048785](https://doi.org/10.1242/bio.048785). URL: <https://www.ncbi.nlm.nih.gov/pubmed/32086251>.
- Liu, Y. et al. (Feb. 26, 2022). "Causal Evidence for a Role of Cerebellar Lobulus Simplex in Prefrontal-Hippocampal Interaction in Spatial Working Memory Decision-Making". In: *Cerebellum*. Edition: 20220226. ISSN: 1473-4230 (Electronic) 1473-4222 (Linking). DOI: [10.1007/s12311-022-01383-7](https://doi.org/10.1007/s12311-022-01383-7). URL: <https://www.ncbi.nlm.nih.gov/pubmed/35218525>.
- Llinás, Rodolfo R. (1988). "The Intrinsic Electrophysiological Properties of Mammalian Neurons: Insights into Central Nervous System Function". In: *Science* 242.4886. Section: 1654, pp. 1654–1664. ISSN: 0036-8075 1095-9203. DOI: [10.1126/science.3059497](https://doi.org/10.1126/science.3059497).
- Logothetis, N. K. et al. (Nov. 22, 2012). "Hippocampal-cortical interaction during periods of subcortical silence". In: *Nature* 491.7425, pp. 547–53. ISSN: 1476-4687 (Electronic) 0028-0836 (Linking). DOI: [10.1038/nature11618](https://doi.org/10.1038/nature11618). URL: <https://www.ncbi.nlm.nih.gov/pubmed/23172213>.
- Lu, L. et al. (2013). "Medial cerebellar nuclear projections and activity patterns link cerebellar output to orofacial and respiratory behavior". In: *Front Neural Circuits* 7. Edition: 20130402, p. 56. ISSN: 1662-5110 (Print) 1662-5110 (Linking). DOI: [10.3389/fncir.2013.00056](https://doi.org/10.3389/fncir.2013.00056). URL: <https://www.ncbi.nlm.nih.gov/pubmed/23565078>.
- Macey, P. M. et al. (Mar. 2005). "Hypoxia reveals posterior thalamic, cerebellar, midbrain, and limbic deficits in congenital central hypoventilation syndrome". In: *J Appl Physiol* (1985) 98.3. Edition: 20041105, pp. 958–69. ISSN: 8750-7587 (Print) 0161-7567 (Linking). DOI: [10.1152/japplphysiol.00969.2004](https://doi.org/10.1152/japplphysiol.00969.2004). URL: <https://www.ncbi.nlm.nih.gov/pubmed/15531561>.
- Maingret, N. et al. (July 2016). "Hippocampo-cortical coupling mediates memory consolidation during sleep". In: *Nat Neurosci* 19.7. Edition: 20160516, pp. 959–64. ISSN: 1546-1726 (Electronic) 1097-6256 (Linking). DOI: [10.1038/nn.4304](https://doi.org/10.1038/nn.4304). URL: <https://www.ncbi.nlm.nih.gov/pubmed/27182818>.
- Malvache, A. et al. (Sept. 16, 2016). "Awake hippocampal reactivations project onto orthogonal neuronal assemblies". In: *Science* 353.6305, pp. 1280–3. ISSN: 1095-9203 (Electronic) 0036-8075 (Linking). DOI: [10.1126/science.aaf3319](https://doi.org/10.1126/science.aaf3319). URL: <https://www.ncbi.nlm.nih.gov/pubmed/27634534>.

- Mauk, M. D. and D. V. Buonomano (2004). "The neural basis of temporal processing". In: *Annu Rev Neurosci* 27, pp. 307–40. ISSN: 0147-006X (Print) 0147-006X (Linking). DOI: [10.1146/annurev.neuro.27.070203.144247](https://doi.org/10.1146/annurev.neuro.27.070203.144247). URL: <https://www.ncbi.nlm.nih.gov/pubmed/15217335>.
- McAfee, S. S. et al. (May 21, 2019). "Cerebellar Lobulus Simplex and Crus I Differentially Represent Phase and Phase Difference of Prefrontal Cortical and Hippocampal Oscillations". In: *Cell Rep* 27.8, 2328–2334 e3. ISSN: 2211-1247 (Electronic). DOI: [10.1016/j.celrep.2019.04.085](https://doi.org/10.1016/j.celrep.2019.04.085). URL: <https://www.ncbi.nlm.nih.gov/pubmed/31116979>.
- (2021). "Cerebellar Coordination of Neuronal Communication in Cerebral Cortex". In: *Front Syst Neurosci* 15. Edition: 20220111, p. 781527. ISSN: 1662-5137 (Print) 1662-5137 (Linking). DOI: [10.3389/fnsys.2021.781527](https://doi.org/10.3389/fnsys.2021.781527). URL: <https://www.ncbi.nlm.nih.gov/pubmed/35087384>.
- McLaughlin, J. and R. E. See (July 2003). "Selective inactivation of the dorsomedial prefrontal cortex and the basolateral amygdala attenuates conditioned-cued reinstatement of extinguished cocaine-seeking behavior in rats". In: *Psychopharmacology (Berl)* 168.1. Edition: 20020905, pp. 57–65. ISSN: 0033-3158 (Print) 0033-3158 (Linking). DOI: [10.1007/s00213-002-1196-x](https://doi.org/10.1007/s00213-002-1196-x). URL: <https://www.ncbi.nlm.nih.gov/pubmed/12845418>.
- Meij, R. van der, M. Kahana, and E. Maris (2012). "Phase-Amplitude Coupling in Human Electro-corticography Is Spatially Distributed and Phase Diverse". In: *Journal of Neuroscience* 32.1. Section: 111, pp. 111–123. ISSN: 0270-6474 1529-2401. DOI: [10.1523/jneurosci.4816-11.2012](https://doi.org/10.1523/jneurosci.4816-11.2012).
- Mewett, D. T., K. J. Reynolds, and H. Nazeran (July 2004). "Reducing power line interference in digitised electromyogram recordings by spectrum interpolation". In: *Med Biol Eng Comput* 42.4, pp. 524–31. ISSN: 0140-0118 (Print) 0140-0118 (Linking). DOI: [10.1007/BF02350994](https://doi.org/10.1007/BF02350994). URL: <https://www.ncbi.nlm.nih.gov/pubmed/15320462>.
- Middleton, F. A. and P. L. Strick (Jan. 15, 2001). "Cerebellar projections to the prefrontal cortex of the primate". In: *J Neurosci* 21.2, pp. 700–12. ISSN: 1529-2401 (Electronic) 0270-6474 (Linking). URL: <https://www.ncbi.nlm.nih.gov/pubmed/11160449>.
- Molinari, M., L. G. Grammaldo, and L. Petrosini (Sept. 1997). "Cerebellar contribution to spatial event processing: right/left discrimination abilities in rats". In: *Eur J Neurosci* 9.9, pp. 1986–92. ISSN: 0953-816X (Print) 0953-816X (Linking). DOI: [10.1111/j.1460-9568.1997.tb00766.x](https://doi.org/10.1111/j.1460-9568.1997.tb00766.x). URL: <https://www.ncbi.nlm.nih.gov/pubmed/9383222>.
- Moruzzi, Giuseppe (1940). "Paleocerebellar Inhibition of Vasomotor and Respiratory Carotid Sinus Reflexes". In: *Journal of Neurophysiology* 3.1. Section: 20, pp. 20–32. ISSN: 0022-3077 1522-1598. DOI: [10.1152/jn.1940.3.1.20](https://doi.org/10.1152/jn.1940.3.1.20).
- Murthy, V. N. and E. E. Fetz (Dec. 1996). "Synchronization of neurons during local field potential oscillations in sensorimotor cortex of awake monkeys". In: *J Neurophysiol* 76.6, pp. 3968–82. ISSN: 0022-3077 (Print) 0022-3077 (Linking). DOI: [10.1152/jn.1996.76.6.3968](https://doi.org/10.1152/jn.1996.76.6.3968). URL: <https://www.ncbi.nlm.nih.gov/pubmed/8985893>.

- Nakajima, M. and M. M. Halassa (June 2017). "Thalamic control of functional cortical connectivity". In: *Curr Opin Neurobiol* 44. Edition: 20170506, pp. 127–131. ISSN: 1873-6882 (Electronic) 0959-4388 (Linking). DOI: [10.1016/j.conb.2017.04.001](https://doi.org/10.1016/j.conb.2017.04.001). URL: <https://www.ncbi.nlm.nih.gov/pubmed/28486176>.
- Nakamura, N. H., M. Fukunaga, and Y. Oku (2018). "Respiratory modulation of cognitive performance during the retrieval process". In: *PLoS One* 13.9. Edition: 20180914, e0204021. ISSN: 1932-6203 (Electronic) 1932-6203 (Linking). DOI: [10.1371/journal.pone.0204021](https://doi.org/10.1371/journal.pone.0204021). URL: <https://www.ncbi.nlm.nih.gov/pubmed/30216372>.
- Nase, G. et al. (Aug. 2003). "Features of neuronal synchrony in mouse visual cortex". In: *J Neurophysiol* 90.2. Edition: 20030417, pp. 1115–23. ISSN: 0022-3077 (Print) 0022-3077 (Linking). DOI: [10.1152/jn.00480.2002](https://doi.org/10.1152/jn.00480.2002). URL: <https://www.ncbi.nlm.nih.gov/pubmed/12702711>.
- Newman, P. P. and H. Reza (Feb. 1979). "Functional relationships between the hippocampus and the cerebellum: an electrophysiological study of the cat". In: *J Physiol* 287, pp. 405–26. ISSN: 0022-3751 (Print) 0022-3751 (Linking). DOI: [10.1113/jphysiol.1979.sp012667](https://doi.org/10.1113/jphysiol.1979.sp012667). URL: <https://www.ncbi.nlm.nih.gov/pubmed/430426>.
- Nicolai, C. von et al. (2014). "Corticostratial Coordination through Coherent Phase-Amplitude Coupling". In: *Journal of Neuroscience* 34.17. Section: 5938, pp. 5938–5948. ISSN: 0270-6474 1529-2401. DOI: [10.1523/jneurosci.5007-13.2014](https://doi.org/10.1523/jneurosci.5007-13.2014).
- Nicole, O. et al. (Mar. 7, 2016). "Soluble amyloid beta oligomers block the learning-induced increase in hippocampal sharp wave-ripple rate and impair spatial memory formation". In: *Sci Rep* 6. Edition: 20160307, p. 22728. ISSN: 2045-2322 (Electronic) 2045-2322 (Linking). DOI: [10.1038/srep22728](https://doi.org/10.1038/srep22728). URL: <https://www.ncbi.nlm.nih.gov/pubmed/26947247>.
- Oh, Seung Wook et al. (2014). "A mesoscale connectome of the mouse brain". In: *Nature* 508.7495. Section: 207, pp. 207–214. ISSN: 0028-0836 1476-4687. DOI: [10.1038/nature13186](https://doi.org/10.1038/nature13186).
- Onslow, A. C., R. Bogacz, and M. W. Jones (Mar. 2011). "Quantifying phase-amplitude coupling in neuronal network oscillations". In: *Prog Biophys Mol Biol* 105.1. Edition: 20100930, pp. 49–57. ISSN: 1873-1732 (Electronic) 0079-6107 (Linking). DOI: [10.1016/j.pbiomolbio.2010.09.007](https://doi.org/10.1016/j.pbiomolbio.2010.09.007). URL: <https://www.ncbi.nlm.nih.gov/pubmed/20869387>.
- Onuki, Y. et al. (Feb. 2015). "Hippocampal-cerebellar interaction during spatio-temporal prediction". In: *Cereb Cortex* 25.2. Edition: 20130822, pp. 313–21. ISSN: 1460-2199 (Electronic) 1047-3211 (Linking). DOI: [10.1093/cercor/bht221](https://doi.org/10.1093/cercor/bht221). URL: <https://www.ncbi.nlm.nih.gov/pubmed/23968839>.
- Osipova, D. et al. (July 12, 2006). "Theta and gamma oscillations predict encoding and retrieval of declarative memory". In: *J Neurosci* 26.28, pp. 7523–31. ISSN: 1529-2401 (Electronic) 0270-6474 (Linking). DOI: [10.1523/JNEUROSCI.1948-06.2006](https://doi.org/10.1523/JNEUROSCI.1948-06.2006). URL: <https://www.ncbi.nlm.nih.gov/pubmed/16837600>.
- Palmen, S. J. et al. (Dec. 2004). "Neuropathological findings in autism". In: *Brain* 127 (Pt 12). Edition: 20040825, pp. 2572–83. ISSN: 1460-2156 (Electronic) 0006-8950 (Linking). DOI: [10.1093/brain/awh287](https://doi.org/10.1093/brain/awh287). URL: <https://www.ncbi.nlm.nih.gov/pubmed/15329353>.

- Papale, A. E. et al. (Dec. 7, 2016). "Interplay between Hippocampal Sharp-Wave-Ripple Events and Vicarious Trial and Error Behaviors in Decision Making". In: *Neuron* 92.5. Edition: 20161117, pp. 975–982. ISSN: 1097-4199 (Electronic) 0896-6273 (Linking). DOI: [10.1016/j.neuron.2016.10.028](https://doi.org/10.1016/j.neuron.2016.10.028). URL: <https://www.ncbi.nlm.nih.gov/pubmed/27866796>.
- Parsons, L. M. et al. (Feb. 13, 2001). "Neuroimaging evidence implicating cerebellum in the experience of hypercapnia and hunger for air". In: *Proc Natl Acad Sci U S A* 98.4, pp. 2041–6. ISSN: 0027-8424 (Print) 0027-8424 (Linking). DOI: [10.1073/pnas.98.4.2041](https://doi.org/10.1073/pnas.98.4.2041). URL: <https://www.ncbi.nlm.nih.gov/pubmed/11172072>.
- Paul, G., B. Elam, and S. J. Verhulst (2007). "A longitudinal study of students' perceptions of using deep breathing meditation to reduce testing stresses". In: *Teach Learn Med* 19.3, pp. 287–92. ISSN: 1040-1334 (Print) 1040-1334 (Linking). DOI: [10.1080/10401330701366754](https://doi.org/10.1080/10401330701366754). URL: <https://www.ncbi.nlm.nih.gov/pubmed/17594225>.
- Paulesu, E., C. D. Frith, and R. S. Frackowiak (Mar. 25, 1993). "The neural correlates of the verbal component of working memory". In: *Nature* 362.6418, pp. 342–5. ISSN: 0028-0836 (Print) 0028-0836 (Linking). DOI: [10.1038/362342a0](https://doi.org/10.1038/362342a0). URL: <https://www.ncbi.nlm.nih.gov/pubmed/8455719>.
- Perl, O. et al. (May 2019). "Human non-olfactory cognition phase-locked with inhalation". In: *Nat Hum Behav* 3.5. Edition: 20190311, pp. 501–512. ISSN: 2397-3374 (Electronic) 2397-3374 (Linking). DOI: [10.1038/s41562-019-0556-z](https://doi.org/10.1038/s41562-019-0556-z). URL: <https://www.ncbi.nlm.nih.gov/pubmed/31089297>.
- Perrett, S. P., B. P. Ruiz, and M. D. Mauk (Apr. 1993). "Cerebellar cortex lesions disrupt learning-dependent timing of conditioned eyelid responses". In: *J Neurosci* 13.4, pp. 1708–18. ISSN: 0270-6474 (Print) 0270-6474 (Linking). URL: <https://www.ncbi.nlm.nih.gov/pubmed/8463846>.
- Person, A. L. and I. M. Raman (2012). "Synchrony and neural coding in cerebellar circuits". In: *Front Neural Circuits* 6. Edition: 20121211, p. 97. ISSN: 1662-5110 (Electronic) 1662-5110 (Linking). DOI: [10.3389/fncir.2012.00097](https://doi.org/10.3389/fncir.2012.00097). URL: <https://www.ncbi.nlm.nih.gov/pubmed/23248585>.
- Pfeiffer, B. E. and D. J. Foster (July 10, 2015). "PLACE CELLS. Autoassociative dynamics in the generation of sequences of hippocampal place cells". In: *Science* 349.6244, pp. 180–3. ISSN: 1095-9203 (Electronic) 0036-8075 (Linking). DOI: [10.1126/science.aaa9633](https://doi.org/10.1126/science.aaa9633). URL: <https://www.ncbi.nlm.nih.gov/pubmed/26160946>.
- Picard, H. et al. (Jan. 2008). "The role of the cerebellum in schizophrenia: an update of clinical, cognitive, and functional evidences". In: *Schizophr Bull* 34.1. Edition: 20070611, pp. 155–72. ISSN: 0586-7614 (Print) 0586-7614 (Linking). DOI: [10.1093/schbul/sbm049](https://doi.org/10.1093/schbul/sbm049). URL: <https://www.ncbi.nlm.nih.gov/pubmed/17562694>.
- Popa, D. et al. (Apr. 10, 2013). "Functional role of the cerebellum in gamma-band synchronization of the sensory and motor cortices". In: *J Neurosci* 33.15, pp. 6552–6. ISSN: 1529-2401 (Electronic) 0270-6474 (Linking). DOI: [10.1523/JNEUROSCI.5521-12.2013](https://doi.org/10.1523/JNEUROSCI.5521-12.2013). URL: <https://www.ncbi.nlm.nih.gov/pubmed/23575852>.

- Rajasethupathy, P. et al. (Oct. 29, 2015). "Projections from neocortex mediate top-down control of memory retrieval". In: *Nature* 526.7575. Edition: 20151005, pp. 653–9. ISSN: 1476-4687 (Electronic) 0028-0836 (Linking). DOI: [10.1038/nature15389](https://doi.org/10.1038/nature15389). URL: <https://www.ncbi.nlm.nih.gov/pubmed/26436451>.
- Ramio-Torrentia, L., E. Gomez, and D. Genis (July 2006). "Swallowing in degenerative ataxias". In: *J Neurol* 253.7. Edition: 20060420, pp. 875–81. ISSN: 0340-5354 (Print) 0340-5354 (Linking). DOI: [10.1007/s00415-006-0122-2](https://doi.org/10.1007/s00415-006-0122-2). URL: <https://www.ncbi.nlm.nih.gov/pubmed/16619126>.
- Ramirez-Villegas, J. F., N. K. Logothetis, and M. Besserve (Nov. 17, 2015). "Diversity of sharp-wave-ripple LFP signatures reveals differentiated brain-wide dynamical events". In: *Proc Natl Acad Sci U S A* 112.46. Edition: 20151104, E6379–87. ISSN: 1091-6490 (Electronic) 0027-8424 (Linking). DOI: [10.1073/pnas.1518257112](https://doi.org/10.1073/pnas.1518257112). URL: <https://www.ncbi.nlm.nih.gov/pubmed/26540729>.
- Rau, H. et al. (May 1993). "Baroreceptor stimulation alters cortical activity". In: *Psychophysiology* 30.3, pp. 322–5. ISSN: 0048-5772 (Print) 0048-5772 (Linking). DOI: [10.1111/j.1469-8986.1993.tb03359.x](https://doi.org/10.1111/j.1469-8986.1993.tb03359.x). URL: <https://www.ncbi.nlm.nih.gov/pubmed/8497561>.
- Rogers, T. D. et al. (Nov. 2011). "Connecting the dots of the cerebro-cerebellar role in cognitive function: neuronal pathways for cerebellar modulation of dopamine release in the prefrontal cortex". In: *Synapse* 65.11. Edition: 20110617, pp. 1204–12. ISSN: 1098-2396 (Electronic) 0887-4476 (Linking). DOI: [10.1002/syn.20960](https://doi.org/10.1002/syn.20960). URL: <https://www.ncbi.nlm.nih.gov/pubmed/21638338>.
- Rojas-Libano, D. et al. (Sept. 1, 2018). "Local cortical activity of distant brain areas can phase-lock to the olfactory bulb's respiratory rhythm in the freely behaving rat". In: *J Neurophysiol* 120.3. Edition: 20180516, pp. 960–972. ISSN: 1522-1598 (Electronic) 0022-3077 (Linking). DOI: [10.1152/jn.00088.2018](https://doi.org/10.1152/jn.00088.2018). URL: <https://www.ncbi.nlm.nih.gov/pubmed/29766764>.
- Rovo, Z., I. Ulbert, and L. Acsady (Dec. 5, 2012). "Drivers of the primate thalamus". In: *J Neurosci* 32.49, pp. 17894–908. ISSN: 1529-2401 (Electronic) 0270-6474 (Linking). DOI: [10.1523/JNEUROSCI.2815-12.2012](https://doi.org/10.1523/JNEUROSCI.2815-12.2012). URL: <https://www.ncbi.nlm.nih.gov/pubmed/23223308>.
- Salman, M. S. (Jan. 2002). "The cerebellum: it's about time! But timing is not everything—new insights into the role of the cerebellum in timing motor and cognitive tasks". In: *J Child Neurol* 17.1, pp. 1–9. ISSN: 0883-0738 (Print) 0883-0738 (Linking). DOI: [10.1177/088307380201700101](https://doi.org/10.1177/088307380201700101). URL: <https://www.ncbi.nlm.nih.gov/pubmed/11913561>.
- Schack, B. et al. (2002). "Phase-coupling of theta–gamma EEG rhythms during short-term memory processing". In: *International Journal of Psychophysiology* 44.2. Section: 143, pp. 143–163. ISSN: 01678760. DOI: [10.1016/s0167-8760\(01\)00199-4](https://doi.org/10.1016/s0167-8760(01)00199-4).
- Schmahmann, J. D. (May 2016). "Cerebellum in Alzheimer's disease and frontotemporal dementia: not a silent bystander". In: *Brain* 139 (Pt 5), pp. 1314–8. ISSN: 1460-2156 (Electronic) 0006-8950 (Linking). DOI: [10.1093/brain/aww064](https://doi.org/10.1093/brain/aww064). URL: <https://www.ncbi.nlm.nih.gov/pubmed/27189578>.

- Sederberg, P. B. et al. (May 2007). "Hippocampal and neocortical gamma oscillations predict memory formation in humans". In: *Cereb Cortex* 17.5. Edition: 20060710, pp. 1190–6. ISSN: 1047-3211 (Print) 1047-3211 (Linking). DOI: 10.1093/cercor/bhl030. URL: <https://www.ncbi.nlm.nih.gov/pubmed/16831858>.
- Shearkhani, O. and K. Takehara-Nishiuchi (Feb. 2013). "Coupling of prefrontal gamma amplitude and theta phase is strengthened in trace eyeblink conditioning". In: *Neurobiol Learn Mem* 100. Edition: 20121223, pp. 117–26. ISSN: 1095-9564 (Electronic) 1074-7427 (Linking). DOI: 10.1016/j.nlm.2012.12.014. URL: <https://www.ncbi.nlm.nih.gov/pubmed/23267870>.
- Sheth, B. R., S. Sandkuhler, and J. Bhattacharya (July 2009). "Posterior Beta and anterior gamma oscillations predict cognitive insight". In: *J Cogn Neurosci* 21.7, pp. 1269–79. ISSN: 0898-929X (Print) 0898-929X (Linking). DOI: 10.1162/jocn.2009.21069. URL: <https://www.ncbi.nlm.nih.gov/pubmed/18702591>.
- Siegel, M., A. K. Engel, and T. H. Donner (2011). "Cortical network dynamics of perceptual decision-making in the human brain". In: *Front Hum Neurosci* 5. Edition: 20110228, p. 21. ISSN: 1662-5161 (Electronic) 1662-5161 (Linking). DOI: 10.3389/fnhum.2011.00021. URL: <https://www.ncbi.nlm.nih.gov/pubmed/21427777>.
- Singer, A. C. et al. (Mar. 20, 2013). "Hippocampal SWR activity predicts correct decisions during the initial learning of an alternation task". In: *Neuron* 77.6, pp. 1163–73. ISSN: 1097-4199 (Electronic) 0896-6273 (Linking). DOI: 10.1016/j.neuron.2013.01.027. URL: <https://www.ncbi.nlm.nih.gov/pubmed/23522050>.
- Sirota, A. et al. (Nov. 26, 2008). "Entrainment of neocortical neurons and gamma oscillations by the hippocampal theta rhythm". In: *Neuron* 60.4, pp. 683–97. ISSN: 1097-4199 (Electronic) 0896-6273 (Linking). DOI: 10.1016/j.neuron.2008.09.014. URL: <https://www.ncbi.nlm.nih.gov/pubmed/19038224>.
- Spellman, T. et al. (June 18, 2015). "Hippocampal-prefrontal input supports spatial encoding in working memory". In: *Nature* 522.7556. Edition: 20150608, pp. 309–14. ISSN: 1476-4687 (Electronic) 0028-0836 (Linking). DOI: 10.1038/nature14445. URL: <https://www.ncbi.nlm.nih.gov/pubmed/26053122>.
- Spoelstra, J., N. Schweighofer, and M. A. Arbib (Apr. 2000). "Cerebellar learning of accurate predictive control for fast-reaching movements". In: *Biol Cybern* 82.4, pp. 321–33. ISSN: 0340-1200 (Print) 0340-1200 (Linking). DOI: 10.1007/s004220050586. URL: <https://www.ncbi.nlm.nih.gov/pubmed/10804064>.
- Strick, P. L., R. P. Dum, and J. A. Fiez (2009). "Cerebellum and nonmotor function". In: *Annu Rev Neurosci* 32, pp. 413–34. ISSN: 1545-4126 (Electronic) 0147-006X (Linking). DOI: 10.1146/annurev.neuro.31.060407.125606. URL: <https://www.ncbi.nlm.nih.gov/pubmed/19555291>.
- Teune, T. M. et al. (2000). "Topography of cerebellar nuclear projections to the brain stem in the rat". In: *Prog Brain Res* 124, pp. 141–72. ISSN: 0079-6123 (Print) 0079-6123 (Linking). DOI: 10.1016/S0079-6123(00)24014-4. URL: <https://www.ncbi.nlm.nih.gov/pubmed/10943123>.

- Timmann, D., S. Watts, and J. Hore (July 1999). "Failure of cerebellar patients to time finger opening precisely causes ball high-low inaccuracy in overarm throws". In: *J Neurophysiol* 82.1, pp. 103–14. ISSN: 0022-3077 (Print) 0022-3077 (Linking). DOI: [10.1152/jn.1999.82.1.103](https://doi.org/10.1152/jn.1999.82.1.103). URL: <https://www.ncbi.nlm.nih.gov/pubmed/10400939>.
- Tomlinson, S. P., N. J. Davis, and R. M. Bracewell (June 2013). "Brain stimulation studies of non-motor cerebellar function: a systematic review". In: *Neurosci Biobehav Rev* 37.5. Edition: 20130313, pp. 766–89. ISSN: 1873-7528 (Electronic) 0149-7634 (Linking). DOI: [10.1016/j.neubiorev.2013.03.001](https://doi.org/10.1016/j.neubiorev.2013.03.001). URL: <https://www.ncbi.nlm.nih.gov/pubmed/23500608>.
- Tomlinson, S. P. et al. (Aug. 22, 2014). "Cerebellar contributions to spatial memory". In: *Neurosci Lett* 578. Edition: 20140705, pp. 182–6. ISSN: 1872-7972 (Electronic) 0304-3940 (Linking). DOI: [10.1016/j.neulet.2014.06.057](https://doi.org/10.1016/j.neulet.2014.06.057). URL: <https://www.ncbi.nlm.nih.gov/pubmed/25004407>.
- Tort, A. B. et al. (Dec. 8, 2009). "Theta-gamma coupling increases during the learning of item-context associations". In: *Proc Natl Acad Sci U S A* 106.49. Edition: 20091123, pp. 20942–7. ISSN: 1091-6490 (Electronic) 0027-8424 (Linking). DOI: [10.1073/pnas.0911331106](https://doi.org/10.1073/pnas.0911331106). URL: <https://www.ncbi.nlm.nih.gov/pubmed/19934062>.
- Tort, Adriano B. L. et al. (2014). "A Canonical Circuit for Generating Phase-Amplitude Coupling". In: *PLoS ONE* 9.8. Section: e102591. ISSN: 1932-6203. DOI: [10.1371/journal.pone.0102591](https://doi.org/10.1371/journal.pone.0102591).
- Towle, V. L. et al. (Aug. 2008). "ECoG gamma activity during a language task: differentiating expressive and receptive speech areas". In: *Brain* 131 (Pt 8). Edition: 20080711, pp. 2013–27. ISSN: 1460-2156 (Electronic) 0006-8950 (Linking). DOI: [10.1093/brain/awn147](https://doi.org/10.1093/brain/awn147). URL: <https://www.ncbi.nlm.nih.gov/pubmed/18669510>.
- Uhlhaas, P. J. et al. (2009). "Neural synchrony in cortical networks: history, concept and current status". In: *Front Integr Neurosci* 3. Edition: 20090730, p. 17. ISSN: 1662-5145 (Electronic) 1662-5145 (Linking). DOI: [10.3389/neuro.07.017.2009](https://doi.org/10.3389/neuro.07.017.2009). URL: <https://www.ncbi.nlm.nih.gov/pubmed/19668703>.
- Vaadia, E. et al. (Feb. 9, 1995). "Dynamics of neuronal interactions in monkey cortex in relation to behavioural events". In: *Nature* 373.6514, pp. 515–8. ISSN: 0028-0836 (Print) 0028-0836 (Linking). DOI: [10.1038/373515a0](https://doi.org/10.1038/373515a0). URL: <https://www.ncbi.nlm.nih.gov/pubmed/7845462>.
- Ven, G. M. van de et al. (Dec. 7, 2016). "Hippocampal Offline Reactivation Consolidates Recently Formed Cell Assembly Patterns during Sharp Wave-Ripples". In: *Neuron* 92.5. Edition: 20161110, pp. 968–974. ISSN: 1097-4199 (Electronic) 0896-6273 (Linking). DOI: [10.1016/j.neuron.2016.10.020](https://doi.org/10.1016/j.neuron.2016.10.020). URL: <https://www.ncbi.nlm.nih.gov/pubmed/27840002>.
- Vertes, R. P. et al. (Mar. 30, 2007). "Nucleus reuniens of the midline thalamus: link between the medial prefrontal cortex and the hippocampus". In: *Brain Res Bull* 71.6. Edition: 20070103, pp. 601–9. ISSN: 0361-9230 (Print) 0361-9230 (Linking). DOI: [10.1016/j.brainresbull.2006.12.002](https://doi.org/10.1016/j.brainresbull.2006.12.002). URL: <https://www.ncbi.nlm.nih.gov/pubmed/17292803>.

- Vugt, M. K. van et al. (Feb. 17, 2010). "Hippocampal gamma oscillations increase with memory load". In: *J Neurosci* 30.7, pp. 2694–9. ISSN: 1529-2401 (Electronic) 0270-6474 (Linking). DOI: [10.1523/JNEUROSCI.0567-09.2010](https://doi.org/10.1523/JNEUROSCI.0567-09.2010). URL: <https://www.ncbi.nlm.nih.gov/pubmed/20164353>.
- Wang, J. et al. (2017). "Enhanced Gamma Activity and Cross-Frequency Interaction of Resting-State Electroencephalographic Oscillations in Patients with Alzheimer's Disease". In: *Front Aging Neurosci* 9. Edition: 20170726, p. 243. ISSN: 1663-4365 (Print) 1663-4365 (Linking). DOI: [10.3389/fnagi.2017.00243](https://doi.org/10.3389/fnagi.2017.00243). URL: <https://www.ncbi.nlm.nih.gov/pubmed/28798683>.
- Warren, C. M. et al. (May 25, 2016). "Catecholamine-Mediated Increases in Gain Enhance the Precision of Cortical Representations". In: *J Neurosci* 36.21, pp. 5699–708. ISSN: 1529-2401 (Electronic) 0270-6474 (Linking). DOI: [10.1523/JNEUROSCI.3475-15.2016](https://doi.org/10.1523/JNEUROSCI.3475-15.2016). URL: <https://www.ncbi.nlm.nih.gov/pubmed/27225761>.
- Watabe-Uchida, M. et al. (June 7, 2012). "Whole-brain mapping of direct inputs to midbrain dopamine neurons". In: *Neuron* 74.5, pp. 858–73. ISSN: 1097-4199 (Electronic) 0896-6273 (Linking). DOI: [10.1016/j.neuron.2012.03.017](https://doi.org/10.1016/j.neuron.2012.03.017). URL: <https://www.ncbi.nlm.nih.gov/pubmed/22681690>.
- Watson, T. C. et al. (2014). "Back to front: cerebellar connections and interactions with the prefrontal cortex". In: *Front Syst Neurosci* 8. Edition: 20140204, p. 4. ISSN: 1662-5137 (Print) 1662-5137 (Linking). DOI: [10.3389/fnsys.2014.00004](https://doi.org/10.3389/fnsys.2014.00004). URL: <https://www.ncbi.nlm.nih.gov/pubmed/24550789>.
- Wesierska, M., C. Dockery, and A. A. Fenton (Mar. 2, 2005). "Beyond memory, navigation, and inhibition: behavioral evidence for hippocampus-dependent cognitive coordination in the rat". In: *J Neurosci* 25.9, pp. 2413–9. ISSN: 1529-2401 (Electronic) 0270-6474 (Linking). DOI: [10.1523/JNEUROSCI.3962-04.2005](https://doi.org/10.1523/JNEUROSCI.3962-04.2005). URL: <https://www.ncbi.nlm.nih.gov/pubmed/15745968>.
- White, J. J. et al. (June 11, 2014). "Cerebellar zonal patterning relies on Purkinje cell neurotransmission". In: *J Neurosci* 34.24, pp. 8231–45. ISSN: 1529-2401 (Electronic) 0270-6474 (Linking). DOI: [10.1523/JNEUROSCI.0122-14.2014](https://doi.org/10.1523/JNEUROSCI.0122-14.2014). URL: <https://www.ncbi.nlm.nih.gov/pubmed/24920627>.
- Whiteside, J. A. and R. S. Snider (July 1953). "Relation of cerebellum to upper brain stem". In: *J Neurophysiol* 16.4, pp. 397–413. ISSN: 0022-3077 (Print) 0022-3077 (Linking). DOI: [10.1152/jn.1953.16.4.397](https://doi.org/10.1152/jn.1953.16.4.397). URL: <https://www.ncbi.nlm.nih.gov/pubmed/13070051>.
- Womelsdorf, T. et al. (June 15, 2007). "Modulation of neuronal interactions through neuronal synchronization". In: *Science* 316.5831, pp. 1609–12. ISSN: 1095-9203 (Electronic) 0036-8075 (Linking). DOI: [10.1126/science.1139597](https://doi.org/10.1126/science.1139597). URL: <https://www.ncbi.nlm.nih.gov/pubmed/17569862>.
- Wulff, Peer et al. (2009). "Hippocampal theta rhythm and its coupling with gamma oscillations require fast inhibition onto parvalbumin-positive interneurons". In: *Proceedings of the National Academy of Sciences* 106.9. Section: 3561, pp. 3561–3566. ISSN: 0027-8424 1091-6490. DOI: [10.1073/pnas.0813176106](https://doi.org/10.1073/pnas.0813176106).

- Xu, F. and D. T. Frazier (Jan. 2002). "Role of the cerebellar deep nuclei in respiratory modulation". In: *Cerebellum* 1.1, pp. 35–40. ISSN: 1473-4222 (Print) 1473-4222 (Linking). DOI: [10.1080/147342202753203078](https://doi.org/10.1080/147342202753203078). URL: <https://www.ncbi.nlm.nih.gov/pubmed/12879972>.
- Xu, F., J. Owen, and D. T. Frazier (Oct. 1995). "Hypoxic respiratory responses attenuated by ablation of the cerebellum or fastigial nuclei". In: *J Appl Physiol* (1985) 79.4, pp. 1181–9. ISSN: 8750-7587 (Print) 0161-7567 (Linking). DOI: [10.1152/jappl.1995.79.4.1181](https://doi.org/10.1152/jappl.1995.79.4.1181). URL: <https://www.ncbi.nlm.nih.gov/pubmed/8567560>.
- Yackle, K. et al. (Mar. 31, 2017). "Breathing control center neurons that promote arousal in mice". In: *Science* 355.6332. Edition: 20170330, pp. 1411–1415. ISSN: 1095-9203 (Electronic) 0036-8075 (Linking). DOI: [10.1126/science.aai7984](https://doi.org/10.1126/science.aai7984). URL: <https://www.ncbi.nlm.nih.gov/pubmed/28360327>.
- Yagi, N. et al. (2017). "Inappropriate Timing of Swallow in the Respiratory Cycle Causes Breathing-Swallowing Discoordination". In: *Front Physiol* 8. Edition: 20170922, p. 676. ISSN: 1664-042X (Print) 1664-042X (Linking). DOI: [10.3389/fphys.2017.00676](https://doi.org/10.3389/fphys.2017.00676). URL: <https://www.ncbi.nlm.nih.gov/pubmed/28970804>.
- Yamamoto, J. et al. (May 8, 2014). "Successful execution of working memory linked to synchronized high-frequency gamma oscillations". In: *Cell* 157.4. Edition: 20140424, pp. 845–57. ISSN: 1097-4172 (Electronic) 0092-8674 (Linking). DOI: [10.1016/j.cell.2014.04.009](https://doi.org/10.1016/j.cell.2014.04.009). URL: <https://www.ncbi.nlm.nih.gov/pubmed/24768692>.
- Yoon, T. et al. (Mar. 2008). "Prefrontal cortex and hippocampus subserve different components of working memory in rats". In: *Learn Mem* 15.3. Edition: 20080219, pp. 97–105. ISSN: 1549-5485 (Electronic) 1072-0502 (Linking). DOI: [10.1101/lm.850808](https://doi.org/10.1101/lm.850808). URL: <https://www.ncbi.nlm.nih.gov/pubmed/18285468>.
- Yu, W. and E. Krook-Magnuson (2015). "Cognitive Collaborations: Bidirectional Functional Connectivity Between the Cerebellum and the Hippocampus". In: *Front Syst Neurosci* 9. Edition: 20151222, p. 177. ISSN: 1662-5137 (Print) 1662-5137 (Linking). DOI: [10.3389/fnsys.2015.00177](https://doi.org/10.3389/fnsys.2015.00177). URL: <https://www.ncbi.nlm.nih.gov/pubmed/26732845>.
- Zelano, C. et al. (Dec. 7, 2016). "Nasal Respiration Entrain Human Limbic Oscillations and Modulates Cognitive Function". In: *J Neurosci* 36.49, pp. 12448–12467. ISSN: 1529-2401 (Electronic) 0270-6474 (Linking). DOI: [10.1523/JNEUROSCI.2586-16.2016](https://doi.org/10.1523/JNEUROSCI.2586-16.2016). URL: <https://www.ncbi.nlm.nih.gov/pubmed/27927961>.
- Zerbi, V. et al. (Aug. 21, 2019). "Rapid Reconfiguration of the Functional Connectome after Chemogenetic Locus Coeruleus Activation". In: *Neuron* 103.4. Edition: 20190618, 702–718 e5. ISSN: 1097-4199 (Electronic) 0896-6273 (Linking). DOI: [10.1016/j.neuron.2019.05.034](https://doi.org/10.1016/j.neuron.2019.05.034). URL: <https://www.ncbi.nlm.nih.gov/pubmed/31227310>.
- Zhang, X. et al. (Feb. 24, 2016). "Impaired theta-gamma coupling in APP-deficient mice". In: *Sci Rep* 6. Edition: 20160224, p. 21948. ISSN: 2045-2322 (Electronic) 2045-2322 (Linking). DOI: [10.1038/srep21948](https://doi.org/10.1038/srep21948). URL: <https://www.ncbi.nlm.nih.gov/pubmed/26905287>.
- Zhivomirov, Hristo (Apr. 2021). URL: <https://mathworks.com/matlabcentral/fileexchange/84933-bimodality-coefficient-calculation-with-matlab>.

Zhong, W. et al. (Apr. 25, 2017). "Selective entrainment of gamma subbands by different slow network oscillations". In: *Proc Natl Acad Sci U S A* 114.17. Edition: 20170410, pp. 4519–4524. ISSN: 1091-6490 (Electronic) 0027-8424 (Linking). DOI: [10.1073/pnas.1617249114](https://doi.org/10.1073/pnas.1617249114). URL: <https://www.ncbi.nlm.nih.gov/pubmed/28396398>.

Vita

Brittany Chapman (née Correia), was born in Collierville, TN in 1995 and grew up in the Memphis area. She completed her undergraduate work at Vanderbilt University in Nashville, TN in 2018 and received a Bachelor of Arts in Neurosciences. She returned to Memphis and began her graduate studies in the College of Graduate Health Sciences at the University of Tennessee Health Science Center in 2018. In March of 2019, she joined the lab of Dr. Detlef Heck where she used a model of cerebellar ataxia to study neuronal and behavioral rhythms. She expects to receive her Ph.D. in Integrated Biomedical Sciences with a Neuroscience concentration in November 2022 and will begin her postdoctoral work at the University of Pennsylvania with Dr. Minghong Ma in 2023.